Critical loads of tall building structures

Pel, E.J.

Award date:
2004

CRITICAL LOADS OF TALL BUILDING STRUCTURES

A-2004.8

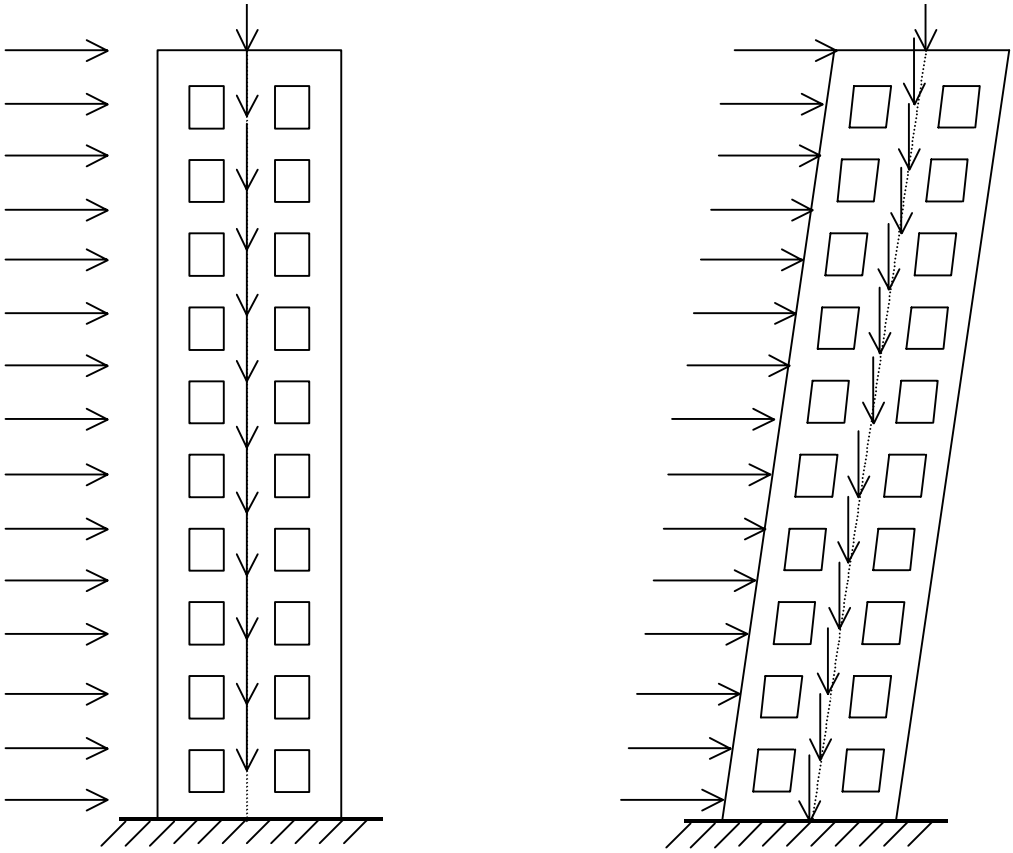

Project:	Critical loads of tall building structures
University:	Eindhoven University of Technology (TU/e)
Department:	Architecture Building & Planning
Group:	Structural Design
Committee:	Dr. ir. J.C.D. Hoenderkamp, chairman
	Prof. ir. H.H. Snijder
	Dr. ir. M.C.M. Bakker
Student:	Ing. E.J. Pel
Identification number:	0500596
Date:	29-6-2004
Country:	The Netherlands

Contents

LIST OF SYMBOLS

Capital letters

symbol	description	dimension
A	cross-sectional area	m^2
A_b	cross-sectional area of beam	m^2
A_c	cross-sectional area of column	m^2
A_d	cross-sectional area of diagonal	m^2
C	rotational spring stiffness	KNm
E	elastic modulus	KN/m^2
EA	axial stiffness	KN
EAc^2	global bending stiffness	KNm^2
EI	individual bending stiffness, bending stiffness	KNm^2
EI_i	stiffness of i-th column	KNm^2
EI_0	overall bending stiffness	KNm^2
F	vertical load	KN
F_d	vertical roof load	KN
F_v	vertical floor load	KN
F_{cr}	critical load (UDL)	KN
$F_{cr;C}$	individual rotational spring critical load (UDL)	KN
$F_{cr;EAc^2}$	global bending critical load (UDL)	KN
$F_{cr;EI}$	individual bending critical load (UDL)	KN
$F_{cr;EI_0}$	overall bending critical load (UDL)	KN
$F_{cr;GA}$	global racking shear critical load (UDL) / shear critical load (UDL)	KN
$F_{cr;GA;cantilever}$	shear critical load of a shear cantilever (UDL)	KN
$F_{cr;GA_c}$	racking shear critical load of the columns (UDL)	KN
$F_{cr;GA_b}$	racking shear critical load of the beams (UDL)	KN
F'_{cr}	critical load (vertical top load + UDL)	KN
$F'_{cr;EAc^2}$	global bending critical load (vertical top load + UDL)	KN
$F'_{cr;EI}$	individual bending critical load (vertical top load + UDL)	KN
$F'_{cr;EI_0}$	overall bending critical load (vertical top load + UDL)	KN
$F'_{cr;GA}$	global racking shear critical load (vertical top load + UDL)	KN
$F'_{cr;GA;cantilever}$	shear critical load of a shear cantilever (vertical top load + UDL)	KN
G	shear modulus	KN/m^2
GA	global racking shear stiffness, shear stiffness	KN
GA_b	racking shear stiffness of the beams	KN
GA_c	racking shear stiffness of the columns (caused by vertical loads)	KN
GA'_c	racking shear stiffness of the columns (caused by horizontal loads)	KN
GA_K	racking shear stiffness of K-braced frame	KN
GA_{Knee}	racking shear stiffness of Knee-braced frame	KN
GA_N	racking shear stiffness of N-braced frame	KN

GA_X	racking shear stiffness of X-braced frame	KN
I	second moment of area	m^4
I_b	second moment of area of beam	m^4
I_c	second moment of area of column	m^4
I_i	second moment of area of i-th column	m^4
I_0	overall second moment of area	m^4
M	bending moment	KNm
M_0	first-order bending moment	KNm
$M_{2.1}$	first step second-order additional bending moment	KNm
$M_{2.2}$	second step second-order additional bending moment	KNm
M_{EAc^2}	global bending moment	KNm
M_{EI}	individual bending moment	KNm
NA_i	neutral axis i-th column	[-]
NA_{frame}	neutral axis frame	[-]
$N_{cantilever}$	normal force in cantilever at the bottom (UDL)	KN
N_{frame}	normal force in frame at the first storey (UDL)	KN
$N'_{cantilever}$	normal force in cantilever at the bottom (vertical top load + UDL)	KN
N'_{frame}	normal force in frame at the first storey (vertical top load + UDL)	KN
P	vertical top load	KN
P_{cr}	(elastic) critical load (vertical top load)	KN
$P_{cr(ANSYS)}$	ANSYS critical load (vertical top load)	KN
$P_{cr;C}$	individual rotational spring critical load (vertical top load)	KN
$P_{cr;EAc^2}$	global bending critical load (vertical top load)	KN
$P_{cr;EI}$	individual bending critical load (vertical top load)	KN
$P_{cr;GA}$	global racking shear critical load (vertical top load) / shear critical load	KN
$P_{cr;GA;cantilever}$	shear critical load of cantilever (vertical top load)	KN
$P_{cr;GA_c}$	racking shear critical load of the columns (vertical top load)	KN
$P_{cr;GA_b}$	racking shear critical load of the beams (vertical top load)	KN
$P_{cr;i}$	critical load of i-th column (vertical top load)	KN
$P_{cr;\max}$	overall critical load (vertical top load)	KN
$P_{cr;P}$	plastic critical load (vertical top load)	KN
P_i	vertical top load on i-th column	KN
Q	horizontal top load	KN
Q_i	horizontal top load on the i-th column	KN
S	amplification factor	[-]
W	horizontal load	KN
W_d	horizontal roof load	KN
W_h	horizontal floor load	KN

Small letters

symbol	description	dimension
a	width of frame, distance between exterior columns	m
b_s	width of sandwich column	m
c'	rotational spring stiffness of individual column	KNm
c	distance between column neutral axis and frame neutral axis	m
c_i	distance between neutral axis i-th column and neutral axis frame	m
c_1	numerical parameter	[-]
c_s	width of the core	m
d	length of diagonal	m
d_s	thickness of the core	m
e	number of columns	[-]
f	uniformly distributed vertical load	KN/m
f_i	uniformly distributed vertical load on i-th column	KN/m
g	horizontal distance from knee-braced top to column	m
h	storey-height of frame	m
i	parameter running from 0 to e	[-]
j	number of stiffness parameters	[-]
k	translational spring stiffness	KN/m
k_{EAc^2}	translational spring stiffness for global bending	KN/m
k_{EI}	translational spring stiffness for individual bending	KN/m
k_{GA}	translational spring stiffness for global racking shear	KN/m
k_i	translational spring stiffness of i-th column	KN/m
l	height of frame / height of structure	m
m	uniformly distributed moment along substitute column	KNm/m
n	critical load ratio	[-]
p	horizontal distance between knee-braced tops	m
r	combination factor	[-]
s	number of stories of frame	[-]
t_s	thickness of face	m
w	horizontal uniformly distributed load	KN/m
w_i	horizontal uniformly distributed load on i-th column	KN/m
x	distance from the origin	m
y	horizontal deformation at the top of the column	m
y_0	first order horizontal deformation at top of the column	m
y_{01}	first order horizontal deformation at top of the first column	m
y_{02}	first order horizontal deformation at top of the second column	m
$y_{2.1}$	first step second-order additional deformation	m
$y_{2.2}$	second step second-order additional deformation	m
y_i	horizontal deformation at top of the i-th column	m
y_C	individual rotational spring deformation at top of the frame	m
y_{EAc^2}	global bending deformation at top of the frame	m
y_{EI}	individual bending deformation at top of the frame	m
y_{EI_0}	overall bending deformation at top of the frame	m

y_{GA}	global racking shear deformation at top of the frame	m
y_{GA_c}	racking shear deformation of the columns at top of the frame	m
y_{GA_b}	racking shear deformation of the beams at top of the frame	m

Greek letters

symbol	description	dimension
α	reduction factor for bending critical loads $P'_{cr;EI}$ and $F'_{cr;EI}$	[-]
α_s	reduction factor	[-]
$\hat{\alpha}$	critical load parameter of substitute column	[-]
β	reduction factor for racking shear critical load (non-continous columns)	[-]
β'	reduction factor for racking shear critical load (continous columns)	[-]
$\overline{\beta}$	stiffness parameter shear-flexure cantilever	[-]
$\hat{\beta}$	stiffness parameter of substute column	[-]
ϕ	rotation	[-]
γ	factor which takes the effect of a different roof load into account	[-]
η	reduction factor, which takes the effects of different normal forces $N_{cantilever}$ and N_{frame} into account	[-]
η'	reduction factor, which takes the effects of different normal forces $N'_{cantilever}$ and N'_{frame} into account	[-]
$\overline{\lambda}$	critical load parameter of shear-flexure cantilever	[-]
ω	reduction factor, which takes the influence of the vertical top load P into account	[-]
ς	ratio between the horizontal and vertical load	[-]
σ	stresses	[-]
ε	strain	[-]
Δ	error	%

Acknowledgements

The author wishes to thank Mrs. dr. ir. M.C.M. Bakker for her help with building the numerical models for the accuracy analysis and her knowledge to overcome the ANSYS FEM program problems. The writer is also grateful to prof. ir. H.H. Snijder for his enthusiasm and help during this project. The chairman dr.ir. J.C.D. Hoenderkamp deserves special thanks for his critical point of view and his interest in this project. I want to thank all for making themselves available for the bi-weekly meetings, for always going through the thick reports during this project and their inspiring discussions during my study. Finally I wishes to thank K.A. Zalka for helping me find some papers for my literature research.

1 Introduction

1.1 Summary

Some approximate equations are presented here for estimating the elastic critical load of planar lateral load resisting braced and rigid frames, which provide the stability in tall buildings.
These equations can be obtained from a stick-spring model by combining the major modes of deformation. Each mode of deformation corresponds to an individual stiffness and an individual critical load. The stick-spring model requires the calculation of the individual stiffnesses, which are necessary for the calculation of the individual critical loads. All these individual critical loads have to be combined into one equation to obtain the elastic critical load of a structure.
The stick-spring model can be used to show the influence of the second order effects on the deformations and bending moments. It is suitable for the preliminary stages of design and can be used to check whether the results of computer analyses are reasonable or not.
A worked example is presented here to show the simplicity of the stick-spring model in the preliminary stages of design of tall building structures. The accuracy of the stick-spring model has been compared to finite element analyses.

1.2 Introduction elastic critical load

To introduce the elastic critical load of a tall building structure, it is modelled into a flexural cantilever as shown in fig. 1.1a. This cantilever has bending stiffness EI, is subjected to a horizontal load $Q = \varsigma P$ and a vertical load P and undergoes bending deformations only. Factor ς represents the ratio between the horizontal and vertical load. The load-deformation diagram of the cantilever is shown in figure 1.1b.

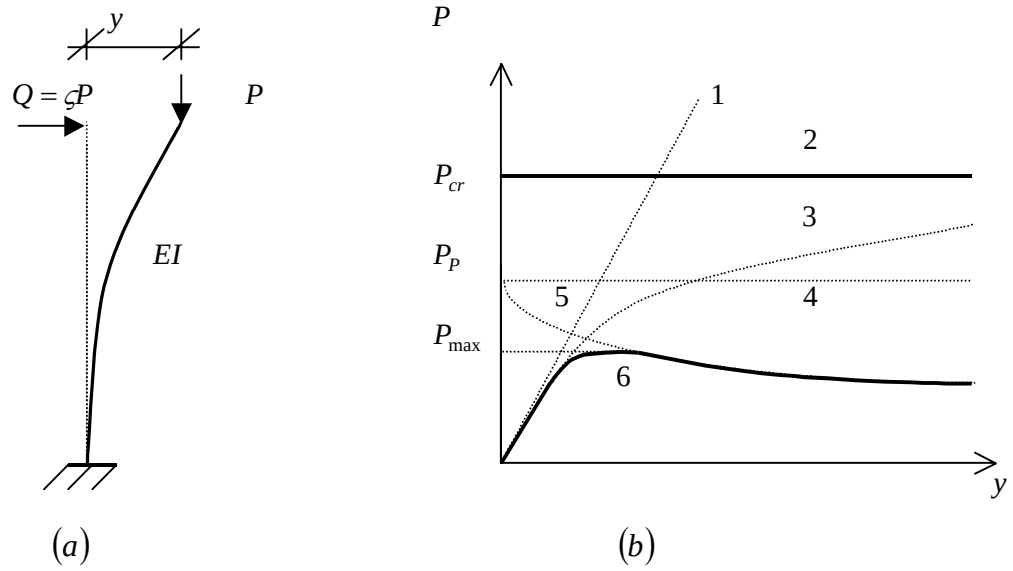

Figure 1.1 Behavior of a flexural cantilever.

First-order elastic (FL+GL)

In a first-order elastic analysis the flexural cantilever is subjected to a horizontal top load only. First-order means that equilibrium is reached in the undeformed state and rotations are small. Elastic means the cantilever returns to its undeformed shape if the horizontal load disappears. This top load causes a first-order horizontal deformation, a shear force and a bending moment in the cantilever. The material of the cantilever is fysically and geometrically lineair, which leads to a lineair elastic relation between load ςP and deformation y (see line 1 fig. 1.1b). Fysically linear (FL) means the material obeys Hooke`s law and there is a lineair elastic relation between stress σ and strain ε. Geometrically lineair (GL) means equilibrium is defined for the undeformed state.

Elastic critical load (Euler)

The same flexural cantilever is subjected to a vertical top load P only. The cantilever collapses if the vertical top load is higher then the elastic critical load, it returns to its original state if the vertical top load is lower then the elastic critical load and it will be standing in the deformed state if the vertical top load is equal to the elastic critical load. The elastic critical load P_{cr} is called the buckling load of the cantilever. A buckling analysis is a second-order analysis. Second-order means that equilibrium is reached in the deformed state and rotations are small. During buckling equilibrium is possible for the same load and for different deformations (see line 2 fig. 1.1b). This is called indifferent equilibrium.

Second-order elastic (FL+GNL)
In a second-order elastic analysis a flexural cantilever is subjected to a horizontal top load ςP and a vertical top load P. The horizontal top load ςP causes a first order-deformation, a shear force and a bending moment in the cantilever. Vertical top load P causes additional horizontal deformations, shear forces and bending moments in the cantilever. These additional deformations, shear forces and bending moments are called second-order effects. The material of the cantilever is fysically lineair and geometrically non-lineair. Geometrically non-lineair means equilibrium is defined for the deformed state, which leads to a non-lineair relation between load P and deformation y
(see line 3 fig. 1.1b).

First-order plastic (FNL+GL)
In a first-order plastic analysis a flexural cantilever is subjected to a horizontal top load ςP only. Plastic means the cantilever will not return to its undeformed shape if the horizontal load disappears. In the elementary collapse analysis a structure collapses if a mechanism appears. The material of the cantilever is fysical non-lineair (FNL). Fysical non-linear means the material does not obey Hooke`s law. In that case only the plastic part of the $\sigma - \varepsilon$ diagram will be used. Equilibrium is possible for the same load and for different deformations (see line 4 fig. 1.1b).

Second-order plastic
In a second-order plastic analysis a flexural cantilever is subjected to a horizontal top load ςP and a vertical top load P. Line 5 represents the relation between load P and deformation y.

Second-order elastic-plastic (FNL+GNL)
In a second-order elastic-plastic analysis a flexural cantilever is subjected to a horizontal top load ςP and a vertical top load P. Elastic-plastic (bi-lineair) means that both the elastic and plastic parts of the $\sigma - \varepsilon$ diagram will be used. The material of this cantilever is fysical non-lineair (FNL).
Transitional line 6 can be obtained by combining line 3 and 5 (see fig. 1.1b).

Note:
In this project only the elastic critical load P_{cr} is important and therefore only line 2 of the load-deformation diagram will be used (see fig. 1.1b).

1.3 Introduction second-order effects

To introduce the second-order effects of a tall building structure, it is modelled into a flexural cantilever as shown in fig. 1.2a. This flexural cantilever has bending stiffness EI and is subjected to a horizontal load Q and a vertical load P. First the cantilever is only subjected to a horizontal load Q (see fig. 1.2b). The horizontal load Q causes a first-order deformation y_0 and a first-order bending moment $M_0 = Ql$. The vertical top load P causes a first step second-order additional bending moment $M_{2;1} = Py_0$, which gives a first step second-order additional deformation $y_{2;1}$ (see fig. 1.2c). This first step second-order additional deformation $y_{2;1}$ in combination with vertical top load P causes a second step second-order additional bending moment $M_{2;2} = Py_{2,1}$, which gives a second step second-order additional deformation $y_{2;2}$ (see fig. 1.2d).
This process will go on, untill the cantilever collapses or equilibrium is reached.
These additional deformations and additional bending moments are called second-order effects.

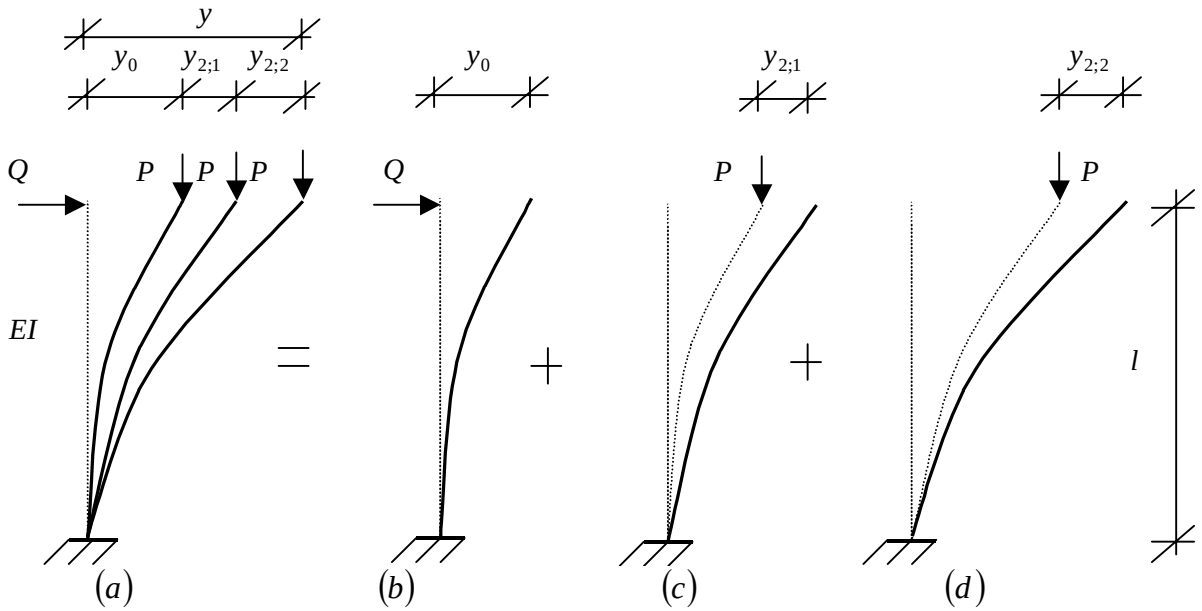

Figure 1.2 First-order and second-order effects.

Horizontal deformation y caused by horizontal load Q and vertical load P is:

$$y = y_0 + y_{2;1} + y_{2;2} + etc \tag{1.1}$$

Consider the deformation of each step is $1/n$ times the deformation of the previous step:

$$y_{2,i+1} = \frac{y_{2;i}}{n} \tag{1.2}$$

and

$$y_{2,1} = \frac{y_0}{n} \tag{1.3}$$

Substituting eq. (1.2) and eq. (1.3) into eq. (1.1) leads to the following expression:

$$y = y_0 + \frac{y_0}{n} + \frac{y_{2;1}}{n} + etc = y_0\left(1 + \frac{1}{n} + \frac{1}{n^2} + etc\right) = y_0 + \frac{y}{n} = \frac{n}{n-1}y_0 \tag{1.4}$$

Where amplification factor S is:

$$S = \frac{n}{n-1} \tag{1.5}$$

Bending moment M can be given by:

$$M = \frac{n}{n-1}M_0 \tag{1.6}$$

The amplification factor S takes the second-order effects caused by vertical top load P into account. Therefore the first-order deformation y_0 and the first-order bending moment M_0 have to be multiplied by amplification S to obtain deformation y (see eq. 1.4) and bending moment M (see eq. 1.6). Amplification factor S is mathematically exact if the first-order deformed shape (see fig. 1.2b) is identical to the first step second-order (see fig. 1.2c) and to the second step second-order deformed shape (see fig. 1.2d) etc.

1.4 Introduction stick-spring model

The stick-spring model was introduced by Dicke [1, 2] to obtain an approximate solution for the critical load of a flexural cantilever subjected to a vertical top load P (see fig. 1.3a).
The flexural cantilever is fixed to the base, has one mode of deformation: individual bending stiffness EI and is subjected to a vertical top load P. First the flexural cantilever is transformed into Rosman`s model [3], where a stick has infinite individual bending stiffness $EI = \infty$ and is supported by the same flexural cantilever (see fig. 1.3b). Now the vertical load P is removed from the cantilever and placed on the stick, which causes a tensile force Q in the horizontal rigid link.

This transformation gives always upperbound approximate solutions for the critical of a flexural cantilever. Rosman`s model can be transformed into the stick-spring model (see fig. 1.3c). In this model the same flexural cantilever is replaced by a horizontal translation spring k, which takes the individual bending stiffness EI into account. Therefore spring stiffness k is a function of the individual bending stiffness of the flexural cantilever $k = f(EI)$.

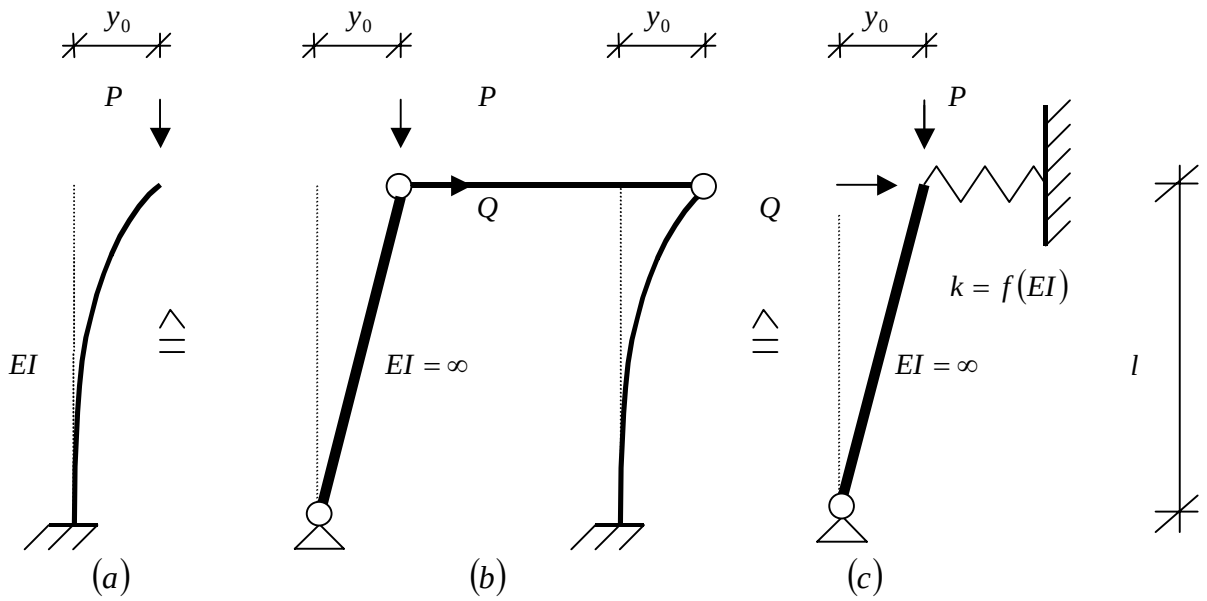

Figure 1.3 Origin stick-spring model.

1.5 Objectives

The main objective of this project is to obtain simplified equations for estimating the elastic critical load of lateral load resisting braced and rigid frames in the preliminary stages of design of tall buildings, which combine the major modes of behavior. Another aim of this project is to check the accuracy of the stick-spring model by a finite element analysis.

1.6 Sway structures

Structures can be divided into sway and non-sway structures. Sway structures are tall and slender structures, which develop global buckling (side-ways deformation) and non-sway structures are low and compact structures, which develop local buckling. In this project only tall and slender one-bay sway structures will be investigated. They are:

- X-braced frames with non-continous columns pin-connected to the base (see fig. 1.4a).
- X-braced frames with continous columns pin-connected to the base (see fig. 1.4b).
- Fixed rigid frames (see fig. 1.4c).
- Flexible rigid frames (see fig. 1.4d).

Highrise X-braced frames are sway structures consisting of beams and diagonals, which are pin-connected to the columns (see fig. 1.4a/b). Highrise rigid frames are sway structures consisting of columns and beams with fully moment resistant joints (see fig. 1.4c/d).

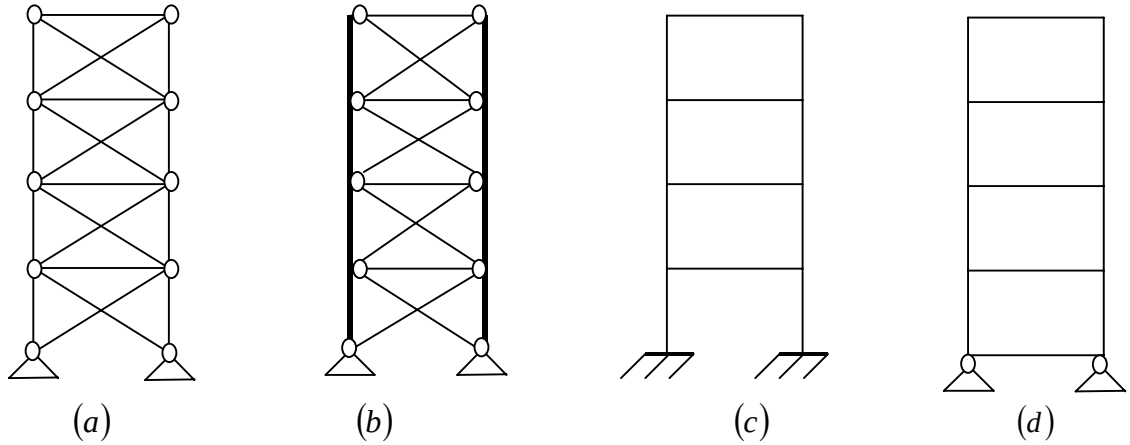

Figure 1.4 Sway frames.

1.7 Assumptions

For this project the following assumptions have been made:

- The material is elastic.
- The loads on the structures are applied statically and hold their direction during buckling (conservative loads).
- The structures are one bay structures.
- The structures are planar.
- The structures are sway structures and only develop global buckling.
- The structures develop small deformations.
- The stiffness parameters of the structures are uniform up the height.
- The height of the investigated structures varies from eight to forty stories.
- All storeys have the same storey-height.
- Imperfections are neglected.
- Residual stresses caused by the rolling proces are neglected.
- Shear deformations in the beams and columns of a rigid frame are neglected.

1.8 Loadcases sway structures

The sway-structures are subjected to three different loadcases (see fig. 1.5):

- Vertical top loads (see fig. 1.5a).
- Uniformly distributed vertical loads (see fig. 1.5b).
- Load combinations (see fig. 1.5c).

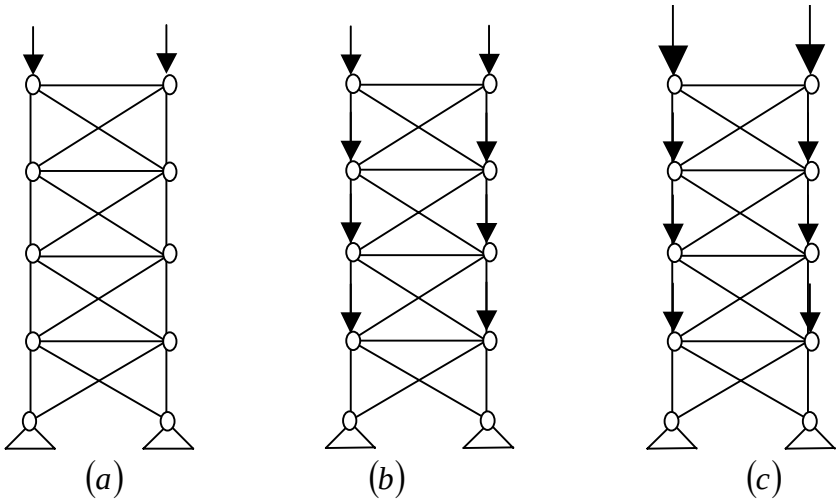

Figure 1.5. Loadcases sway structures.

1.9 Report layout

This report consists of nine chapters. Chapter two gives a history search with a summary of all important analytical models for the elastic stability of structures. Chapter three discusses additive theorems. Chapter four introduces the stick-spring model subjected to three different loadcases for the stability analysis. In chapter five the stick-spring model is used to obtain an approximate critical load for a flexural cantilever with one mode of deformation: individual bending stiffness EI.
In chapter six the stick-spring model is used to obtain an approximate critical load for a braced frame with non-continous columns pin-connected to the base and with two modes of deformation: global bending stiffness EAc^2 and racking shear stiffness GA. In chapter six the stick-spring model is also used to obtain an approximate critical load for a braced frame, but now with continous columns pin-connected to the base and with two modes of deformation: overall bending stiffness EI_0 and racking shear stiffness GA. In chapter seven the stick-spring model is used to obtain an approximate critical load for a rigid frame fix-connected to the base and with four modes of deformation: individual bending stiffness EI, global bending stiffness EAc^2, racking shear stiffness of the columns GA_c and racking shear stiffness of the beams GA_b.
In chapter seven the stick-spring model is also used to obtain an approximate critical load for a rigid frame, but now flexibly connected to the base and with five modes of deformation: individual bending stiffness EI, individual rotational stiffness C, global bending stiffness EAc^2, racking shear stiffness of the columns GA_c and racking shear stiffness of the beams GA_b.
Chapter eight gives a discusion and the conclusions of this project and chapter nine describes recommendations for further research.

2 Analytical models for the stability analysis

Several simplified analytical models are introduced here for the stability analysis.
These models can be used for estimating the critical load of braced and rigid frames.
They are:

- Flexural cantilever.
- Shear-flexure cantilever.
- Substitute column.
- Sandwich column with thin faces.
- Sandwich column with thick faces.

Each analytical model will be discussed independently.

2.1 Flexural cantilever

A "flexural cantilever" is a column fixed to the base, has bending stiffness EI and undergoes bending deformations only (see fig. 2.1).

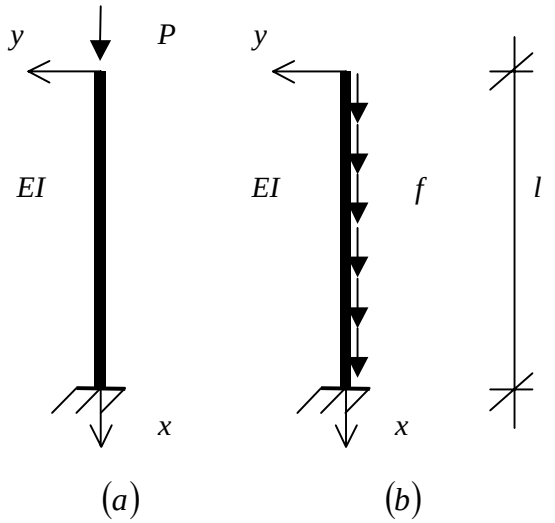

Figure 2.1. Flexural cantilever.

2.1.1 Vertical top load

Euler [4] derived in 1744 a differential equation for a flexural cantilever subjected to a vertical top load P (see fig. 2.1a)

$$\frac{d^2y}{dx^2} = -\frac{Py}{EI} \tag{2.1}$$

and obtained a formula for the critical load

$$P_{cr;EI} = \frac{\pi^2 EI}{4l^2} \tag{2.2}$$

2.1.2 Uniformly distributed vertical load

In 1936 Timoshenko [5] found a differential equation for a flexural cantilever subjected to an uniformly distributed vertical load f (see fig. 2.1b)

$$\frac{d^3y}{dx^3} + \frac{fx}{EI}\frac{dy}{dx} = 0 \qquad \text{or} \qquad \frac{d^2y}{dx^2} = -\frac{Fy}{EI} \tag{2.3}$$

,where $F = fl$ and suggested a formula for the critical load

$$F_{cr;EI} = \frac{7.837EI}{l^2} \tag{2.4}$$

2.2 Shear-flexure cantilever

A "shear-flexure cantilever" is a column fixed to the base, has bending stiffness EI, shear stiffness GA and undergoes bending and shear deformations (see fig. 2.2).

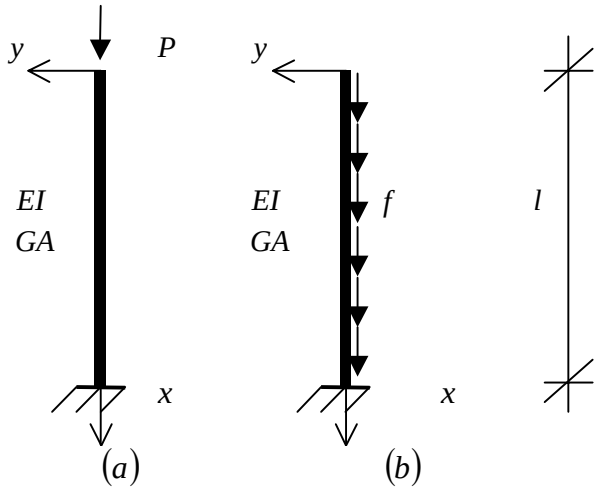

Figure 2.2. Shear-flexure cantilever.

2.2.1 Vertical top load

In 1936 Timoshenko [5] derived a differential equation for a shear-flexure cantilever subjected to a vertical top load P (see fig. 2.2a)

$$\frac{d^2y}{dx^2} = -\frac{Py}{EI} + \frac{P}{GA}\frac{d^2y}{dx^2} \tag{2.5}$$

and obtained a formula for the critical load

$$P_{cr} = \frac{P_{cr;EI}}{1+\frac{P_{cr;EI}}{P_{cr;GA}}} \qquad \text{or} \qquad \frac{1}{P_{cr}} = \frac{1}{P_{cr;EI}} + \frac{1}{P_{cr;GA}} \tag{2.6}$$

, where the bending critical load is

$$P_{cr;EI} = \frac{\pi^2 EI}{4l^2} \tag{2.7}$$

and the shear critical load is

$$P_{cr;GA} = GA \tag{2.8}$$

Equation (2.6) can also be found by applying the Föppl-Papkovics theorem [6, 7] (see section 3.3). For this case the Föppl-Papkovics formula is mathematical exact, because the bending buckling shape (see fig. 2.3a) is identical to the shear buckling shape (see fig. 2.3b). The shear buckling shape has no definite buckling shape, which means the shear buckling shape can assume any form even the form of the bending buckling shape.

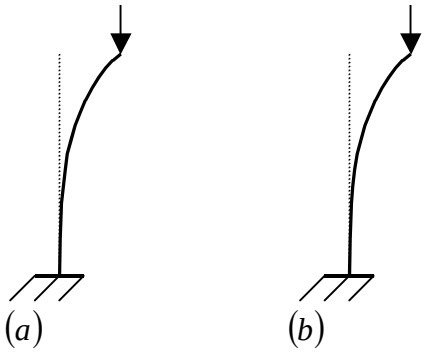

Fig 2.3 Buckling shapes of a shear-flexure cantilever subjected to a vertical top load.

2.2.2 Uniformly distributed vertical load

In 1979 [8] Zalka found a differential equation for a shear-flexure cantilever subjected to an uniformly distributed vertical load f (see fig. 2.2b)

$$y'''' - \frac{f}{GA}\left(3y''' + xy''''\right) + \frac{f}{EI}\left(y' + xy''\right) = 0 \tag{2.9}$$

and obtained a mathematically exact formula for the critical load by making use of a table or graph in which a critical load parameter $\overline{\lambda}$ is a function of a stiffness parameter $\overline{\beta}$

$$F_{cr} = \overline{\lambda} F_{cr;GA} \tag{2.10}$$

, where the stiffness parameter is

$$\overline{\beta} = \frac{F_{cr;GA}}{F_{cr;EI}} \tag{2.11}$$

He also suggested a simplified approximate formula for the critical load by applying the Föppl-Papkovics theorem [6, 7], which leads to

$$\frac{1}{F_{cr}} = \frac{1}{F_{cr;EI}} + \frac{1}{F_{cr;GA}} \tag{2.12}$$

, where the bending critical load is

$$F_{cr;EI} = \frac{7.837EI}{l^2} \tag{2.13}$$

and the shear critical load is

$$F_{cr;GA} = GA \tag{2.14}$$

For this case the Föppl-Papkovics formula is always conservative, because the bending buckling shape (see fig. 2.4a) is not identical to the shear buckling shape (see fig. 2.4b). The shear buckling shape has a definite buckling shape, which means the shear buckling shape can assume only one form.

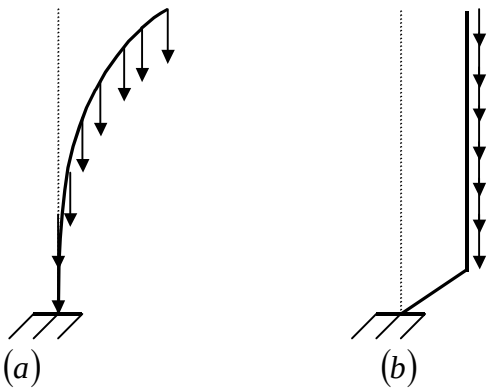

Fig 2.4 Buckling shapes of a shear-flexure cantilever subjected to a vertical UDL.

2.3 Substitute column

A "substitute column" is a flexural column fixed to the base with bending stiffness EI, which is supported by a uniformly distributed moment $m = f(GA)$ and undergoes bending and shear deformations (see fig. 2.5).

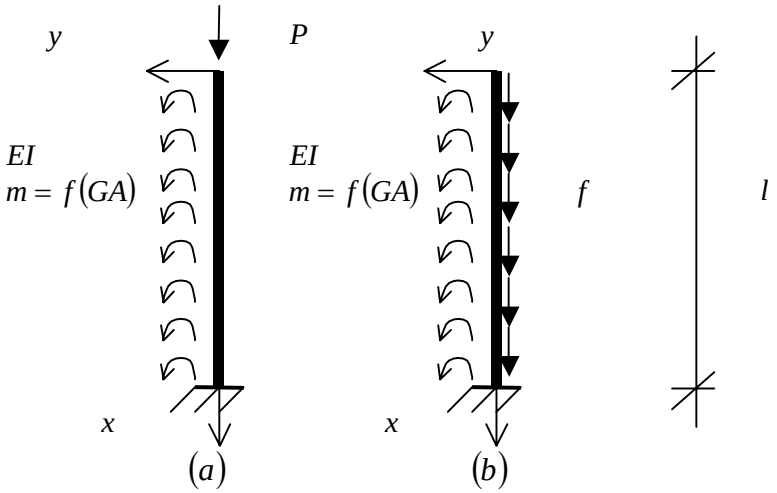

Figure 2.5. Substitute column.

2.3.1 Vertical top load

In 1961 Csonka [9] derived a differential equation for a substitute column subjected to a vertical top load P (see fig. 2.5a)

$$\frac{d^2y}{dx^2} = -\left(\frac{P - GA}{EI}\right) \tag{2.15}$$

and obtained a formula for the critical load

$$P_{cr} = P_{cr;EI} + P_{cr;GA} \tag{2.16}$$

, where the bending critical load is

$$P_{cr;EI} = \frac{\pi^2 EI}{4l^2} \tag{2.17}$$

and the shear critical load is

$$P_{cr;GA} = GA \tag{2.18}$$

Equation (2.16) can also be found by applying the Southwells theorem [10] (see section 3.2).
For this case the Southwell formula is mathematical exact, because the bending buckling shape (see fig. 2.3a) is identical to the shear buckling shape (see fig. 2.3b). The shear buckling shape has no definite buckling shape, which means the shear buckling shape can assume any form even the form of the bending buckling shape.

2.3.2 Uniformly distributed vertical load

In 1980 Zalka [11] found a differential equation for a substitute column subjected to an uniformly distributed vertical load f (see fig. 2.5b)

$$y''' + \left(\frac{F - GA}{EI}\right)y' = 0 \quad \text{or} \qquad \frac{d^2 y}{dx^2} = -\left(\frac{F - GA}{EI}\right) \tag{2.19}$$

and obtained a mathematically exact formula for the critical load by making use of a table or graph in which a critical load parameter $\hat{\alpha}$ is a function of a stiffness parameter $\hat{\beta}$

$$F_{cr} = \hat{\alpha}F_{cr;EI} = \hat{\alpha}F_{cr;EI} - F_{cr;GA} + F_{cr;GA} = \left(\hat{\alpha} - \hat{\beta}\right)F_{cr;EI} + F_{cr;GA} \tag{2.20}$$

, where the critical load parameter is

$$\hat{\alpha} = \frac{F_{cr}}{F_{cr;EI}} \tag{2.21}$$

and the stiffness parameter is

$$\hat{\beta} = \frac{F_{cr;GA}}{F_{cr;EI}} \tag{2.22}$$

He also suggested a simple approximate formula for the critical load by applying the Southwell theorem [10]

$$F_{cr} = F_{cr;EI} + F_{cr;GA} \tag{2.23}$$

, where the bending critical load is

$$F_{cr;EI} = \frac{7.837EI}{l^2} \tag{2.24}$$

and the shear critical load is

$$F_{cr;GA} = GA \tag{2.25}$$

For this case the Southwell formula (see eq. (2.23)) is always conservative, because the bending buckling shape (see fig. 2.4a) is not identical to the shear buckling shape (see fig. 2.4b).
The shear buckling shape has a definite buckling shape, which means the shear buckling shape can assume only one form. Equation (2.23) can give conservative errors of 47 % in comparison with the mathematically exact formula (see eq. (2.20))

2.4 Sandwich column with thin faces

A sandwich column with thin faces is a multi-layer column fixed to the base with global bending stiffness EAc^2 and racking shear stiffness GA, which undergoes global bending and racking shear deformations (see fig. 2.6). Most sandwich columns consist of three layers: two faces with thickness t_s and a core with thickness c_s. Structures are called sandwich columns with thin faces, if the following relationships hold:

- The thickness t_s of the faces can be neglected, because $t_s <<< c_s$, which leads to $c_s \approx d_s$.
- The individual bending stiffness of the faces $EI = 0$ can be neglected.
- The individual bending moment in the faces $M_{EI} = 0$ can be neglected.

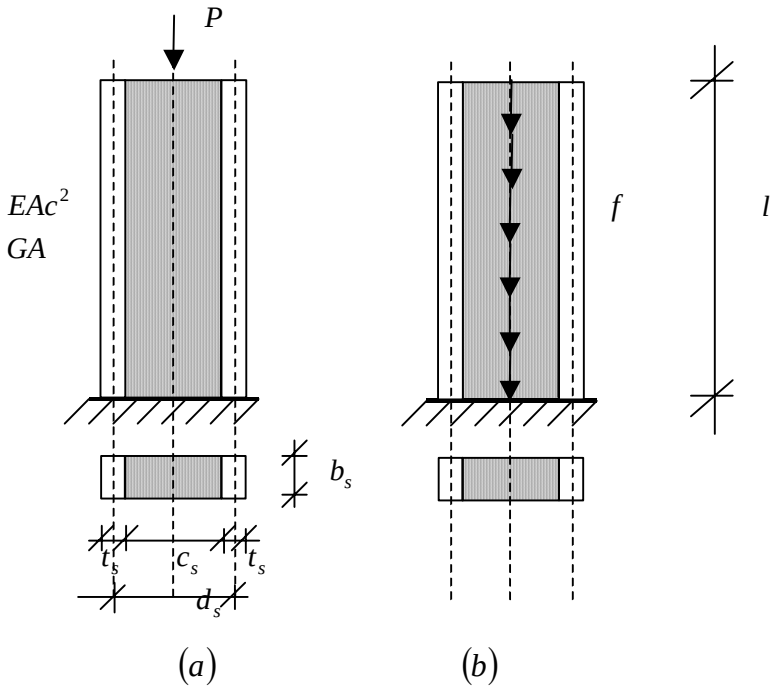

Figure 2.6. Sandwich column with thin faces.

2.4.1 Vertical top load

In 1984 [12] Hegedüs and Kollár derived a differential equation for a sandwich column with thin faces subjected to a vertical top load P (see fig. 2.6a)

$$EAc^2 \frac{d^4\phi}{dx^4} + P\left(\frac{d^2\phi}{dx^2} - \frac{EAc^2}{GA}\frac{d^4\phi}{dx^4}\right) = 0 \qquad \text{or} \qquad \frac{d^2y}{dx^2} = -\frac{Py}{EAc^2} + \frac{P}{GA}\frac{d^2y}{dx^2} \tag{2.26}$$

, where $\phi = y / l$ and obtained a formula for the critical load

$$\frac{1}{P_{cr}} = \frac{1}{P_{cr;EAc^2}} + \frac{1}{P_{cr;GA}} \tag{2.27}$$

, where the global bending critical load is

$$P_{cr;EAc^2} = \frac{\pi^2 EI}{4l^2} \tag{2.28}$$

and the shear critical load is

$$P_{cr;GA} = GA \tag{2.29}$$

Equation (2.27) can also be found by applying the Föppl-Papkovics theorem.
For this case the Föppl-Papkovics formula is mathematical exact, because the global bending buckling shape (see fig. 2.3a) is identical to the racking shear buckling shape (see fig. 2.3b).
The racking shear buckling shape has no definite buckling shape, which means the racking shear buckling shape can assume any form even the form of the global bending buckling shape.

2.4.2 Uniformly distributed vertical load

In 1979 [8] Zalka found a differential equation for a sandwich column with thin faces subjected to an uniformly distributed vertical load f (see fig. 2.6b)

$$y'''' - \frac{f}{GA}\left(3y''' + xy''''\right) + \frac{f}{EAc^2}\left(y' + xy''\right) = 0 \tag{2.30}$$

and obtained a mathematically exact formula for the critical load by making use of a table or graph in which a critical load parameter $\overline{\lambda}$ is a function of a stiffness parameter $\overline{\beta}$

$$F_{cr} = \overline{\lambda} F_{cr;GA} \tag{2.31}$$

, where the stiffness parameter is

$$\overline{\beta} = \frac{F_{cr;GA}}{F_{cr;EAc^2}} \tag{2.32}$$

He also suggested a simplified approximate formula for the critical load by applying the Föppl-Papkovics theorem [6, 7], which leads to

$$\frac{1}{F_{cr}} = \frac{1}{F_{cr;EAc^2}} + \frac{1}{F_{cr;GA}} \tag{2.33}$$

, where the bending critical load is

$$F_{cr;EI} = \frac{7.837 EAc^2}{l^2} \tag{2.34}$$

and the shear critical load is

$$F_{cr;GA} = GA \tag{2.35}$$

For this case the Föppl-Papkovics formula (see eq. (2.33)) is always conservative,
because the global bending buckling shape (see fig. 2.4a) is not identical to the racking shear buckling shape (see fig. 2.4b). The racking shear buckling shape has a definite buckling shape,
which means the shear buckling shape can assume only one form.

2.5 Sandwich column with thick faces

A sandwich column with thick faces is a multi-layer column fixed to the base with individual bending stiffness EI, global bending stiffness EAc^2 and racking shear stiffness GA,
which undergoes individual bending, global bending and racking shear deformations (see fig. 2.7).
Structures are called sandwich columns with thick faces, if the following relationships hold:

- The thickness $t_s \neq 0$ of the faces can`t be neglected and plays an important role.
- The individual bending stiffness $EI \neq 0$.
- The individual bending moment $M_{EI} \neq 0$.

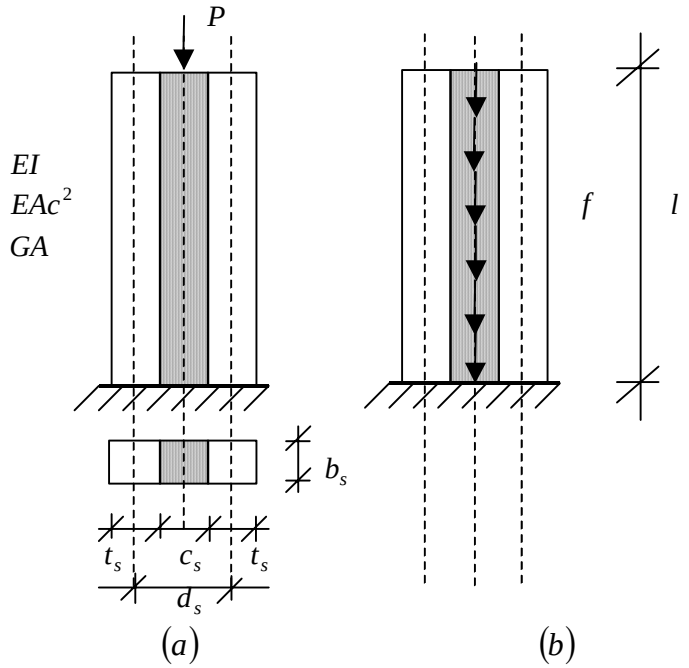

Figure 2.7. Sandwich column with thick faces.

2.5.1 Vertical top load

In 1984 [13] Hegedüs and Kollár derived a differential equation for a sandwich column with thick faces subjected to a vertical top load (see fig. 2.7a)

$$\frac{EAc^2 EI}{GA}\frac{d^4\phi}{dx^4} - \left(EAc^2 + EI\right)\frac{d^2\phi}{dx^2} + P\left(\frac{EAc^2}{GA}\frac{d^2\phi}{dx^2} - \phi\right) = 0 \tag{2.36}$$

or

$$\frac{EAc^2 + EI}{EAc^2}\frac{d^2y}{dx^2} = -\frac{Py}{EAc^2} + \frac{P}{GA}\frac{d^2y}{dx^2} + \frac{EI}{GA}\frac{d^2y}{dx^2}$$

, where $\phi = y/l$ and obtained a formula for the critical load

$$P_{cr} = \left[\frac{1}{P_{cr;EAc^2}} + \frac{1}{P_{cr;GA}}\right]^{-1} + P_{cr;EI} \tag{2.37}$$

Equation (2.37) can also be found by applying the Föppl-Papkovics [6, 7] and Southwell theorem [10]. For this case the formula is mathematical exact, because the individual bending buckling shape is identical to the global bending and racking shear buckling shape. The shear buckling shape has no definite buckling shape, which means the shear buckling shape can assume any form even the form of the individual bending and global bending buckling shape.

2.5.2 Uniformly distributed vertical load

In 1984 [13] Hegedüs and Kollár found a differential equation for a sandwich column with thick faces subjected to an uniformly distributed vertical load (see fig. 2.7b)

$$\frac{EAc^2EI}{GA}\frac{d^4\phi}{dx^4}-\left(EAc^2+EI\right)\frac{d^2\phi}{dx^2}+F\left(\frac{EAc^2}{GA}\frac{d^2\phi}{dx^2}-\phi\right)=0 \tag{2.38}$$

or

$$\frac{EAc^2+EI}{EAc^2}\frac{d^2y}{dx^2}=-\frac{Fy}{EAc^2}+\frac{F}{GA}\frac{d^2y}{dx^2}+\frac{EI}{GA}\frac{d^2y}{dx^2}$$

, where $\phi = y/l$ and obtained a mathematically exact formula by making use of a table for numerical parameter c_1

$$F_{cr}=c_1\frac{EAc^2+EI}{l^2} \tag{2.39}$$

They also suggested a simplified approximate formula for the critical load by applying the Föppl-Papkovics theorem [6, 7] and the Southwell theorem [10]

$$F_{cr}=\left[\frac{1}{F_{cr;EAc^2}}+\frac{1}{F_{cr;GA}}\right]^{-1}+F_{cr;EI} \tag{2.40}$$

For this case the combination of the Föppl-Papkovics and Southwell formula is always conservative, because the individual bending and global bending buckling shape are not identical to the racking shear buckling shape. The racking shear buckling shape has a definite buckling shape, which means the racking shear buckling shape can assume only one form.

3 Additive Theorems

Additive theorems are useful tools for dealing with complex problems in a simple way.
Equations for the overall critical load of a complex structure often rely on additive theorems and therefore a short summary of the theorems is given below. These theorems can only be used in the linear theory of stability for estimating the overall critical load of a structure.
A detailed analysis with mathematical background and the limitation of application of additive theorems is given by Tarnai [14, 15]. The principle of all additive theorems used in the stability analysis of structures is as follows. The buckling problem of an original structure is to complex and therefore the structure is divided into simpler part problems. Each part problem corresponds to a different buckling shape and a different individual critical load, which can be computed by a FEM program by always assuming a different stiffness parameter to be infinite or zero.
The overall critical load of the original complex structure can now be obtained by a summation of the individual critical loads of the part problems. This can be done by direct summation of the individual critical loads (Southwell) or by inverse summation of the individual critical loads (Föppl-Papkovics).
The big advantage of additive theorems is that a solution of the part problems is usually available whether the solution of the original complex problem is very difficult to obtain.
Three theorems will be introduced:

- The Dunkerley Theorem.
- The Southwell Theorem (parallel connection).
- The Föppl-Papkovics Theorem (serial connection).

3.1 The Dunkerley Theorem

Dunkerley [16] first used his formula for the vibration problem of shafts. The Dunkerley theorem applied to stability problems is defined as follows. The principle of this theory is as follows.
If a load system of an elastic structure can be considered as the sum of two loadsystems,
then the inverse addition of the critical loads which belong to the two loadsystems gives a conservative estimate of the overall critical load of the structure.

$$\frac{1}{F'_{cr}} \leq \frac{1}{F_{cr}} + \frac{1}{P_{cr}} \tag{3.1}$$

This theorem makes it possible to investigate structures subjected to a combination of load systems. For example a combination between a vertical top load and a uniformly distributed load.
The Dunkerley formula can also be used in a different form:

$$\frac{F}{F_{cr}} + \frac{P}{P_{cr}} \leq 1 \tag{3.2}$$

3.2 The Southwell Theorem

Southwell [10] first applied his theorem to vibration problems. Southwell`s theorem applied to stability problems is defined as follows. The elastic system is characterized by e stiffness parameters. The elastic system is first considered with all stiffness parameters zero except for the i-th one, which is left unchanged. Then the critical load of the i-th column is calculated.
This procedure is then repeated and always another stiffness parameter is left unchanged, while the values of all the others are assumed to be zero. This theory is based on parallel connection of columns and leads to the following four conditions (see fig. 3.1):

- The horizontal displacement of the resultant column is identical to the horizontal displacements of the individual columns:

$$y = y_1 = y_2 = y_3 \tag{3.3}$$

- The stiffness EI of the resultant column is equal to the sum of the individual stiffnesses.

$$EI = \sum_{i=1}^{e} EI_i = EI_1 + EI_2 + EI_3 \tag{3.4}$$

- The horizontal top loading Q on the resultant column is equal to the sum of the horizontal loading on the individual columns:

$$Q = \sum_{i=1}^{e} Q_i = Q_1 + Q_2 + Q_3 \tag{3.5}$$

- The vertical top loading P on the resultant column is equal to the sum of the vertical loading on the individual columns:

$$P = \sum_{i=1}^{e} P_i = P_1 + P_2 + P_3 \tag{3.6}$$

If the columns are parallel connected, then the sum of the individual critical loads of these parts gives a lower bound to the overall critical of a structure:

$$P_{cr} \geq \sum_{i=1}^{e} P_{cr;i} = P_{cr;1} + P_{cr;2} + P_{cr;3} \tag{3.7}$$

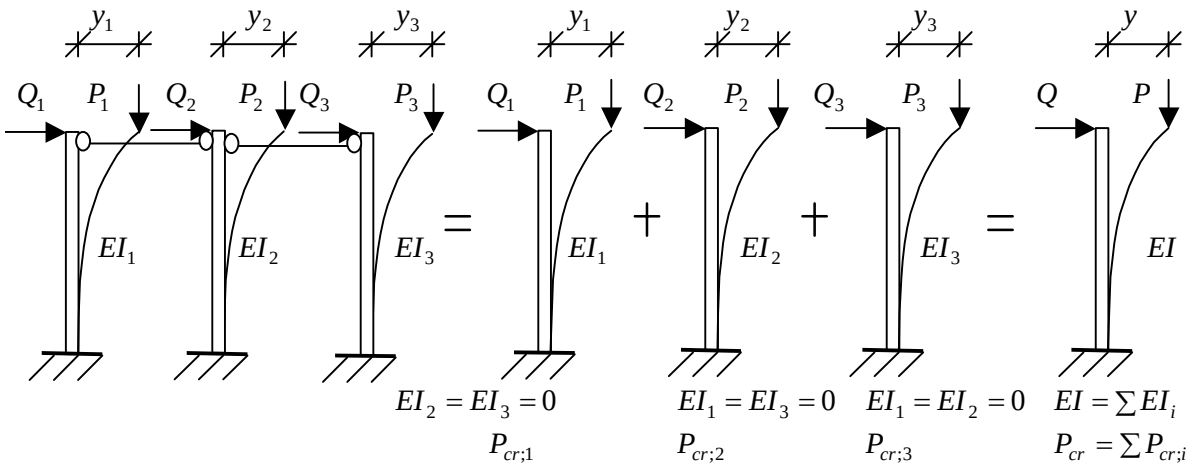

Figure 3.1 Southwell`s model: parallel connection of columns.

3.3 The Föppl-Papkovics Theorem

Föppl [6] and Papkovics [7] developed a theory for the stability of elastic structures, based on the partial stiffening of its elements. The principle of his theorem is as follows. The elastic system is characterized by e stiffness parameters. The system is first considered with all stiffness parameters infinite except for the i-th one, which is left unchanged. Then the critical load of the i-th column is calculated. This procedure is then repeated and always another stiffness parameter is left unchanged, while the values of all the others is assumed to be infinite. This theory is based on serial connection of columns and leads to the following four conditions (see fig. 3.2):

- The horizontal displacement of the resultant column is identical to the sum of the displacements of the individual columns:

$$y = \sum_{i=1}^{e} y_i = y_1 + y_2 + y_3 \tag{3.8}$$

- The stiffness EI of the resultant column is equal to the reciprocal sum of the individual stiffnesses.

$$\frac{1}{EI} = \sum_{i=1}^{e} \frac{1}{EI_i} = \frac{1}{EI_1} + \frac{1}{EI_2} + \frac{1}{EI_3} \tag{3.9}$$

- The horizontal top loading Q on the resultant column is equal to the horizontal loading on the individual columns:

$$Q = Q_1 = Q_2 = Q_3 \tag{3.10}$$

- The vertical top loading P on the resultant column is equal to the vertical loading on the individual column:

$$P = P_1 = P_2 = P_3 \tag{3.11}$$

If the columns are serial connected, then the reciprocal sum of the individual critical loads of these parts gives a lower bound to the overall critical load of a structure:

$$\frac{1}{P_{cr}} \le \sum_{i=1}^{e} \frac{1}{P_{cr;i}} = \frac{1}{P_{cr;1}} + \frac{1}{P_{cr;2}} + \frac{1}{P_{cr;3}} \tag{3.12}$$

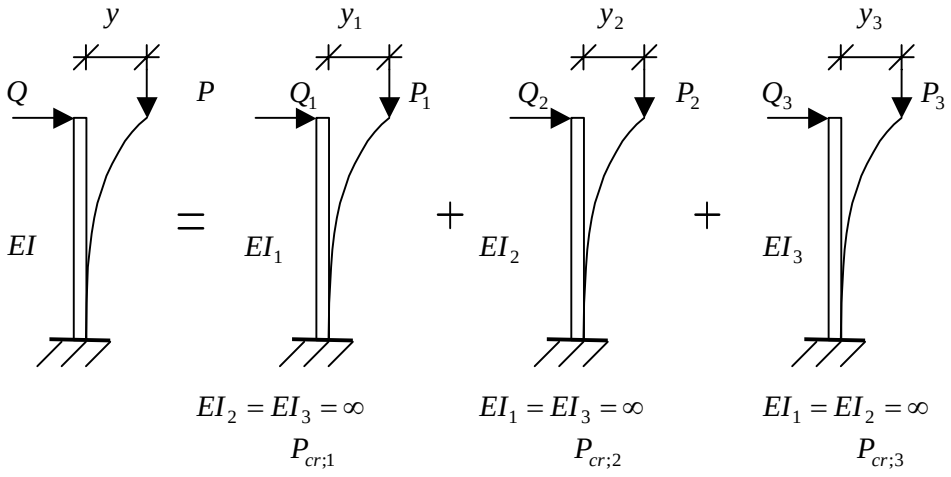

Figure 3.2 Föppl-Papkovics model: serial connection of columns.

4 Stick-spring model

The stick-spring model was introduced by Dicke [1, 2] to obtain an approximate solution for the overall critical load of a flexural cantilever subjected to a vertical top load P (see section 4.1). This model will be further developed for a uniformly distributed vertical load F (see section 4.2) and for a combination of a vertical top load P and uniformly distributed vertical load F (see section 4.3).

4.1 Vertical top load

As has been shown earlier (see section 1.4) a flexural cantilever subjected to a vertical top load P (see fig. 4.1a) can be transformed into a stick-spring model subjected to a vertical top load P and a horizontal load Q (see fig. 4.1b). In this model a flexural cantilever is replaced by a horizontal translation spring k, which takes the individual bending stiffness EI into account. Therefore spring stiffness k is a function of the individual bending stiffness of the flexural cantilever $k = f(EI)$.

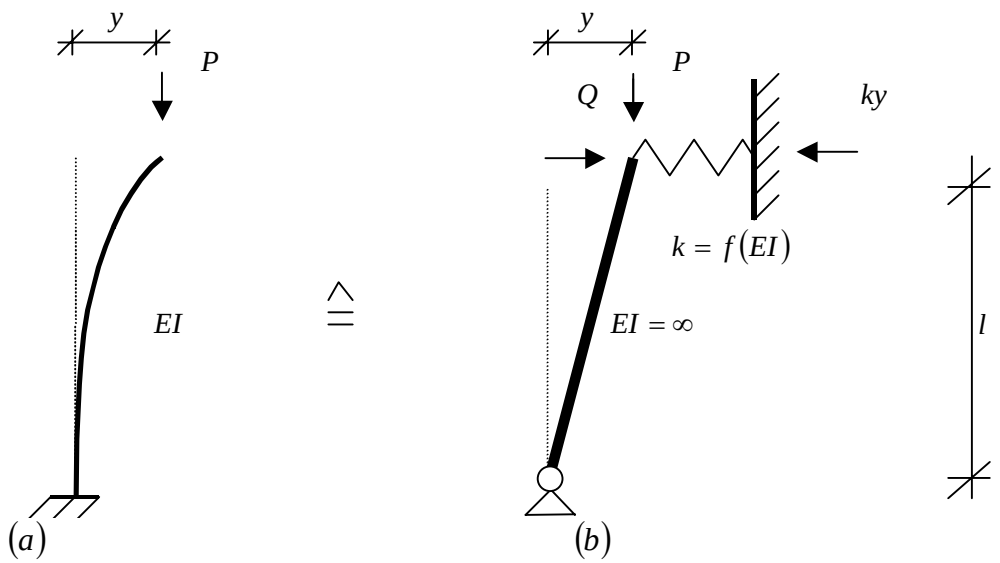

Figure 4.1 Original stick-spring model for loadcase P.

In fig. 4.1b the deformed shape of the stick-spring model is shown, equilibrium is reached when:

$$Ql + Py = kyl \tag{4.1}$$

Eq. (4.1) can be rearranged to find the horizontal displacement y at the top:

$$y = \frac{Ql}{kl - P} \tag{4.2}$$

If the denominater is zero, instability occurs and the critical load is [1, 2]:

$$P_{cr} = kl \tag{4.3}$$

In absence of vertical top load P the first-order deformation at the top is:

$$y_0 = \frac{Q}{k} \tag{4.4}$$

Substituting eq. (4.3) and eq. (4.4) into eq. (4.2) leads to the following expression:

$$y = \frac{kl}{kl - P} y_0 = \frac{P_{cr}}{P_{cr} - P} y_0 = \frac{\frac{P_{cr}}{P}}{\frac{P_{cr}}{P} - 1} y_0 = \frac{n}{n-1} y_0 \tag{4.5}$$

Where the critical load ratio is:

$$n = \frac{P_{cr}}{P} \tag{4.6}$$

The amplification factor $\frac{n}{n-1}$ takes the second-order effects caused by vertical top load P into account. If the critical load ratio is higher then ten the influence of the second order effects can be neglected, because the inluence of the second order effects is less then 10 %.

4.2 Uniformly distributed vertical load

In a similar way a flexural cantilever subjected to a uniformly distributed vertical load f (see fig. 4.2a) can be transformed into a stick-spring model subjected to uniformly distributed vertical load f and a uniformly distributed horizontal load w (see fig. 4.2b).

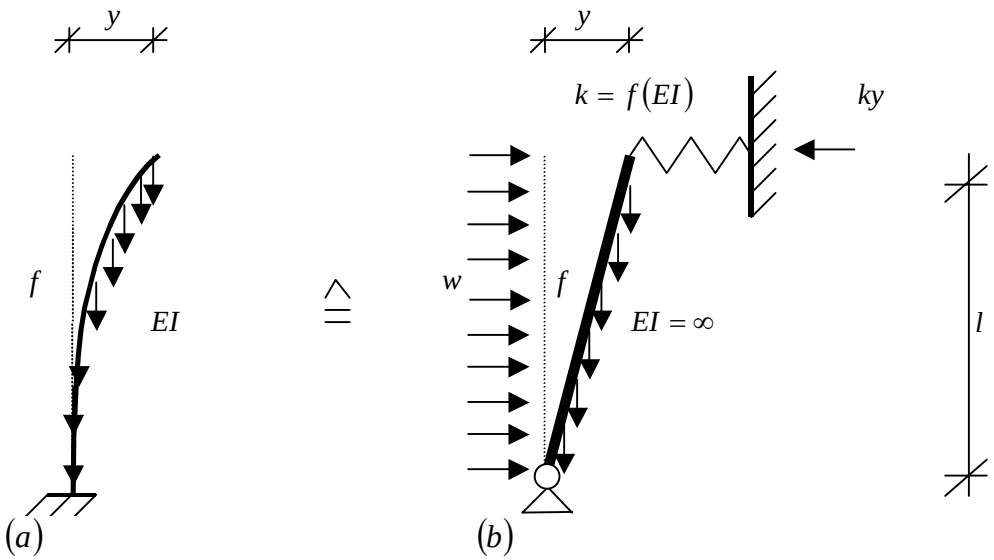

Figure 4.2 Original stick-spring model for loadcase F .

In fig. 4.2b the deformed shape of the stick-spring model is shown, equilibrium is reached when:

$$0.5wl^2 + 0.5fly = kyl \tag{4.7}$$

The vertical load F is:

$$F = fl \tag{4.8}$$

The horizontal load W is:

$$W = wl \tag{4.9}$$

Substituting eq. (4.8) and eq. (4.9) into eq. (4.7) leads to:

$$0.5Wl + 0.5Fy = kyl \tag{4.10}$$

Eq. (4.10) can be rearranged to find the horizontal displacement y at the top:

$$y = \frac{Wl}{2kl - F} \tag{4.11}$$

If the denominater is zero, instability occurs and the critical load is:

$$F_{cr} = 2kl \tag{4.12}$$

In absence of a vertical UDL f the first-order deformation at the top is:

$$y_0 = \frac{wl}{2k} = \frac{W}{2k} \tag{4.13}$$

Substituting eq. (4.12) and eq. (4.13) into eq. (4.11) leads to the following expression:

$$y = \frac{2kl}{2kl - F} y_0 = \frac{F_{cr}}{F_{cr} - F} y_0 = \frac{\frac{F_{cr}}{F}}{\frac{F_{cr}}{F} - 1} y_0 = \frac{n}{n-1} y_0 \tag{4.14}$$

Where the critical load ratio is:

$$n = \frac{F_{cr}}{F} \tag{4.15}$$

The amplification factor $\frac{n}{n-1}$ takes the second-order effects caused by vertical UDL f into account.

4.3 Load combination

In a similar way a flexural cantilever subjected to a combination of a vertical top load P and a uniformly distributed vertical load f (see fig. 4.3a) can be transformed into a stick-spring model subjected to a vertical top load P, a horizontal top load Q, a uniformly distributed vertical load f and a uniformly distributed horizontal load w (see fig. 4.3b).

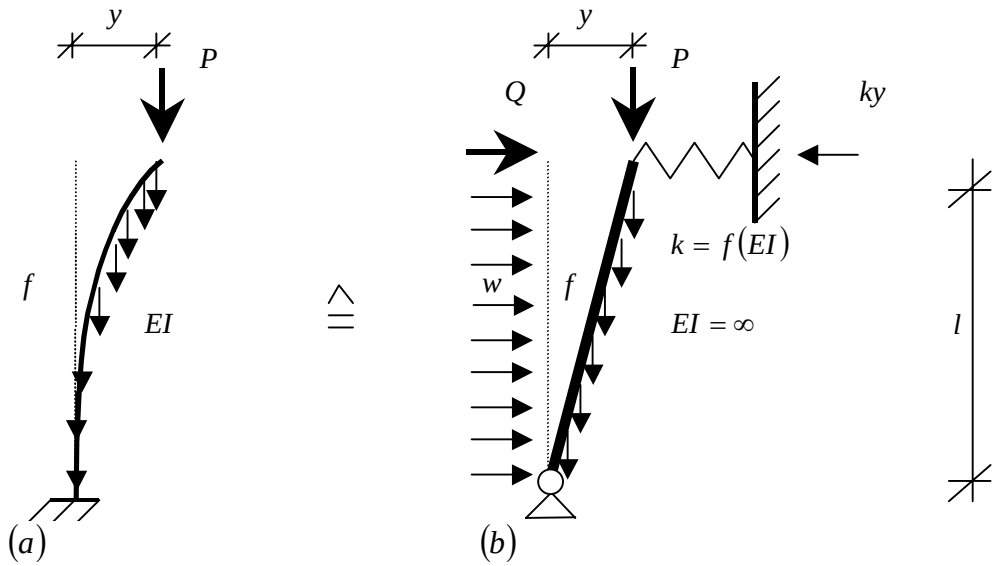

Figure 4.3 Original stick-spring model for loadcase $P + F$.

In fig. 4.3b the deformed shape of the stick-spring model is shown, equilibrium is reached when:

$$Ql + 0.5wl^2 + Py + 0.5fly = kyl \tag{4.16}$$

Substituting eq. (4.8) and eq. (4.9) into eq. (4.16) leads to:

$$Ql + 0.5Wl + Py + 0.5Fy = kyl \tag{4.17}$$

Relations between the vertical loads P and F and relations between the horizontal loads Q and W are needed to solve eq. (4.17). The relation between the vertical top load P and vertical UDL F can be obtained from fig. 4.4. Fig. 4.4a shows a cantilever column, subjected to vertical floor loads F_v and a vertical roof load F_d. The vertical loads can be replaced by a vertical UDL f. This is only correct if the vertical roof load F_d is half of the typical floor loading F_v. If the vertical roof load F_d is larger then half of the floor loading F_v, the vertical loads can be replaced by a combination of a vertical UDL f (see fig. 4.4b) and a vertical top load P (see fig. 4.4c).

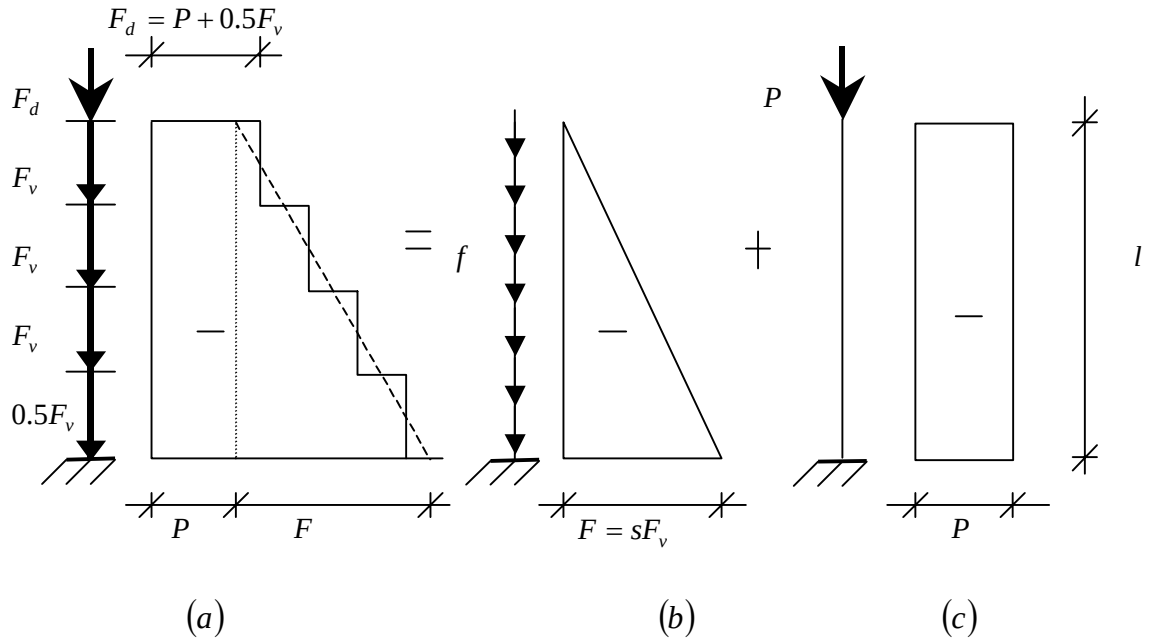

Fig. 4.4 Cantilever subjected to different vertical loadcases.

The vertical roof load is:

$$F_d = \gamma F_v \tag{4.18}$$

Where factor γ takes the effect of a different roof load F_d into account.
The vertical load F is:

$$F = sF_v \tag{4.19}$$

Where s is the number of stories.
The vertical top load P is (see fig. 4.4):

$$P = F_d - 0.5F_v \tag{4.20}$$

The vertical top load P can be rearranged by substituting eq. (4.18) and eq. (4.19) into eq. (4.20):

$$P = F_v(\gamma - 0.5) = \frac{F(\gamma - 0.5)}{s} \tag{4.21}$$

The relation between the horizontal top load Q and horizontal UDL W can be obtained from fig. 4.5 in a similar way as has been done for the relation between vertical top load P and vertical UDL F.

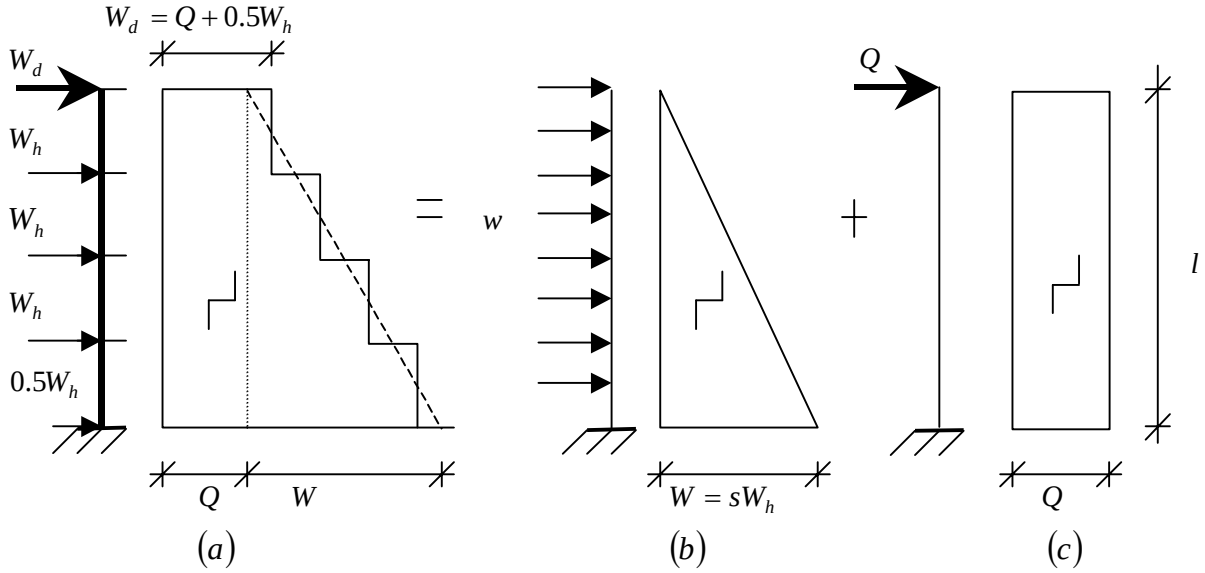

Fig. 4.5 Cantilever subjected to different horizontal loadcases.

The horizontal roof load is:

$$W_d = \gamma W_h \tag{4.22}$$

The horizontal load W is:

$$W = sW_h \tag{4.23}$$

The horizontal top load Q is (see fig. 4.5):

$$Q = W_d - 0.5W_h \tag{4.24}$$

The horizontal top load Q can rearranged by substituting eq. (4.22) and eq. (4.23) into eq. (4.24):

$$Q = W_h(\gamma - 0.5) = \frac{W(\gamma - 0.5)}{s} \tag{4.25}$$

Substituting eq. (4.21) and eq. (4.25) into eq. (4.17) leads to the following expression:

$$\frac{Wl(\gamma - 0.5)}{s} + 0.5Wl + \frac{F(\gamma - 0.5)}{s}y + 0.5Fy = kyl \tag{4.26}$$

Eq. (4.26) can be rearranged to find the horizontal displacement y at the top:

$$y = \frac{Wl}{\frac{2kl}{\left[\frac{2(\gamma - 0.5)}{s} + 1\right]} - F} = \frac{Wl}{\frac{2kl}{\left[\frac{s + 2\gamma - 1}{s}\right]} - F} = \frac{Wl}{2\omega kl - F} \tag{4.27}$$

If the denominater is zero, instability occurs and the critical load is:

$$F'_{cr} = 2\omega kl = \omega F_{cr} \tag{4.28}$$

Where reduction factor ω takes the influence of the vertical top load P into account, which leads to:

$$\omega = \frac{s}{s + 2\gamma - 1} \tag{4.29}$$

If $\gamma = 0.5$, then $\omega = 1$ and $F'_{cr} = F_{cr}$.
In absence of vertical top load P and uniformly distributed vertical load f the first-order deformation at the top is:

$$y_0 = \frac{Q}{k} + \frac{W}{2k} = \frac{W\left[\frac{(2\gamma - 1)}{s} + 1\right]}{2k} = \frac{W\left(\frac{s + 2\gamma - 1}{s}\right)}{2k} = \frac{W}{2\omega k} \tag{4.30}$$

Substituting eq. (4.28) and eq. (4.30) into eq. (4.27) leads to the following expression:

$$y = \frac{2\omega kl}{2\omega kl - F} y_0 = \frac{F'_{cr}}{F'_{cr} - F} y_0 = \frac{\frac{F'_{cr}}{F}}{\frac{F'_{cr}}{F} - 1} y_0 = \frac{n}{n-1} y_0 \tag{4.31}$$

Where the critical load ratio is

$$n = \frac{F'_{cr}}{F} \tag{4.32}$$

The amplification factor $\frac{n}{n-1}$ takes the second-order effects caused by vertical load $P + F$ into account.

5 Flexural cantilever

5.1 Vertical top load

A stick-spring model is used here to obtain an approximate solution for the overall critical load of a flexural cantilever subjected to a vertical top load P (see fig. 5.1a). As earlier has been shown a flexural cantilever subjected to a vertical top load P can be transformed into a stick-spring model subjected to a vertical top load P and a horizontal load Q (see fig. 5.1b).

In this model a flexural cantilever is replaced by a horizontal translation spring k , which takes the individual bending stiffness EI into account. Therefore spring stiffness k is a function of the individual bending stiffness of the flexural cantilever $k = f(EI)$.

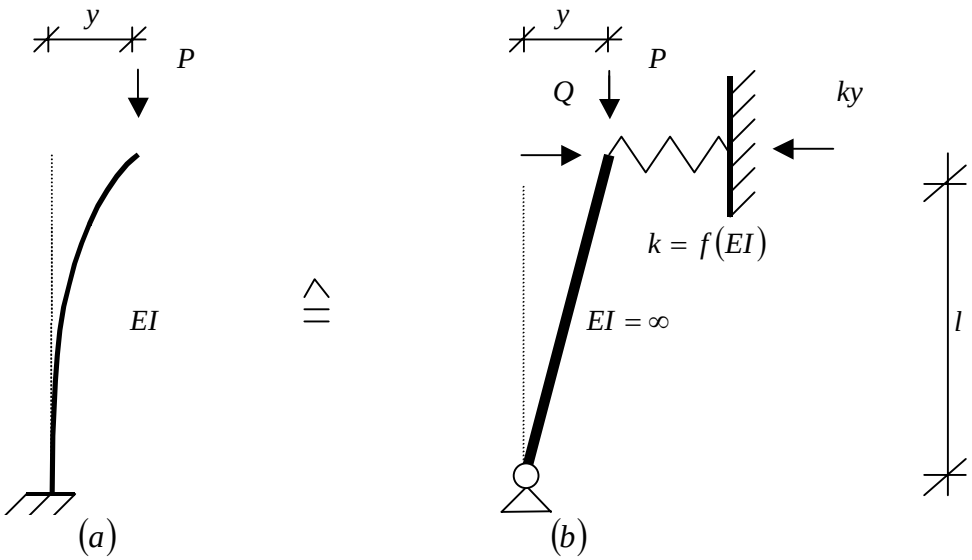

Figure 5.1 Transformation flexural cantilever into a stick-spring model for loadcase P.

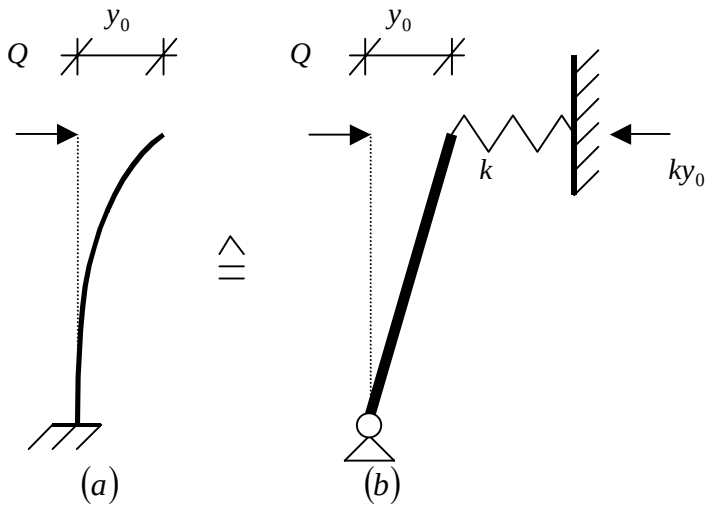

Figure 5.2 First-order deformations flexural cantilever caused by horizontal top load Q.

The behaviour of a flexural cantilever, which is subjected to a horizontal top load Q, consists of one mode of deformation: individual bending deformation y_{EI}.
The first-order deformation at the top of the flexural cantilever is (see fig. 5.2a):

$$y_0 = \frac{Ql^3}{3EI} \tag{5.1}$$

The first-order deformation at the top of the stick-spring model is (see fig. 5.2b):

$$y_0 = \frac{Q}{k} \tag{5.2}$$

Both deformations are the same yielding the horizontal translational spring stiffness k:

$$k = \frac{3EI}{l^3} \tag{5.3}$$

It has also been shown that the critical load of the stick-spring model is (see eq. (4.3)):

$$P_{cr} = kl \tag{5.4}$$

After substituting eq. (5.3) into eq. (5.4) the critical load of the stick-spring model is [1, 2]:

$$P_{cr} = \frac{3EI}{l^2} \tag{5.5}$$

The actual individual bending critical load of a flexural cantilever for loadcase P is [4]:

$$P_{cr} = P_{cr;EI} = \frac{\pi^2 EI}{4l^2} = \frac{2.4674EI}{l^2} \tag{5.6}$$

The individual bending critical load of the stick-spring model (see eq. (5.5)) is about 21.6% larger then the actual individual bending critical load of a flexural cantilever (see eq. (5.6)),
because the individual bending deflection shape of a flexural cantilever is not identical to the individual bending buckling shape of a flexural cantilever. The deflection shape of a flexural cantilever is a third order function and the buckling shape of a flexural cantilever is a cosine function.

5.2 Uniformly distributed vertical load

In a similar way a stick-spring model is used here (see fig. 5.3b) to obtain an approximate solution for the overall critical load of a flexural cantilever subjected to a uniformly distributed vertical load f (see fig. 5.3a).

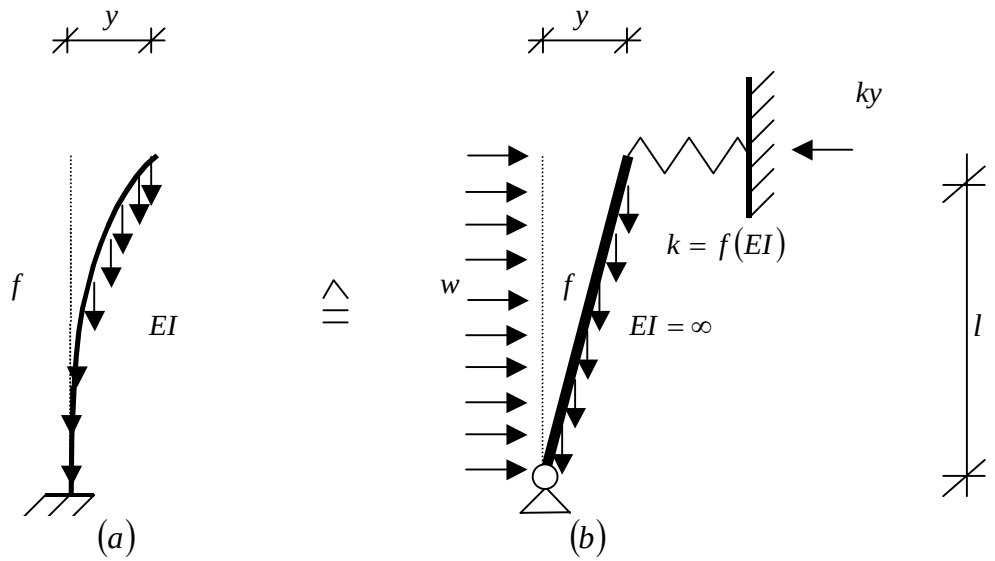

Figure 5.3 Transformation flexural cantilever into a stick-spring model for loadcase F.

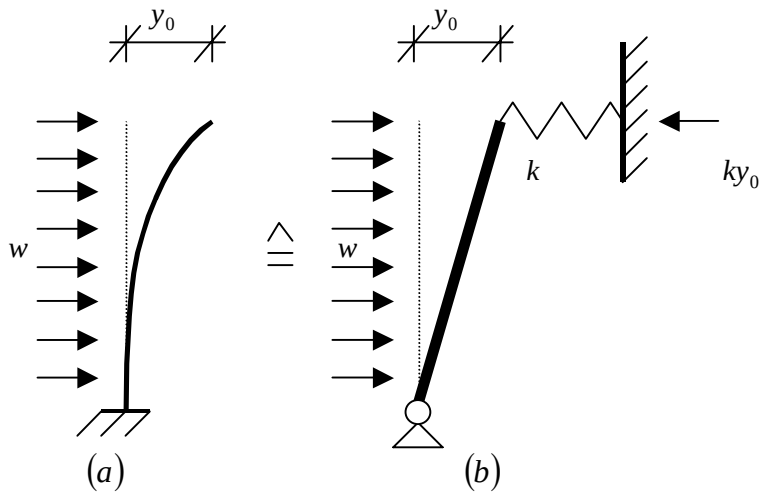

Figure 5.4 Deformations flexural cantilever caused by horizontal UDL w.

The first-order deformation at the top of the flexural cantilever is (see fig. 5.4a):

$$y_0 = \frac{wl^4}{8EI} \tag{5.7}$$

The first-order deformation at the top of the stick-spring model is (see fig. 5.4b):

$$y_0 = \frac{wl}{2k} \tag{5.8}$$

Both deformations are the same yielding the horizontal translational spring stiffness k :

$$k = \frac{4EI}{l^3} \tag{5.9}$$

It has also been shown that the critical load of the stick-spring model is (see eq. (4.12)):

$$F_{cr} = 2kl \tag{5.10}$$

After substituting eq. (5.9) into eq. (5.10) the critical load of the stick-spring model is [1, 2]:

$$F_{cr} = \frac{8EI}{l^2} \tag{5.11}$$

The actual individual bending critical load of a flexural cantilever for loadcase F is [5]:

$$F_{cr} = F_{cr;EI} = \frac{7.837EI}{l^2} \tag{5.12}$$

The individual bending critical load of the stick-spring model (see eq. (5.11)) is about 2.1% larger then the actual individual bending critical load of a flexural cantilever (see eq. (5.12)), because the individual bending deflection shape of a flexural cantilever is not identical to the individual bending buckling shape of a flexural cantilever. The deflection shape of a flexural cantilever is a fourth order function and the buckling shape of a flexural cantilever can be approximated by a cosine function.

5.3 Load combination

In a similar way a stick-spring model is used here (see fig. 5.5b) to obtain an approximate solution for the overall critical load of a flexural cantilever subjected to a vertical top load P and a uniformly distributed vertical load f (see fig. 5.5a).

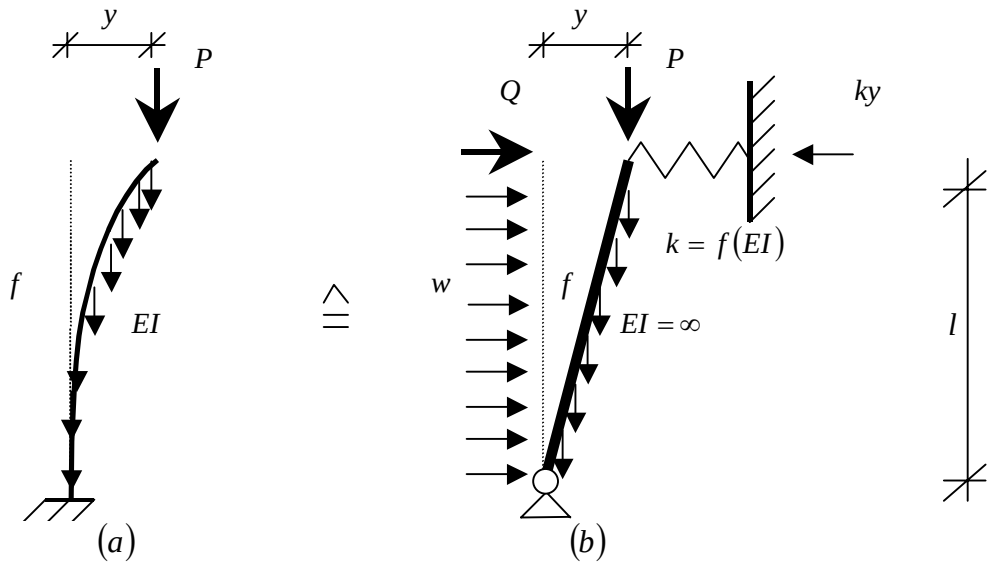

Figure 5.5 Transformation flexural cantilever into stick-spring model (vertical UDL).

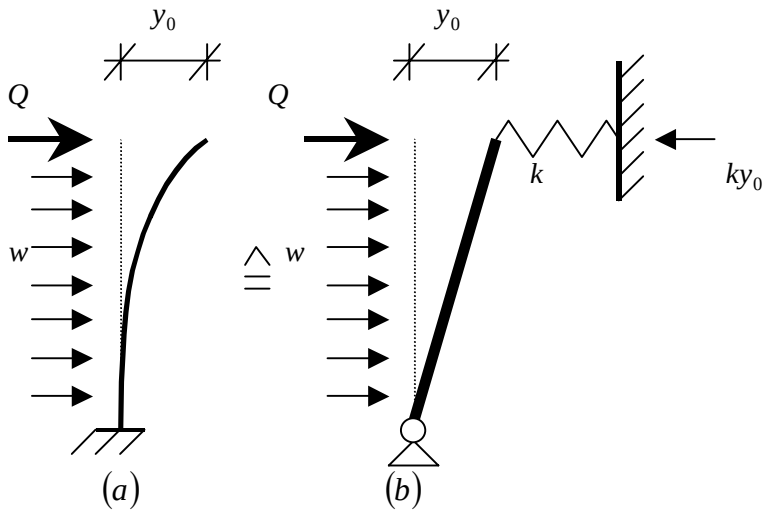

Figure 5.6 Deformations flexural cantilever caused by horizontal top load Q and horizontal UDL w.

The first-order deformation at the top of the flexural cantilever is (see fig. 5.6a):

$$y_0 = \frac{Ql^3}{3EI} + \frac{wl^4}{8EI} \tag{5.13}$$

By substituting eq. (4.9) and eq. (4.25) into eq. (5.13) the first-order deformation at the top of the flexural cantilever can be rearranged into:

$$y_0 = \frac{Wl^3}{3EI}\left(\frac{\gamma - 0.5}{s}\right) + \frac{Wl^3}{8EI} \tag{5.14}$$

It has also been shown that the first-order deformation at the top of the stick-spring model is (see eq. (4.30) and fig. 5.16b)):

$$y_0 = \frac{W}{2\omega k} \tag{5.15}$$

Both deformations are the same yielding:

$$\frac{1}{2\omega k} = \frac{l^3}{3EI}\left(\frac{\gamma - 0.5}{s}\right) + \frac{l^3}{8EI} \tag{5.16}$$

It has been shown that the critical load of the stick-spring model is (see eq. (4.28)):

$$F'_{cr} = 2\omega k l \tag{5.17}$$

After substituting eq. (5.16) into eq. (5.17) the critical load of the stick-spring model is:

$$\frac{1}{F'_{cr}} = \frac{1}{2\omega k l} = \frac{l^2}{3EI}\left(\frac{\gamma - 0.5}{s}\right) + \frac{l^2}{8EI} \tag{5.18}$$

In general, the critical load in eq. (5.18) can be written as:

$$\frac{1}{F'_{cr}} = \frac{1}{P_{cr;EI}}\left(\frac{\gamma - 0.5}{s}\right) + \frac{1}{F_{cr;EI}} \tag{5.19}$$

Where the critical loads obtained from the stick-spring model are for :

- Individual bending for loadcase P [1, 2]:

$$P_{cr;EI} = \frac{3EI}{l^2} \tag{5.20}$$

- Individual bending for loadcase F [1, 2]:

$$F_{cr;EI} = \frac{8EI}{l^2} \tag{5.21}$$

But the actual critical loads are for:

- Individual bending for loadcase P [4]:

$$P_{cr;EI} = \frac{\pi^2 EI}{4l^2} \tag{5.22}$$

- Individual bending for loadcase F [5]:

$$F_{cr;EI} = \frac{7.837EI}{l^2} \tag{5.23}$$

Eq. (5.18) gives an overestimated individual bending critical load, because the individual bending critical loads (see eq. (5.20) and eq. (5.21)) are overestimated in the stick-spring-model.
If the actual values for individual bending (see eq. (5.22) and eq. (5.23)) are substituted in eq. (5.19) the critical load can be rearranged into:

$$\frac{1}{F'_{cr}} = \frac{4l^2}{\pi^2 EI}\left(\frac{\gamma - 0.5}{s}\right) + \frac{l^2}{7.837EI} \tag{5.24}$$

The ratio for the individual bending critical loads is:

$$\frac{F_{cr;EI}}{P_{cr;EI}} = \frac{7.837EI}{l^2}\frac{4l^2}{\pi^2 EI} = 3.176 \tag{5.25}$$

By substituting eq. (5.25) into eq. (5.24) the critical load can be rearranged into:

$$\frac{1}{F'_{cr}} = \frac{1}{F_{cr;EI}}\left[3.176\left(\frac{\gamma - 0.5}{s}\right) + 1\right] = \frac{1}{\alpha F_{cr;EI}} = \frac{1}{F'_{cr;EI}} \tag{5.26}$$

The actual individual bending critical load for a flexural cantilever for loadcase $P + F$ is [17]:

$$F'_{cr} = F'_{cr;EI} = \alpha F_{cr;EI} = \frac{7.837\alpha EI}{l^2} \tag{5.27}$$

Where:
α is a reduction factor for the bending critical load, which takes the influence of the vertical top load P into account and can be given by:

$$\alpha = \frac{1}{3.176\left(\frac{\gamma - 0.5}{s}\right) + 1} = \frac{1}{\frac{3.176(\gamma - 0.5) + s}{s}} = \frac{s}{s + 3.176(\gamma - 0.5)} \tag{5.28}$$

Eq. (5.27) gives a conservative critical load, because the individual bending buckling shape for loadcase P (see fig. 5.1a) is not identical to the individual bending buckling shape for loadcase F (see fig. 5.3a).

6 One bay braced frames

6.1 Braced frames with non-continous columns

A braced frame with non-continous columns is a structure consisting of columns, beams and diagonals, which are pin-connected to each other (see fig. 6.1).
The columns of the frame are non-continous and pin-connected to the base.

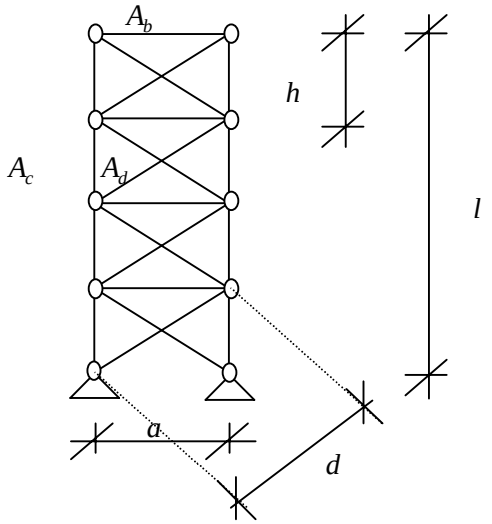

Figure 6.1 Braced frames pin-connected to base.

The buckling behaviour of a braced frame with non-continous columns pin-connected to the base can be divided into 2 modes of deformation:

- Global bending (EAc^2): axial deformation in the columns (shortening at one side and lengthening at the other side) (see fig. 6.2a).
- Racking shear (GA): axial strains in the diagonals (see fig. 6.2b).

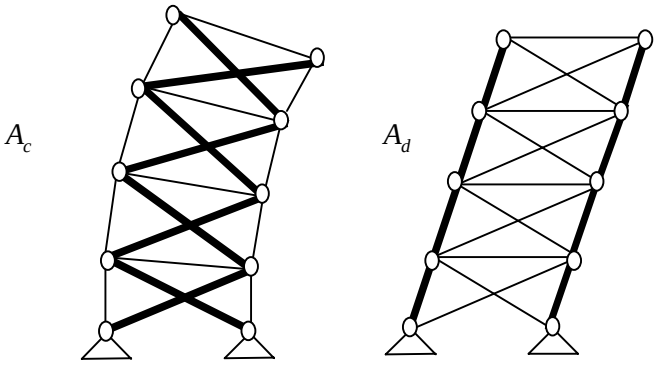

Fig 6.2 Modes of deformation of a braced frame with non-continious columns.

Assumptions:

- The columns, beams and diagonals are hinged connected to each other.
- The braced frame is pin-connected to the base.
- The columns are non-continous and therefore the individual bending stiffness is zero $EI = 0$.

- The braced frame has two lateral stiffness parameters $EAc^2 = f(A_c)$ and $GA = f(A_b, A_d)$.
- There is no connection between the diagonals.

6.1.1 Vertical top loads

A stick-spring model is introduced here to obtain an approximate solution for the overall critical load of a one-bay braced frame with non-continous columns (see fig. 6.3a). The braced frame is subjected to vertical top loads and can be transformed into a shear-flexure cantilever with global bending stiffness $EAc^2 = f(A_c)$ and racking shear stiffness $GA = f(A_b, A_d)$ (see fig. 6.3b).
This shear-flexure cantilever can be transformed into a stick-spring model (see fig. 6.3c).
In this model a shear-flexure cantilever is replaced by a horizontal translation spring k, which takes the global bending stiffness EAc^2 and the racking shear stiffness GA of the shear-flexure cantilever into account. Therefore spring stiffness k is a function of the global bending stiffness EAc^2 and of the racking shear stiffness GA of the shear-flexure cantilever $k = f(EAc^2, GA)$.

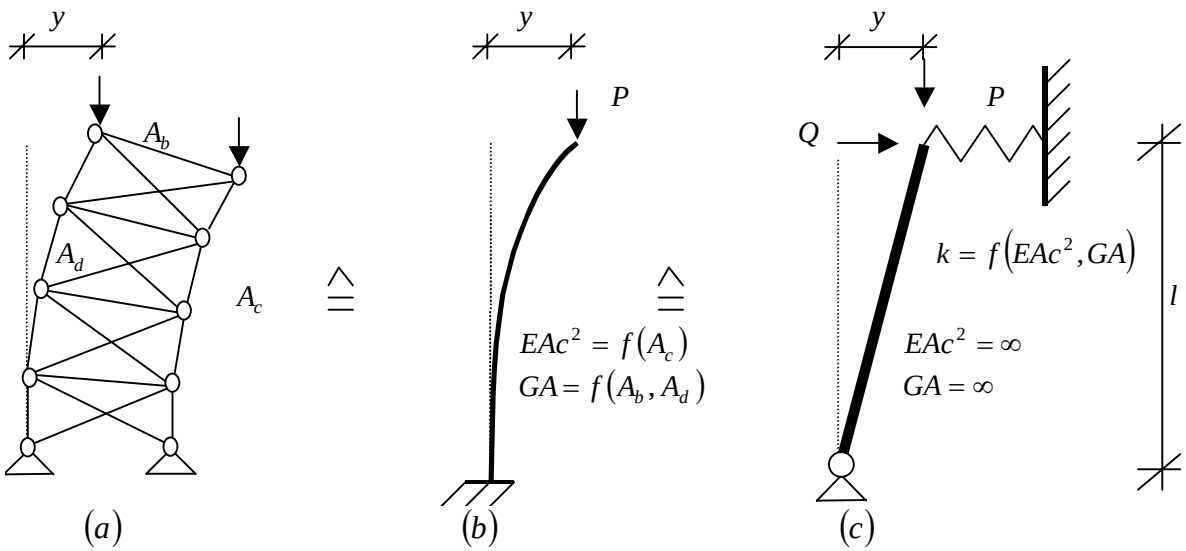

Figure 6.3 Transformation braced frame into stick-spring model (vertical top loads).

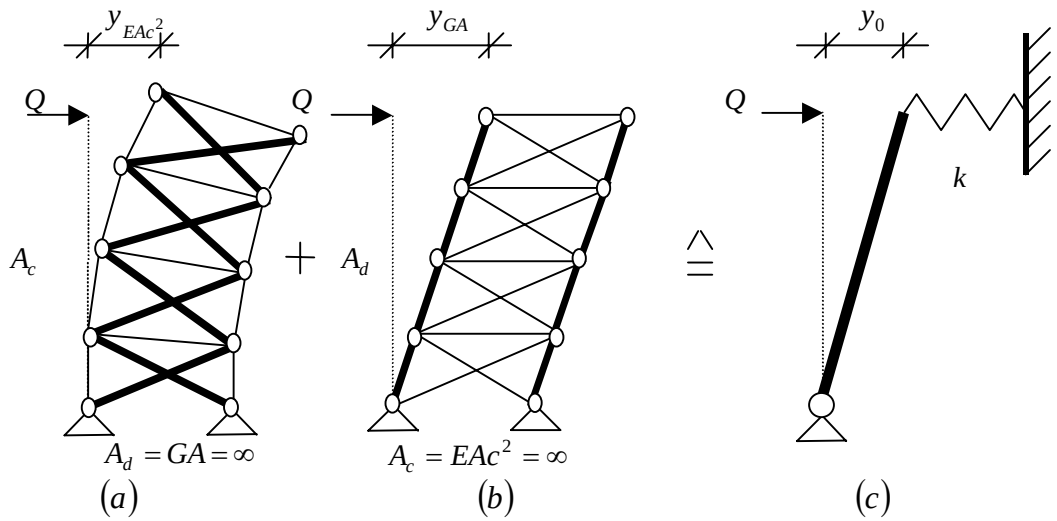

Figure 6.4 Deformations braced frame caused by horizontal load Q.

The first-order deformation at the top of the braced frame is (see fig. 6.4a/b):

$$y_0 = y_{EAc^2} + y_{GA} = \frac{Ql^3}{3EAc^2} + \frac{Ql}{GA} \tag{6.1}$$

The first-order deformation at the top of the stick-spring model is (see fig. 6.4c):

$$y_0 = \frac{Q}{k} \tag{6.2}$$

Both deformations are the same yielding the horizontal translational spring stiffness k:

$$\frac{1}{k} = \frac{l^3}{3EAc^2} + \frac{l}{GA} \tag{6.3}$$

It has been shown that the critical load of the stick-spring model is (see eq. (4.3)):

$$P_{cr} = kl \tag{6.4}$$

After substituting eq. (6.3) into eq. (6.4) the critical load of the stick-spring model is:

$$\frac{1}{P_{cr}} = \frac{1}{kl} = \frac{l^2}{3EAc^2} + \frac{1}{GA} \tag{6.5}$$

In general, the critical load of eq. (6.5) can written as:

$$\frac{1}{P_{cr}} = \frac{1}{P_{cr;EAc^2}} + \frac{1}{P_{cr;GA}} \tag{6.6}$$

Where the critical loads obtained from the stick-spring model are for:

- Global bending [1, 2]:

$$P_{cr;EAc^2} = \frac{3EAc^2}{l^2} \tag{6.7}$$

- Racking shear [5]:

$$P_{cr;GA} = GA \tag{6.8}$$

But the actual critical loads are for:

- Global bending [4]:

$$P_{cr;EAc^2} = \frac{\pi^2 EAc^2}{4l^2} \tag{6.9}$$

- Racking shear [5]:

$$P_{cr;GA} = GA \tag{6.10}$$

The global bending critical load of the stick-spring model (see eq. (6.7)) is about 21.6% larger then the actual global bending critical load of a braced frame (see eq. (6.9)), because the global bending deflection shape of a braced frame is not identical to the global bending buckling shape of a braced frame. The deflection shape of a braced frame is a third order function and the buckling shape of a braced frame is a cosine function.

The racking shear critical load of the stick-spring model (see eq. (6.8)) is equal to the actual racking shear critical load of a braced frame (see eq. (6.10)), because the racking shear deflection shape of a braced frame (see fig. 6.5a) is identical to the racking shear buckling shape of a braced frame (see fig. 6.5b). The racking shear buckling shape of a braced has not a definite buckling shape, which means the racking shear buckling shape can assume any form even the form of the racking shear deflection shape. Therefore different racking shear buckling shapes have one eigenvalue and one critical load. If a braced frame has eight storeys, eight different racking shear buckling shapes have one eigenvalue and one critical load.

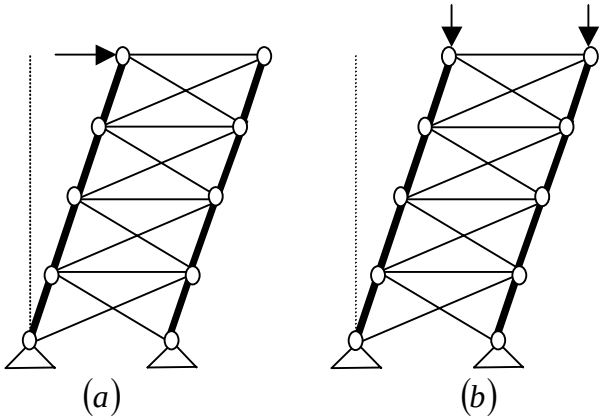

Figure 6.5 Racking shear shapes of braced frames caused by top loads.

If the actual values for global bending (see eq. (6.9)) and racking shear (see eq. (6.10)) are substituted into eq. (6.6) the critical load of a braced frame becomes:

$$\frac{1}{P_{cr}} = \frac{4l^2}{\pi^2 EAc^2} + \frac{1}{GA} \tag{6.11}$$

Eq. (6.5) gives in most cases an overestimated critical load, because the global bending critical load (see eq. (6.7)) is overestimated by 21.6% in the stick-spring model. If the actual values for global bending (see eq. (6.9)) and racking shear (see eq. (6.10)) are substituted into eq. (6.6) the critical load is now conservative (see eq. (6.11)), because the global bending buckling shape (see fig. 6.6a) is not identical to the racking shear buckling shape (see fig. 6.6b).

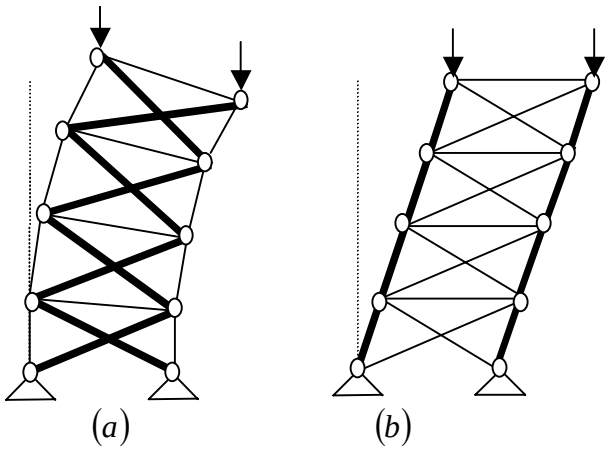

Figure 6.6 Buckling shapes for loadcase P .

6.1.2 Uniformly distributed vertical loads

In fig. 6.7a a braced frame with non-continous columns is subjected to vertical point loads F_v accept for the point loads at the roof and at the bottom of the frame which are $0.5F_v$.
In a similar way the stick-spring model can be used here to obtain an approximate solution for the overall critical load of a braced frame. First a braced frame subjected to vertical point loads is transformed into a shear-flexure cantilever subjected to a vertical UDL f (see fig. 6.7b), which then can be transformed into a stick-spring model (see fig. 6.7c).

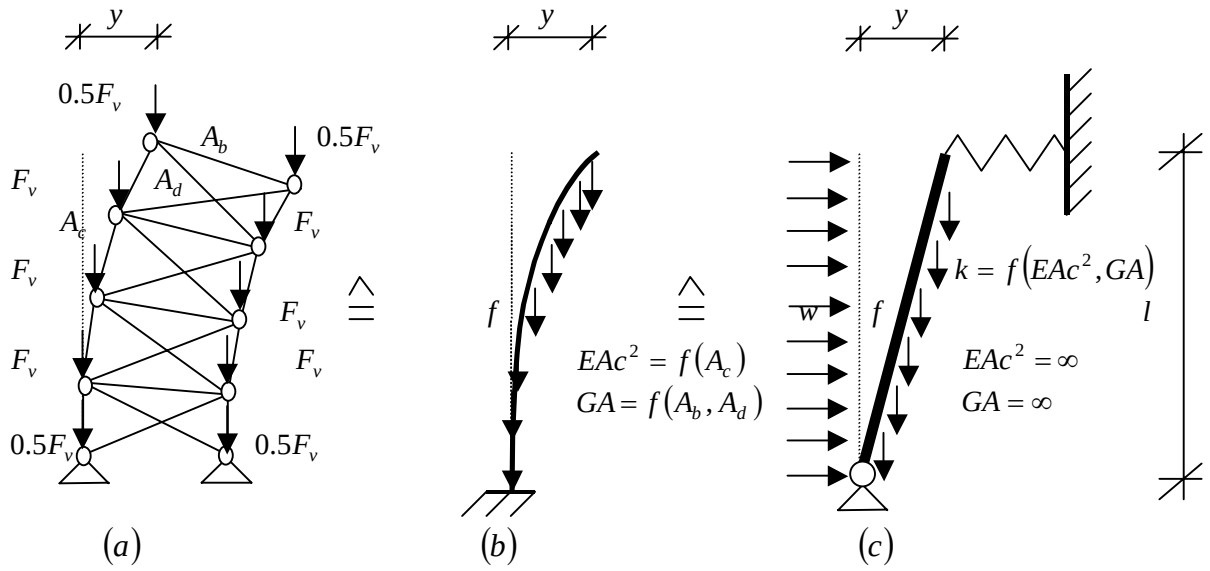

Figure 6.7 Transformation braced frame into stick-spring model (uniformly distributed vertical loads).

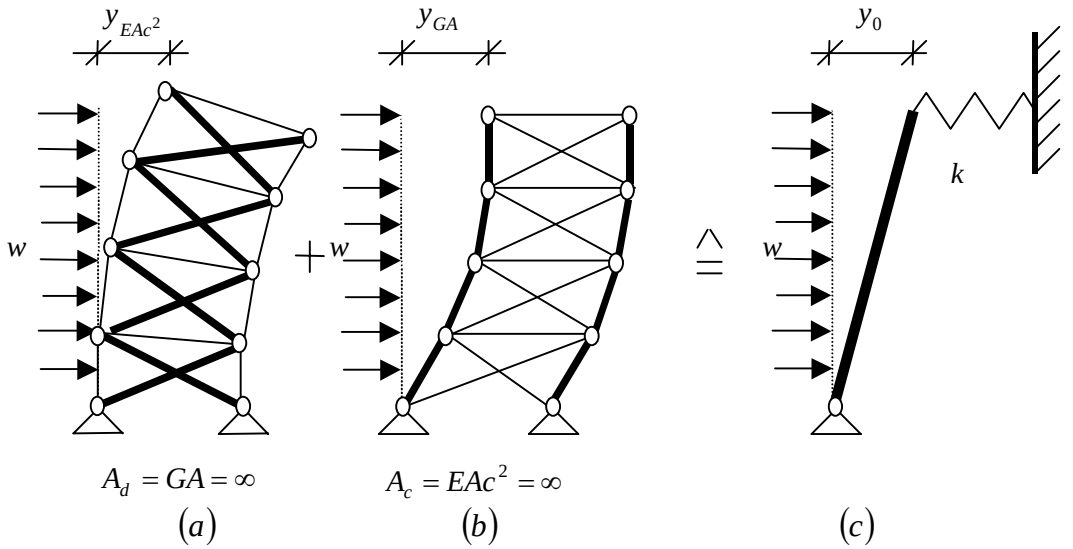

Figure 6.8 Deformations X-braced frame caused by horizontal UDL w.

The first-order deformation at the top of the braced frame is (see fig. 6.8a/b):

$$y_0 = y_{EAc^2} + y_{GA} = \frac{wl^4}{8EAc^2} + \frac{wl^2}{2GA} \tag{6.12}$$

The first-order deformation at the top of the stick-spring model is (see fig. 6.8c):

$$y_0 = \frac{wl}{2k} \tag{6.13}$$

Both deformations are the same yielding the horizontal translational spring stiffness k:

$$\frac{1}{k} = \frac{l^3}{4EAc^2} + \frac{l}{GA} \tag{6.14}$$

It has been shown that the critical load of the stick-spring model is (see eq. (4.12)):

$$F_{cr} = 2kl \tag{6.15}$$

After substituting eq. (6.14) into eq. (6.15) the critical load of the stick-spring model is:

$$\frac{1}{F_{cr}} = \frac{1}{2kl} = \frac{l^2}{8EAc^2} + \frac{1}{2GA} \tag{6.16}$$

In general, the critical load of eq. (6.16) can be written as:

$$\frac{1}{F_{cr}} = \frac{1}{F_{cr;EAc^2}} + \frac{1}{F_{cr;GA}} \tag{6.17}$$

Where the critical loads obtained from the stick-spring model are for:

- Global bending [1, 2]:

$$F_{cr;EAc^2} = \frac{8EAc^2}{l^2} \tag{6.18}$$

- Racking shear [18-21]:

$$F_{cr;GA} = 2GA \tag{6.19}$$

But the actual critical loads are for:

- Global bending [5]:

$$F_{cr;EAc^2} = \frac{7.837EAc^2}{l^2} \tag{6.20}$$

- Racking shear (see eq. (6.28)):

$$F_{cr;GA} = \eta GA \tag{6.21}$$

Where η is a factor which takes the effect of the different normal forces $N_{cantilever}$ and N_{frame} into account for loadcase F:

$$\eta = \frac{s}{s - 0.5} \tag{6.22}$$

The global bending critical load of the stick-spring model (see eq. (6.18)) is about 2.1% larger then the actual global bending critical load of a braced frame (see eq. (6.20)), because the global bending deflection shape of a braced frame is not identical to the global bending buckling shape of a braced frame. The deflection shape of the braced frame is a fourth order function and the buckling shape of the braced frame can be approximated by a cosine function.

The racking shear critical load of the stick-spring model (see eq. (6.19)) is about 100% larger then the actual racking shear critical load of eq. (6.21), because the racking shear deflection shape of a braced frame (see fig. 6.9a) is not identical to the racking shear buckling shape of a braced frame (see fig. 6.9b). The racking shear buckling shape of a braced has a definite buckling shape, which means the racking shear buckling shape can assume only one form.
Therefore the racking shear buckling shape has one eigenvalue and one critical load.

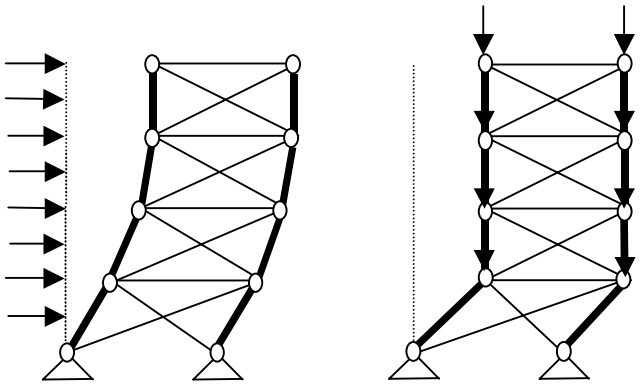

Figure 6.9 Racking shear shapes braced frame caused by UDL.

If the actual values for global bending (see eq. (6.20)) and racking shear (see eq. (6.21)) are substituted into eq. (6.17) the critical load of a braced frame becomes:

$$\frac{1}{F_{cr}} = \frac{l^2}{7.837EAc^2} + \frac{1}{\eta GA} \tag{6.23}$$

Eq. (6.16) gives in most cases an overestimated critical load, because the global bending critical load (see eq. (6.18)) is overestimated by 2.1% and the racking shear critical load (see eq. (6.19)) is overestimated by nearly 100 % in the stick-spring model. If the actual values for global bending (see eq. (6.20)) and racking shear (see eq. (6.21)) are substituted into eq. (6.17) the critical load is now conservative (see eq. (6.23)), because the global bending buckling shape (see fig. 6.10a) is not identical to the racking shear buckling shape (see fig. 6.10b).

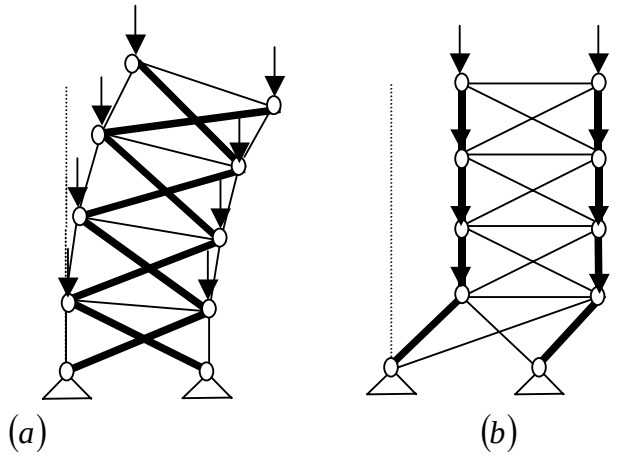

Figure 6.10 Buckling shapes for loadcase F *with* $F_{cr;GA} = \eta GA$.

Now the derivation of the actual racking shear critical load of a braced frame will be given (see eq. (6.21)). A lower bound for the racking shear critical load of a braced frame subjected to floor loads F_v can be found by assuming a shear cantilever subjected to UDL f, which gives:

$$F_{cr;GA;cantilever} = GA \tag{6.24}$$

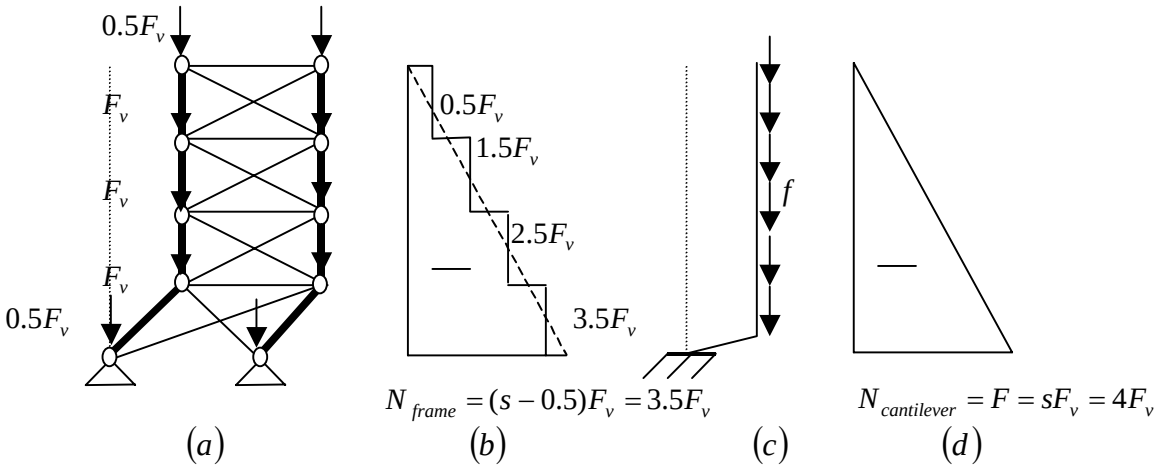

Figure 6.11 Influence of normal force on the racking shear critical load $F_{cr;GA}$.

From the racking shear buckling shape of a braced frame it can be seen that the first-storey sways and the other storeys remain vertical (see fig. 6.11a). The normal force N_{frame} in a braced frame at the first storey is (see fig. 6.11b):

$$N_{frame} = (s - 0.5)F_v \tag{6.25}$$

From the racking shear buckling shape of a shear cantilever it can be seen that a cantilever sways at the bottom and the rest remains vertical (see fig. 6.11c). The normal force $N_{cantilever}$ in a cantilever at the bottom is: (see fig. 6.11d):

$$N_{cantilever} = F = sF_v \tag{6.26}$$

At buckling the normal force in the shear cantilever is half a floor load larger ($0.5F_v$) then the normal force in a braced frame. Therefore the racking shear critical load of a shear cantilever is lower then the racking shear critical load of a braced frame and eq. (6.24) has to be rearranged, to take the effect of the larger normal force into consideration, which leads to the actual racking shear critical load of a braced frame:

$$F_{cr;GA} = \frac{N_{cantilever}}{N_{frame}} GA \tag{6.27}$$

Substituting eq. (6.25) and eq. (6.26) into eq. (6.27) leads to the actual racking shear critical load of a braced frame subjected to floor loads F_v:

$$F_{cr;GA} = \eta GA \tag{6.28}$$

Formula (6.28) gives a mathematically exact racking shear critical load, because the racking shear buckling shape of a braced frame (see fig. 6.11a) is identical to the racking shear buckling shape of a shear cantilever (see fig. 6.11c) if factor η is taken into account.

6.1.3 Load combinations

In fig. 6.12a a braced frame with non-continous columns is subjected to vertical point loads F_v accept for the point load at the roof, which is F_d and the load at the bottom, which is $0.5F_v$.
In a similar way the stick-spring model can be used here to obtain an approximate solution for the overall critical load of a braced frame. First a braced frame subjected to vertical point loads is transformed into a shear-flexure cantilever subjected to a vertical top load P and a vertical UDL f (see fig. 6.12b), which then can be transformed into a stick-spring model (see fig. 6.12c).

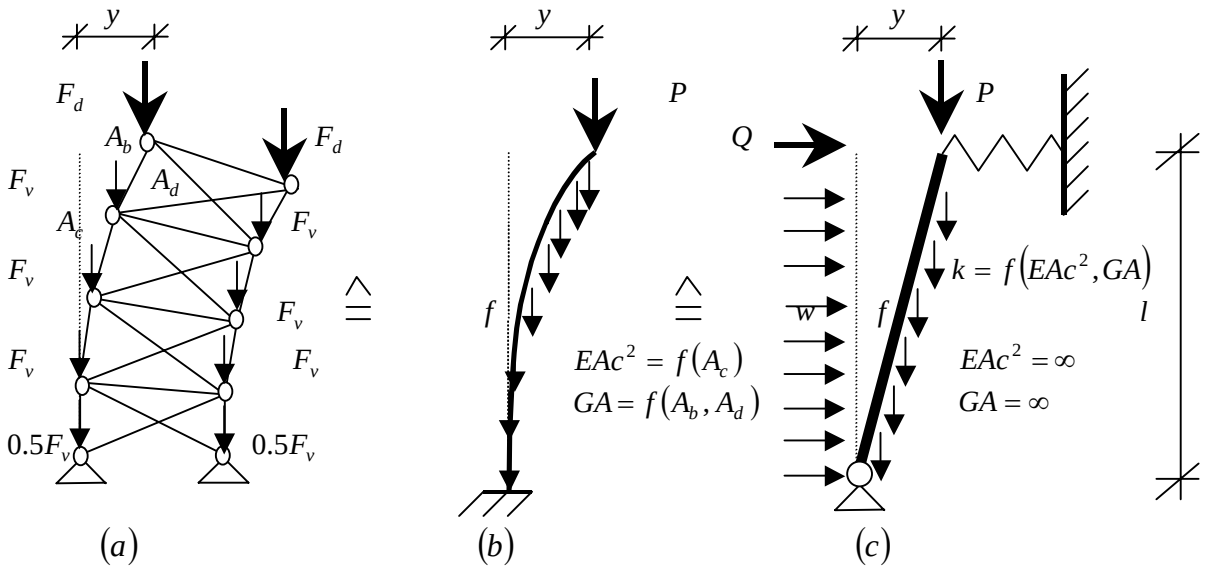

Figure 6.12 Transformation braced frame into stick-spring model (load combination).

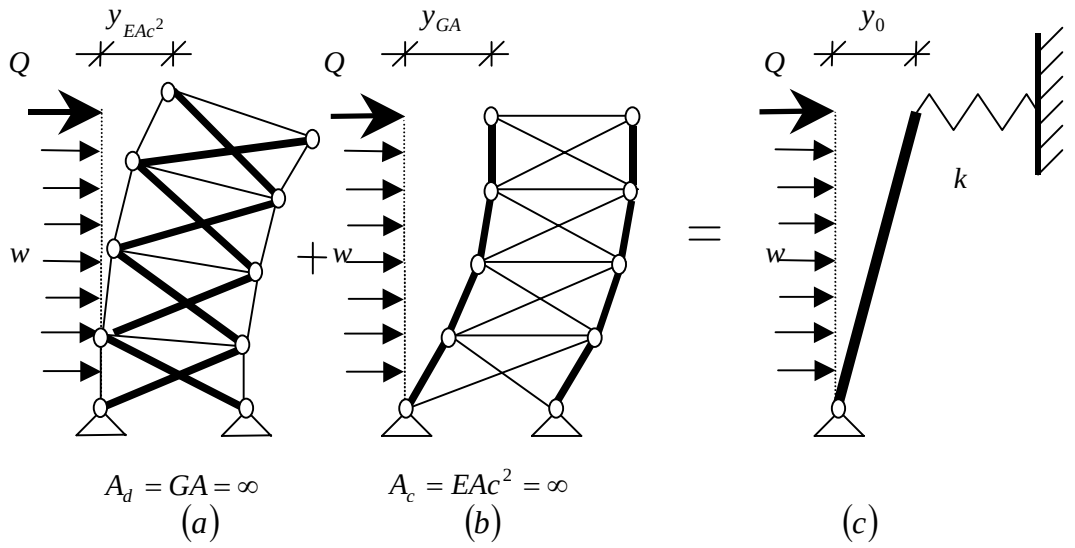

Figure 6.13 Deformations X-braced frame caused by load combination.

The first-order deformation at the top of the braced frame is (see fig. 6.13a/b):

$$y_0 = y_{EAc^2} + y_{GA} = \frac{Ql^3}{3EAc^2} + \frac{wl^4}{8EAc^2} + \frac{Ql}{GA} + \frac{wl^2}{2GA} \tag{6.29}$$

By substituting eq. (4.9) and eq. (4.25) into eq. (6.29) the first-order deformation at the top of the braced frame can be rearranged into:

$$y_0 = \frac{Wl^3}{3EAc^2}\left(\frac{\gamma - 0.5}{s}\right) + \frac{Wl^3}{8EAc^2} + \frac{Wl}{GA}\left(\frac{\gamma - 0.5}{s}\right) + \frac{Wl}{2GA} \tag{6.30}$$

It has been shown that the first-order deformation at the top of the stick-spring model is (see eq. (4.30) and fig. 6.13c):

$$y_0 = \frac{W}{2\omega k} \tag{6.31}$$

Both deformations are the same yielding k:

$$\frac{1}{2\omega k} = \frac{l^3}{3EAc^2}\left(\frac{\gamma - 0.5}{s}\right) + \frac{l^3}{8EAc^2} + \frac{l}{GA}\left(\frac{\gamma - 0.5}{s}\right) + \frac{l}{2GA} \tag{6.32}$$

It has been shown that the critical load of the stick-spring model is (see eq. (4.28)):

$$F'_{cr} = 2\omega kl \tag{6.33}$$

After substituting eq. (6.32) into eq. (6.33) the critical load of the stick-spring model is:

$$\frac{1}{F'_{cr}} = \frac{1}{2\omega kl} = \frac{l^2}{3EAc^2}\left(\frac{\gamma - 0.5}{s}\right) + \frac{l^2}{8EAc^2} + \frac{1}{GA}\left(\frac{\gamma - 0.5}{s}\right) + \frac{1}{2GA} \tag{6.34}$$

In general, the critical load in eq. (6.34) can be written as:

$$\frac{1}{F'_{cr}} = \frac{1}{P_{cr;EAc^2}}\left(\frac{\gamma - 0.5}{s}\right) + \frac{1}{F_{cr;EAc^2}} + \frac{1}{P_{cr;GA}}\left(\frac{\gamma - 0.5}{s}\right) + \frac{1}{F_{cr;GA}} \tag{6.35}$$

Where the critical loads obtained from the stick-spring model are for:

- Global bending for loadcase P [1, 2]:

$$P_{cr;EAc^2} = \frac{3EAc^2}{l^2} \tag{6.36}$$

- Global bending for loadcase F [1, 2]:

$$F_{cr;EAc^2} = \frac{8EAc^2}{l^2} \tag{6.37}$$

- Racking shear for loadcase P [5]:

$$P_{cr;GA} = GA \tag{6.38}$$

- Racking shear for loadcase F [18-21]:

$$F_{cr;GA} = 2GA \tag{6.39}$$

But the actual critical loads are for:

- Global bending for loadcase P [4]:

$$P_{cr;EAc^2} = \frac{\pi^2 EAc^2}{4l^2} \tag{6.40}$$

- Global bending for loadcase F [5]:

$$F_{cr;EAc^2} = \frac{7.837 EAc^2}{l^2} \tag{6.41}$$

- Racking shear for loadcase P [5]:

$$P_{cr;GA} = GA \tag{6.42}$$

- Racking shear of a shear cantilever for loadcase F [22]:

$$F_{cr;GA;cantilever} = GA \tag{6.43}$$

Eq. (6.34) gives an overestimated critical load, because the global bending critical loads (see eq. (6.36) and eq. (6.37)) and the racking shear critical load (see eq. (6.39)) are overestimated in the stick-spring-model. If the actual values for global bending (see eq. (6.40) and eq. (6.41)) and racking shear (see eq. (6.42) and eq. (6.43)) are substituted into eq. (6.35) the critical load is:

$$\frac{1}{F'_{cr}} = \frac{4l^2}{\pi^2 EAc^2}\left(\frac{\gamma - 0.5}{s}\right) + \frac{l^2}{7.837 EAc^2} + \frac{1}{GA}\left(\frac{\gamma - 0.5}{s}\right) + \frac{1}{GA} \tag{6.44}$$

The ratio for the global bending critical loads is:

$$\frac{F_{cr;EAc^2}}{P_{cr;EAc^2}} = \frac{7.837 EAc^2}{l^2}\frac{4l^2}{\pi^2 EAc^2} = 3.176 \tag{6.45}$$

The ratio for the racking shear critical loads is:

$$\frac{F_{cr;GA}}{P_{cr;GA}} = \frac{GA}{GA} = 1 \tag{6.46}$$

By substituting eq. (6.45) and eq. (6.46) into eq. (6.44) the critical load is:

$$\frac{1}{F'_{cr}} = \frac{1}{F_{cr;EAc^2}}\left[3.176\left(\frac{\gamma - 0.5}{s}\right) + 1\right] + \frac{1}{F_{cr;GA}}\left[\left(\frac{\gamma - 0.5}{s}\right) + 1\right] = \frac{1}{\alpha F_{cr;EAc^2}} + \frac{1}{\beta F_{cr;GA}} \tag{6.47}$$

In general, the critical load of eq. (6.47) can be written as:

$$\frac{1}{F'_{cr}} = \frac{1}{F'_{cr;EAc^2}} + \frac{1}{F'_{cr;GA}} \tag{6.48}$$

Where the critical loads are for:

- Global bending [17]:

$$F'_{cr;EAc^2} = \alpha F_{cr;EAc^2} = \frac{7.837\alpha EAc^2}{l^2} \tag{6.49}$$

, where α is a reduction factor for the bending critical load, which takes the influence of the vertical top load P into account is:

$$\alpha = \frac{s}{s + 3.176(\gamma - 0.5)} \tag{6.50}$$

- Racking shear of a shear cantilever:

$$F'_{cr;GA;cantilever} = \beta GA \tag{6.51}$$

, where β is a reduction factor for the racking shear critical load, which takes the influence of the vertical top load P into account is:

$$\beta = \frac{1}{\left(\frac{\gamma - 0.5}{s}\right) + 1} = \frac{1}{\frac{(\gamma - 0.5) + s}{s}} = \frac{s}{s + \gamma - 0.5} \tag{6.52}$$

Formula (6.49) gives a conservative critical load, because the global bending buckling shape for loadcase P (see fig. 6.6a) is not identical to the global bending buckling shape for loadcase F (see fig. 6.10a).

A lower bound for the racking shear critical load of a braced frame can be found by assuming a shear cantilever. It has been shown that the racking shear critical load of a shear cantilever is (see eq. 6.51)):

$$F'_{cr;GA;cantilever} = \beta GA \tag{6.53}$$

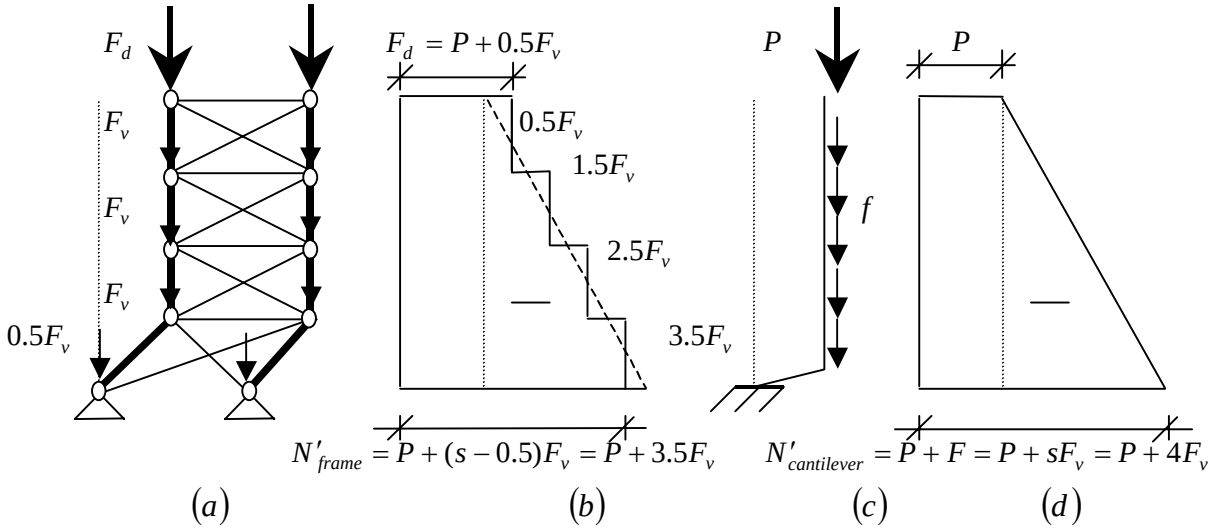

Figure 6.14 Influence normal force on racking shear critical load $F'_{cr;GA}$.

From the racking shear buckling shape of a braced frame it can be seen that the first-storey sways and the other storeys remain vertical (see fig. 6.14a). The normal force N'_{frame} in a braced frame at the first storey is (see fig. 6.14b):

$$N'_{frame} = (s-0.5)F_v + P = (s-0.5)F_v + (\gamma-0.5)F_v = (s+\gamma-1)F_v \tag{6.54}$$

From the racking shear buckling shape of a shear cantilever it can be seen that a cantilever sways at the bottom and the rest remains vertical (see fig. 6.14c). The normal force $N'_{cantilever}$ in a braced frame at the bottom is (see fig. 6.14d):

$$N'_{cantilever} = sF_v + P = sF_v + (\gamma-0.5)F_v = (s+\gamma-0.5)F_v \tag{6.55}$$

At buckling the normal force in a shear cantilever is half a floor load larger ($0.5F_v$) then the normal force in a braced frame. Therefore the racking shear critical load of a shear cantilever is lower then the racking shear critical load of a braced frame and eq. (6.53) has to be rearranged, to take the effect of the larger normal force into consideration, which leads to:

$$F'_{cr;GA} = \frac{N'_{cantilever}}{N'_{frame}}\beta GA \tag{6.56}$$

Substituting eq. (6.54) and eq. (6.55) into eq. (6.56) leads to the actual shear critical load:

$$F'_{cr;GA} = \eta'\beta GA \tag{6.57}$$

Where η' is a factor which takes the effect of the different normal forces $N'_{cantilever}$ and N'_{frame} into account for loadcase $P+F$:

$$\eta' = \frac{N'_{cantilever}}{N'_{frame}} = \frac{s+\gamma-0.5}{s+\gamma-1} \tag{6.58}$$

For the case when the roof load is half the floor load ($\gamma = 0.5$), which is identical to a UDL, η' is:

$$\eta' = \eta = \frac{s}{s-0.5}$$

Formula (6.57) gives a mathematically exact racking shear critical load, because the racking shear buckling shape of a cantilever (see fig. 6.14c) is identical to the racking shear buckling shape of a braced frame (see fig. 6.14a).

If the actual values for global bending (see eq. (6.49)) and racking shear (see eq. (6.57)) are substituted into eq. (6.48) the critical load of a braced frame becomes:

$$\frac{1}{F'_{cr}} = \frac{l^2}{7.837\alpha EAc^2} + \frac{1}{\eta'\beta GA} \tag{6.59}$$

Formula (6.59) gives a conservative critical load, because the global bending buckling shape for loadcase $P+F$ (6.15a) is not identical to the racking shear buckling shape for loadcase $P+F$ (see fig. 6.15b).

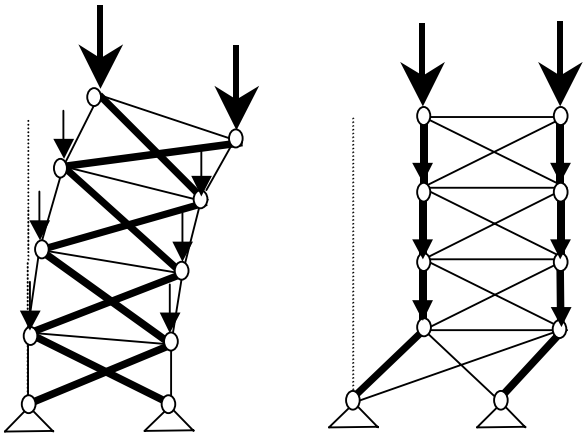

(a) (b)

Figure 6.15 Buckling shapes for loadcase $P + F$ *with* $F'_{cr;GA} = \eta' \beta GA$.

6.2 Lateral stiffnesses of braced frame with non-continous columns

6.2.1 Global bending stiffness

The global bending stiffness caused by the axial deformation in the columns (shortening of the columns at one side and lengthening at the other side) can be obtained from (see fig. 6.16):

$$EAc^2 = \sum EA_c c_i^2 \tag{6.60}$$

where E is the elastic modulus, A_{ci} is the cross-sectional area of the column and c_i is the distance between the neutral axis of the column NA_1 and the neutral axis of the X-braced frame NA_{frame}.

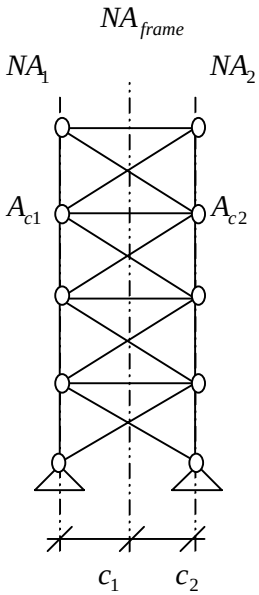

Figure 6.16 Global bending stiffness braced frame with non-continous columns.

6.2.2 Racking shear stiffness

The racking shear stiffness GA can be defined as the resistance of a structure against shear.
The racking shear stiffness GA of an X-braced frame is caused by axial strains in the diagonals.
Values of the racking shear stiffness can be obtained by analysing one storey of an X-braced frame.
The racking shear stiffness of different bracing types has been derived earlier [23].
The racking shear stiffness of an one-bay X-braced frame is (see fig. 6.17a):

$$GA_X = \frac{2a^2 hEA_d}{d^3} \tag{6.61}$$

The racking shear stiffness of an one-bay K-braced frame is (see fig. 6.17b):

$$GA_K = a^2 hE\left[\frac{2d^3}{A_d} + \frac{a^3}{4A_b}\right]^{-1} \tag{6.62}$$

The racking shear stiffness of an one-bay N-braced frame is (see fig. 6.17c):

$$GA_N = a^2 hE\left[\frac{d^3}{A_d} + \frac{a^3}{A_b}\right]^{-1} \tag{6.63}$$

The racking shear stiffness of an one-bay Knee-braced frame is (see fig. 6.17d):

$$GA_{Knee} = 2m^2 hE\left[\frac{d^3}{A_d} + \frac{g^3}{A_b} + \frac{g^2 p^2 h^2}{6aI_b}\right]^{-1} \tag{6.64}$$

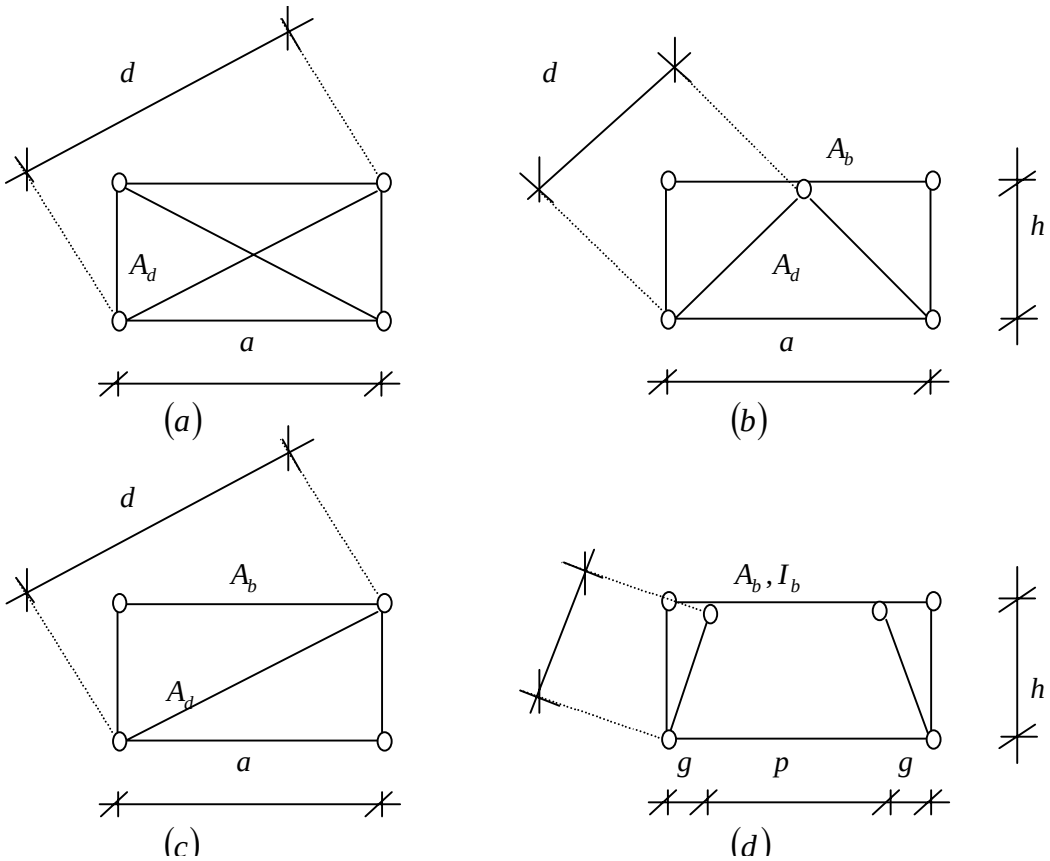

Figure 6.17 Bracing types.

6.3 Accuracy

To establish the accuracy of the stick-spring model, critical loads of a number of one-bay X-braced frames were estimated using the stick-spring model and a finite element analyses. Finite element program ANSYS was used to obtain the eigenvalues of the braced frames. The braced frames have non-continous columns and pinned supports and the height of the frames varied from eight to forty stories. The X-braced frames are subjected to three different loadcases (see fig. 1.5):

- Vertical top loads (see fig. 1.5a).
- Uniformly distributed vertical loads (see fig. 1.5b).
- Load combinations (see fig. 1.5c).

Five different cases will be investigated for one-bay X-braced frames:

- Global bending deformation only (see fig. 6.18a).
- Racking shear deformation only (see fig. 6.18b).
- All deformations together (see fig. 6.18a/b).
- Influence of varying cross-sectional area of the columns A_c on the critical load.
- Influence of varying cross-sectional area of the diagonals A_d on the critical load.

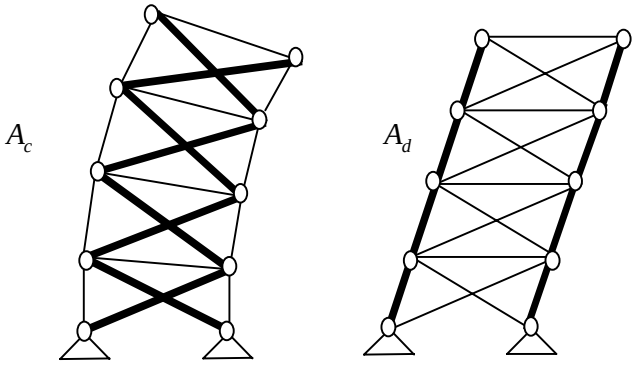

Fig 6.18 Cases to investigate for braced frames with non-continous columns.

The first two cases only represent theoretical cases, but the inclusion of them is very important to make a well-based judgement on the accuracy of the stick-spring model.
The critical loads found with the finite element method are assumed to be exact.

The errors are calculated as follows $\Delta = \dfrac{P_{cr} - P_{cr(ANSYS)}}{P_{cr(ANSYS)}} \times 100\%$.

If the error is negative the stick-spring model gives a conservative value for the critical load.

6.3.1 Numerical model

The numerical model is built up from LINK1 elements. LINK1 elements can only sustain normal forces (see fig. 6.19). The columns, beams and diagonals are all LINK1 elements with a cross-sectional area A_c, A_d or A_b. All the connections between these LINK1 elements are hinged. The columns are pin-connected to the base. For this investigation it is assumed that the braced frame has an uniform cross-sectional area of the columns A_c, of the diagonals A_d and of the beams A_b up the height.

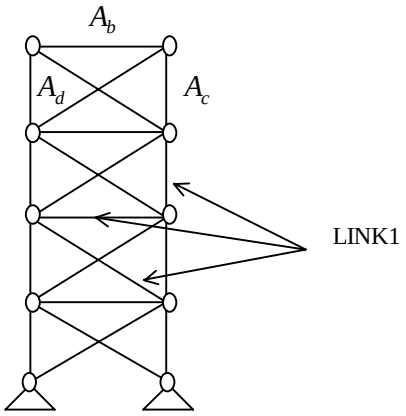

Figure 6.19 Numerical model for a braced frame with non-continous columns.

6.3.2 Example

An eight storey high one bay X-braced frame with non-continous columns (see fig. 6.20) has a global bending stiffness EAc^2, a racking shear stiffness GA and is subjected to three different loadcases. The characteristics of the braced frame can be found in table 6.1.

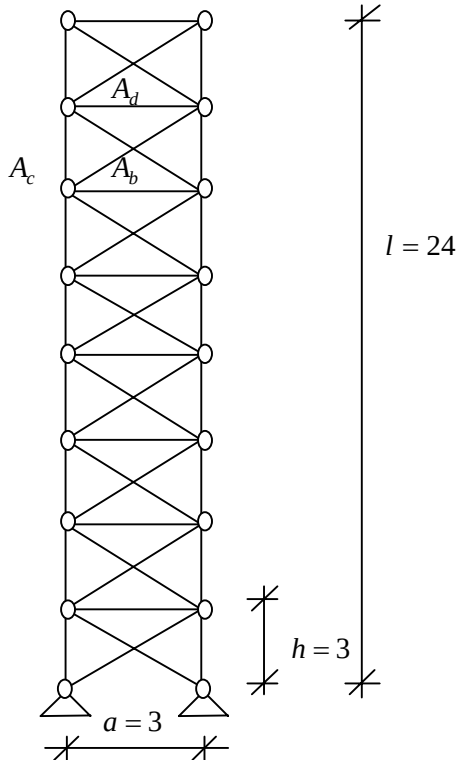

Figure 6.20. Example of braced frames with non-continous columns.

Table 6.1. Characteristics

Columns UC305x137 (305x305x137 mm)	
Cross-sectional area:	A_c=1.744E-02 m^2
Second moment of area:	I_c=3.281E-04 m^4
Beams UB356x45 (356x171x45 mm)	
Cross-sectional area:	A_b=5.733E-03m^2
Second moment of area:	I_b=1.207E-04 m^4
Diagonals 250x15 mm	
Cross-sectional area:	A_d=3.75E-03 m^2
Second moment of area:	I_d=1.953E-05 m^4
Elastic modulus:	E=2.00E+05 MN/m^2

6.3.2.1 Stiffness parameters

The global bending stiffness is (see eq. (6.60)):

$$EAc^2 = \sum EA_{ci}c_i^{\,2} = 2EA_c c_i^{\,2} = 2\times 2\times 10^5 \times 1.744\cdot 10^{-2}\times 1.5^2 = 15696MN$$

The racking shear stiffness is (see eq. (6.61)):

$$GA_X = \frac{2a^2 hEA_d}{d^3} = \frac{2\times 3^2\times 3\times 2\times 10^5\times 3.75\times 10^{-3}}{\left(3\sqrt{2}\right)^3} = 530.3MN$$

6.3.2.2 Vertical top load

The global bending critical load is (see eq. (6.9)):

$$P_{cr;EAc^2} = \frac{\pi^2 EAc^2}{4l^2} = \frac{\pi^2\times 15696}{4\times 24^2} = 67.24MN$$

The racking shear critical load is (see eq. (6.10)):

$$P_{cr;GA} = GA = 530.3MN$$

The critical load is (see eq. (6.6)):

$$P_{cr} = \left[\frac{1}{P_{cr;EAc^2}} + \frac{1}{P_{cr;GA}}\right]^{-1} = \left[\frac{1}{67.24} + \frac{1}{530.32}\right]^{-1} = 59.67MN$$

6.3.2.3 Vertical UDL

The global bending critical load is (see eq. (6.20)):

$$F_{cr;EAc^2} = \frac{7.837EAc^2}{l^2} = \frac{7.837 \times 15696}{24^2} = 213.6MN$$

Reduction factor η is (see eq. (6.22)):

$$\eta = \frac{s}{s-0.5} = \frac{8}{8-0.5} = \frac{16}{15} = 1.0666$$

The racking shear critical load is (see eq. (6.21)):

$$F_{cr;GA} = \eta GA = 1.0666 \times 530.3 = 565.7MN$$

The critical load is (see eq. (6.17)):

$$F_{cr} = \left[\frac{1}{F_{cr;EAc^2}} + \frac{1}{F_{cr;GA}} \right]^{-1} = \left[\frac{1}{213.6} + \frac{1}{565.7} \right]^{-1} = 155.0MN$$

6.3.2.4 Load combinations

If the vertical top load is 4 times the floor loading factor γ is (see eq. (4.18)):

$$\gamma = \frac{F_d}{F_v} = 4$$

Reduction factor for the bending critical load α is (see eq. (6.50)):

$$\alpha = \frac{s}{s + 3.176(\gamma - 0.5)} = \frac{8}{8 + 3.176(4 - 0.5)} = 0.4185$$

The global bending critical load is (see eq. (6.49)):

$$F'_{cr;EAc^2} = \frac{7.837\alpha EAc^2}{l^2} = \alpha F_{cr;EAc^2} = 0.4185 \times 213.6 = 89.37MN$$

Reduction factor for the racking shear critical load β is (see eq. (6.52)):

$$\beta = \frac{s}{s + \gamma - 0.5} = \frac{8}{8 + 4 - 0.5} = 0.6957$$

Reduction factor η' is (see eq. (6.58)):

$$\eta' = \frac{s + \gamma - 0.5}{s + \gamma - 1} = \frac{8 + 4 - 0.5}{8 + 4 - 1} = 1.0455$$

The racking shear critical load is (see eq. (6.57)):

$$F'_{cr;GA} = \eta'\beta GA = 1.0455 \times 0.6957 \times 530.3 = 385.7MN$$

The critical load is (see eq. (6.48)):

$$F'_{cr} = \left[\frac{1}{F'_{cr;EAc^2}} + \frac{1}{F'_{cr;GA}} \right]^{-1} = \left[\frac{1}{89.37} + \frac{1}{385.7} \right]^{-1} = 72.56MN$$

All critical loads in this example calculated by the stick-spring model are in bold type and can be found in tables 6.2-6.11.

6.3.3 Results

The figures and tables below present the results of the critical loads obtained from the stick-spring model and the numerical analysis. Table 6.2 shows the accurracy of the global bending critical loads $P_{cr;EAc^2}$ and $F_{cr;EAc^2}$ and table 6.3 of the racking shear critical loads $P_{cr;GA}$ and $F_{cr;GA}$ and table 6.4 of the critical loads P_{cr} and F_{cr}. Table 6.5 shows the accuraccy of the global bending critical load $F'_{cr;EAc^2}$, table 6.6 of the racking shear critical load $F'_{cr;GA} = \eta'\beta GA$, table 6.7 of the critical load F'_{cr}. Table 6.8 and 6.9 show the accurracy of the critical loads P_{cr} and F_{cr} by varying the cross-sectional area of the columns A_c and table 6.10 and 6.11 show the accurracy of the critical loads P_{cr} and F_{cr} by varying the cross-sectional area of the diagonals A_d. The errors for practical tall building structures are given in red.

Table 6.2. Critical loads for braced frames with non-continous columns, global bending deformation only.

Number of storeys s [-]	Vertical top load P with $P_{cr;EAc^2} = \frac{\pi^2 EAc^2}{4l^2}$ (see eq. (6.9))			UDL $F(\gamma = 0.5)$ with $F_{cr;EAc^2} = \frac{7.837 EAc^2}{l^2}$ (see eq. (6.20))		
	Critical loads P_{cr} [MN]			Critical loads F_{cr} [MN]		
	Stick-spring model	ANSYS	Error Δ [%]	Stick-spring model	ANSYS	Error Δ [%]
8	**67.24**	67.93	-1.0	**213.6**	216.1	-1.2
16	16.81	16.84	-0.2	53.39	53.54	-0.3
24	7.47	7.48	-0.1	23.73	23.76	-0.1
32	4.20	4.20	-0.1	13.35	13.36	-0.1
40	2.69	2.69	0.0	8.54	8.55	0.0

Table 6.3. Critical loads for braced frames with non-continous columns, racking shear deformation only.

Number of storeys s [-]	Vertical top load P with $P_{cr;GA} = GA$ (see eq. (6.10))			UDL $F(\gamma = 0.5)$ with $F_{cr;GA} = \eta GA$ (see eq. (6.21))		
	Critical loads P_{cr} [MN]			Critical loads F_{cr} [MN]		
	Stick-spring model	ANSYS	Error Δ [%]	Stick-spring model	ANSYS	Error Δ [%]
8	**530.3**	530.3	0.0	**565.7**	565.7	0.0
16	530.3	530.3	0.0	547.4	547.4	0.0
24	530.3	530.3	0.0	541.6	541.6	0.0
32	530.2	530.2	0.0	538.7	538.8	0.0
40	530.2	530.2	0.0	537.0	537.0	0.0

Table 6.4. Critical loads for braced frames with non-continous columns, all deformations together.

Number of storeys s [-]	Vertical top load P			UDL $F(\gamma = 0.5)$		
	Critical loads P_{cr} [MN] (see eq. (6.6))			Critical loads F_{cr} [MN] (see eq. (6.17))		
	Stick-spring model	ANSYS	Error Δ [%]	Stick-spring model	ANSYS	Error Δ [%]
8	**59.67**	60.06	-0.6	**155.0**	179.7	-14
16	16.29	16.32	**-0.2**	48.65	51.04	**-4.7**
24	7.37	7.37	**-0.1**	22.73	23.26	**-2.2**
32	4.17	4.17	**-0.1**	13.03	13.20	**-1.3**
40	2.68	2.68	**-0.0**	8.41	8.48	**-0.8**

Table 6.5. Critical loads for braced frames with non-continous columns, $P+F$, global bending def. only.

Number of storeys s [-]	Load combination $P+F$ with $F'_{cr;EAc^2}=\frac{7.837\alpha EAc^2}{l^2}$ (see eq. (6.49))											
	Critical loads F'_{cr} [MN]											
	$\gamma=1$			$\gamma=4$			$\gamma=16$			$\gamma=64$		
	Stick-spring model	ANSYS	Error Δ [%]	Stick-spring model	ANSYS	Error Δ [%]	Stick-spring model	ANSYS	Error Δ [%]	Stick-spring model	ANSYS	Error Δ [%]
8	178.2	181.5	-1.8	**89.37**	91.38	-2.2	29.85	30.30	-1.5	8.15	8.15	-1.0
16	48.57	48.92	-0.7	31.50	32.01	-1.6	13.10	13.26	-1.2	3.92	3.92	-0.6
24	22.26	22.35	-0.4	16.22	16.43	-1.3	7.78	7.88	-1.3	2.52	2.52	-0.6
32	12.72	12.76	-0.3	9.91	10.02	-1.1	5.26	5.33	-1.4	1.83	1.83	-0.7
40	8.22	8.24	-0.3	6.69	6.76	-1.1	3.83	3.88	-1.4	1.41	1.41	-0.8

Table 6.6. Critical loads for braced frames with non-continous columns, $P+F$, racking shear def. only.

Number of storeys s [-]	Load combination $P+F$ with $F'_{cr;GA}=\eta'\beta GA$ (see eq. (6.57))											
	Critical loads F'_{cr} [MN]											
	$\gamma=1$			$\gamma=4$			$\gamma=16$			$\gamma=64$		
	Stick-spring model	ANSYS	Error Δ [%]	Stick-spring model	ANSYS	Error Δ [%]	Stick-spring model	ANSYS	Error Δ [%]	Stick-spring model	ANSYS	Error Δ [%]
8	530.3	530.3	0.0	**385.7**	385.7	0.0	184.5	184.5	0.0	59.76	59.76	0.0
16	530.3	530.3	0.0	446.6	446.6	0.0	273.7	273.7	0.0	107.4	107.4	0.0
24	530.3	530.3	0.0	471.4	471.4	0.0	326.3	326.4	0.0	146.3	146.3	0.0
32	530.3	530.3	0.0	484.8	484.9	0.0	361.0	361.1	0.0	178.6	178.6	0.0
40	530.3	530.3	0.0	493.3	493.3	0.0	385.6	385.7	0.0	205.9	206.0	0.0

Table 6.7. Critical loads for braced frames with non-continous columns, $P+F$, all deformations together.

Number of storeys s [-]	Load combination $P+F$ (see eq. (6.48))											
	Critical loads F'_{cr} [MN]											
	$\gamma=1$			$\gamma=4$			$\gamma=16$			$\gamma=64$		
	Stick-spring model	ANSYS	Error Δ [%]	Stick-spring model	ANSYS	Error Δ [%]	Stick-spring model	ANSYS	Error Δ [%]	Stick-spring model	ANSYS	Error Δ [%]
8	133.4	153.6	-13	**72.56**	79.97	-9.3	25.70	26.80	-4.1	7.17	7.29	-1.7
16	44.49	46.76	**-4.8**	29.43	30.83	**-4.6**	12.50	12.83	**-2.6**	3.79	3.82	**-1.0**
24	21.36	21.90	**-2.5**	15.68	16.15	**-2.9**	7.60	7.76	**-2.2**	2.48	2.50	**-0.9**
32	12.42	12.61	**-1.5**	9.71	9.92	**-2.1**	5.18	5.29	**-2.0**	1.81	1.83	**-0.9**
40	8.09	8.17	**-1.0**	6.60	6.71	**-1.7**	3.79	3.86	**-1.8**	1.40	1.42	**-1.0**

Table 6.8. Varying cross-sectional area of the columns A_c for loadcase P , all deformations together.

Characteristics			Vertical top load P (see eq. (6.6))				
Columns	A_c [m2]	EAc^2 MN]	Error Δ [%]				
			s=8	s=16	s=24	s=32	s=40
Bar (d=10)	7.854e-5	70.686	-1.5	-0.4	-0.3	-0.2	-0.2
HE 100A	2.124e-3	1911.6	-0.9	-0.3	-0.1	-0.1	-0.1
HE 400A	1.59e-2	13310	-0.7	**-0.2**	**-0.1**	**0.0**	**0.0**
HE 800A	2.858e-2	25722	-0.6	**-0.2**	**-0.1**	**-0.1**	**0.0**
HE 1000M	4.442e-2	39978	-0.6	**-0.2**	**-0.1**	**0.0**	**0.0**
HD 400x1086	1.815e-3	124740	-0.4	-0.1	-0.1	0.0	0.0
Fictive profile	0.25	225000	-0.3	-0.1	-0.1	0.0	0.0
Fictive profile	1	900000	-0.1	-0.1	-0.1	0.0	0.0
Fictive profile	10	9000000	0.0	0.0	0.0	0.0	0.0
Fictive profile	10000	900000000	0.0	0.0	0.0	0.0	0.0

Table 6.9. Varying cross-sectional area of the columns A_c for loadcase F, all deformations together.

Characteristics			UDL F (see eq. (6.17))				
Columns	A_c [m2]	EAc^2 [MN]	Error Δ [%]				
			s=8	s=16	s=24	s=32	s=40
Bar (d=10)	7.854e-5	70.686	-2.9	-0.8	-0.4	-0.2	0.0
HE 100A	2.124e-3	1911.6	-3.5	-1.0	-0.4	-0.2	-0.2
HE 400A	1.59e-2	13310	-13	**-4.3**	**-2.1**	**-1.2**	**-0.8**
HE 800A	2.858e-2	25722	-18	**-7.1**	**-3.5**	**-2.1**	**-1.4**
HE 1000M	4.442e-2	39978	-22	**-10**	**-5.2**	**-3.1**	**-2.1**
HD 400x1086	1.815e-3	124740	-23	-21	-13	-8.4	-5.8
Fictive profile	0.25	225000	-15	-26	-19	-13	-9.5
Fictive profile	1	900000	-4.3	-15	-27	-26	-23
Fictive profile	10	9000000	-0.5	-1.8	-3.8	-6.6	-9.9
Fictive profile	10000	900000000	0.0	0.0	0.0	0.0	0.0

Table 6.10. Varying cross-sectional area of the diagonals A_d for loadcase P, all deformations together.

Charecteristics			Vertical top load P (see eq. (6.6))				
Diagonals	A_d [m2]	GA [MN]	Error Δ [%]				
			s=8	s=16	s=24	s=32	s=40
Bar (d=10)	7.854e-5	11.11	-0.1	-0.1	-0.1	0.0	0.0
RHS 40x40x3	4.343e-4	61.42	-0.4	-0.2	-0.1	0.0	0.0
RHS 80x80x6.3	1.815e-3	256.68	-0.6	**-0.2**	**-0.1**	**0.0**	**0.0**
RHS 160x160x8	4.795e-3	678.12	-0.7	**-0.2**	**-0.1**	**-0.1**	**0.0**
RHS 250x250x12.5	1.171e-2	1656.04	-0.7	**-0.2**	**-0.1**	**0.0**	**0.0**
RHS 400x400x16	2.43e-1	3436.54	-0.8	**-0.2**	**-0.1**	**-0.1**	**0.0**
Fictive profile	10000	9000000000	-1.0	-0.2	-0.1	-0.1	-0.1

Table 6.11. Varying cross-sectional area of the diagonals A_d for loadcase F, all deformations together.

Charecteristics			UDL F (see eq. (6.17))				
Diagonals	A_d [m2]	GA [MN]	Error Δ [%]				
			s=8	s=16	s=24	s=32	s=40
Bar (d=10)	7.854e-5	11.11	-5.2	-18	-28	-25	-21
RHS 40x40x3	4.343e-4	61.42	-22	-22	-14	-9.0	-6.2
RHS 80x80x6.3	1.815e-3	256.68	-21	**-8.6**	**-4.3**	**-2.6**	**-1.7**
RHS 160x160x8	4.795e-3	678.12	-12	**-3.8**	**-1.8**	**-1.0**	**-0.7**
RHS 250x250x12.5	1.171e-2	1656.04	-6.1	**-1.5**	**-0.8**	**-0.5**	**-0.3**
RHS 400x400x16	2.43e-1	3436.54	-3.6	**-1.0**	**-0.5**	**-0.3**	**-0.2**
Fictive profile	10000	9000000000	-1.2	-0.3	-0.1	-0.1	-0.1

Observations

- **The buckling behavior of a braced frame with non-continous columns can be divided into global bending and racking shear.**

- **The dominant buckling shape for highrise braced frames is global bending.**

- **The critical load of a braced frame subjected loadcase P is lower then of a braced subjected to loadcase F,** because the point of impact of the resulting vertical load is higher. The critical load depends on the point of impact of the resulting vertical load.

- **The racking shear buckling shape of a braced for loadcase P has not a definite buckling shape, which means the racking shear buckling shape can assume any form.**
  Therefore different racking shear buckling shapes have one eigenvalue and one critical load. If a braced frame has eight storeys, eight different racking shear buckling shapes have one eigenvalue and one critical load.

- **The racking shear buckling shapes of a braced for loadcases F and $P+F$ have a definite buckling shape, which means the racking shear buckling shape can assume only one form.** Therefore the racking shear buckling shape has one eigenvalue and one critical load.

- **The global bending critical loads $P_{cr;EAc^2}=\frac{\pi^2 EAc^2}{4l^2}$, $F_{cr;EAc^2}=\frac{7.837EAc^2}{l^2}$ and $F'_{cr;EAc^2}=\frac{7.837\alpha EAc^2}{l^2}$ are conservative,** because all errors are negative (see table 6.2 and 6.5).

- **The racking shear critical loads are $P_{cr;GA}=GA$, $F_{cr;GA}=\eta GA$ and $F'_{cr;GA}=\eta'\beta GA$,** because the errors are zero (see table 6.3 and 6.6). This is because the racking shear buckling shape of a shear cantilever is identical to the racking shear buckling shape of a braced frame.

- **The critical loads $P_{cr}=\left[\frac{4l^2}{\pi^2 EAc^2}+\frac{1}{GA}\right]^{-1}$, $F_{cr}=\left[\frac{l^2}{7.837EAc^2}+\frac{1}{\eta GA}\right]^{-1}$ and $F'_{cr}=\left[\frac{l^2}{7.837\alpha EAc^2}+\frac{1}{\eta'\beta GA}\right]^{-1}$ are conservative,** because the errors are negative (see table 6.2-6.11). This is because the global bending buckling shape is not identical to the racking shear buckling shape.

- **The maximum errors for the theoretical tall building structures are (see table** 6.2-6.11**).**
  The highest conservative error for loadcase P is: -1.5 %.
  The highest conservative error for loadcase F is: -28 %.
  The highest conservative error for loadcase $P+F$ is: -13 %.

- **The maximum errors for the practical tall building structures are (see table** 6.2-6.11 in red**).**
  The highest conservative error for loadcase P is: -0.2 %.
  The highest conservative error for loadcase F is: -10 %.
  The highest conservative error for loadcase $P+F$ is: -4.8 %.

- **All suggested formula give good results for the preliminary design of practical highrise braced frames with non-continous columns within a maximum error of 10%.**

- **All observations are only valid for X-braced frames of eight till forty stories pin-connected to the base with non-continous columns.**

- **All observations are only valid for the investigated cases in this parameterstudy.**

6.4 Braced frames with continous columns

A braced frame with continous columns is a structure consisting of columns, beams and diagonals, which are pin-connected to each other (see fig. 6.21). The columns of the frame are continous and pin-connected to the base.

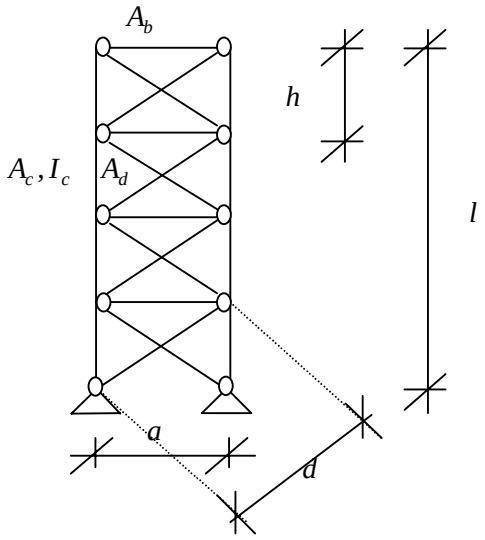

Figure 6.21 Braced frame with continous columns pin-connected to base.

The buckling behaviour of a braced frame with continous columns pin-connected to the base can be divided into 2 modes of deformation:

- Overall bending deformation (EI_0): single curvature bending in the continous columns and axial deformation in the columns (see fig. 6.22a).
- Racking shear deformation (GA): axial strains in the diagonals (see fig. 6.22b).

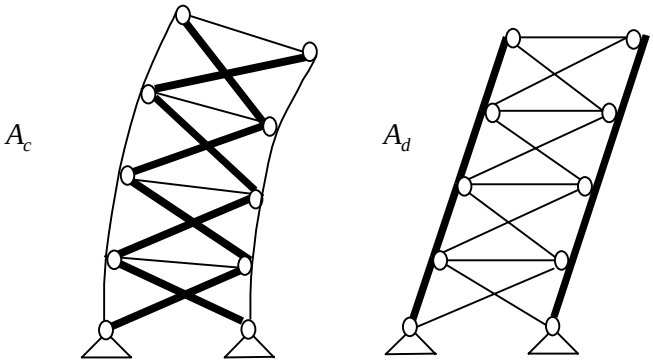

Fig 6.22 Modes of behavior of a braced frame with continious columns.

Assumptions:

- The beams and diagonals are hinged connected to continous columns.
- The braced frame is pin-connected to the base.
- The columns are continous up the height and therefore the individual bending stiffness is not zero $EI \neq 0$.
- The braced frame has two lateral stiffness parameters $EI_0 = f(A_c, I_c)$ and $GA = f(A_b, A_d)$.
- There is no connection between the diagonals.

6.4.1 Vertical top loads

A stick-spring model is introduced here to obtain an approximate solution for the overall critical load of a one-bay braced frame with continous columns (see fig. 6.23a). The braced frame is subjected to vertical top loads and can be transformed into a shear-flexure cantilever with overall bending stiffness $EI_0 = f(A_c, I_c)$ and racking shear stiffness $GA = f(A_b, A_d)$ (see fig. 6.23b).
This shear-flexure cantilever can be transformed into a stick-spring model (see fig. 6.23c).
In this model a shear-flexure cantilever is replaced by a horizontal translation spring k,
which takes the overall bending stiffness EI_0 and the racking shear stiffness GA of the shear-flexure cantilever into account. Therefore spring stiffness k is a function of the overall bending stiffness EI_0 and of the racking shear stiffness GA of the shear-flexure cantilever $k = f(EI_0, GA)$.

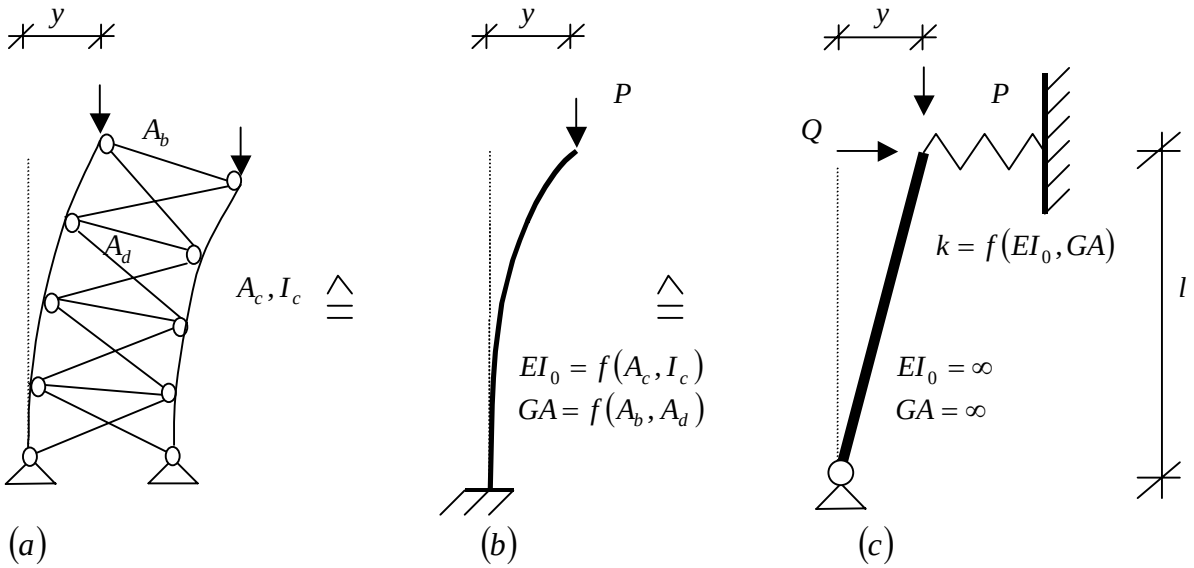

Figure 6.23 Transformation braced frame (continous) into stick-spring model (vertical top loads).

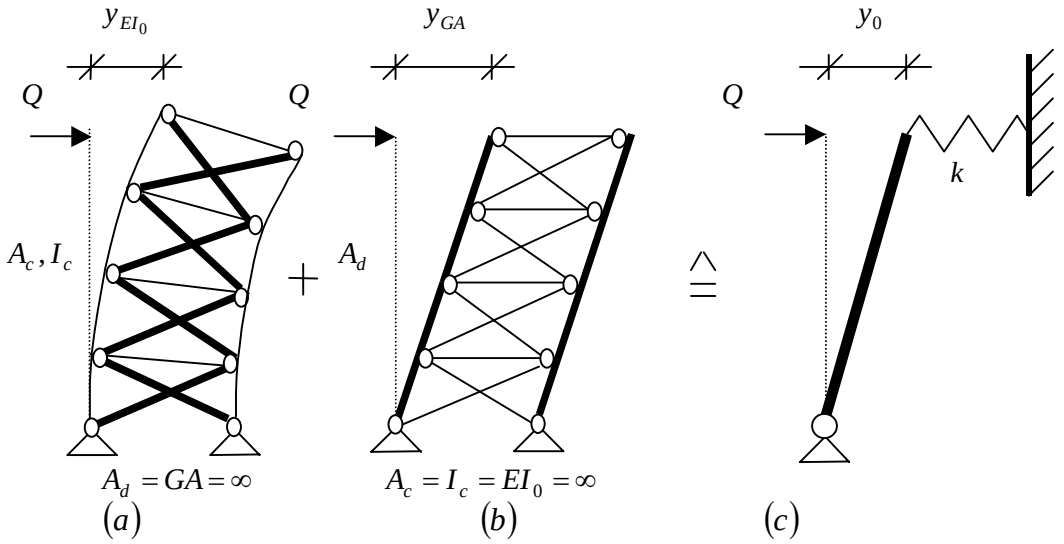

Figure 6.24 Deformations braced frame (continous) caused by horizontal load Q.

The first-order deformation at the top of the braced frame is (see fig. 6.24a/b):

$$y_0 = y_{EI_0} + y_{GA} = \frac{Ql^3}{3EI_0} + \frac{Ql}{GA} \tag{6.65}$$

The overall bending stiffness can be obtained from [5]:

$$EI_0 = EAc^2 + EI \tag{6.66}$$

After substituting eq. (6.66) into eq. (6.65) the first-order deformation can be rearranged into:

$$y_0 = \frac{Ql^3}{3EI + 3EAc^2} + \frac{Ql}{GA} \tag{6.67}$$

The first-order deformation at the top of the stick-spring model is (see fig. 6.24c):

$$y_0 = \frac{Q}{k} \tag{6.68}$$

Both deformations are the same yielding the horizontal translational spring stiffness k:

$$\frac{1}{k} = \frac{l^3}{3EI + 3EAc^2} + \frac{l}{GA} \tag{6.69}$$

It has been shown that the critical load of the stick-spring model is (see eq. (4.3)):

$$P_{cr} = kl \tag{6.70}$$

After substituting eq. (6.69) into eq. (6.70) the critical load of the stick-spring model is:

$$\frac{1}{P_{cr}} = \frac{1}{kl} = \frac{l^2}{3EI + 3EAc^2} + \frac{1}{GA} \tag{6.71}$$

In general, the critical load of eq. (6.71) can be written as:

$$\frac{1}{P_{cr}} = \frac{1}{P_{cr;EI} + P_{cr;EAc^2}} + \frac{1}{P_{cr;GA}} \tag{6.72}$$

Where the critical loads obtained from the stick-spring model are for:

- Individual bending [1, 2]

$$P_{cr;EI} = \frac{3EI}{l^2} \tag{6.73}$$

- Global bending [1, 2]:

$$P_{cr;EAc^2} = \frac{3EAc^2}{l^2} \tag{6.74}$$

- Racking shear [5]:

$$P_{cr;GA} = GA \tag{6.75}$$

But the actual critical loads are for:

- Individual bending [4]:

$$P_{cr;EI} = \frac{\pi^2 EI}{4l^2} \tag{6.76}$$

- Global bending [4]:

$$P_{cr;EAc^2} = \frac{\pi^2 EAc^2}{4l^2} \tag{6.77}$$

- Racking shear [5]:

$$P_{cr;GA} = GA \tag{6.78}$$

The racking shear critical load of the stick-spring model (see eq. (6.75)) is equal to the actual racking shear critical load of a braced frame (see eq. (6.78)), because the racking shear deflection shape of a braced frame (see fig. 6.25a) is identical to the racking shear buckling shape of a braced frame (see fig. 6.25b). The racking shear buckling shape of a braced has a definite buckling shape, which means the racking shear buckling shape can assume only one form.
Therefore the racking shear buckling shape has one eigenvalue and one critical load.

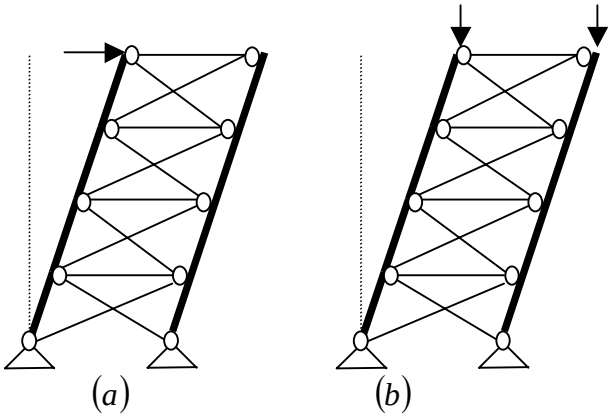

Figure 6.25 Racking shear shapes braced frame (continous) caused by top loads.

If the actual values for individual bending (see eq. (6.76)), global bending (see eq. (6.77)) and racking shear (see eq. (6.78)) are substituted into eq. (6.72) the critical load of a braced frame is:

$$\frac{1}{P_{cr}} = \frac{4l^2}{\pi^2 EI + \pi^2 EAc^2} + \frac{1}{GA} \tag{6.79}$$

Eq. (6.71) gives in most cases an overestimated critical load, because the individual bending critical load (see eq. (6.73)) and the global bending critical load (see eq. (6.74)) are overestimated by 21.6% in the stick-spring model. If the actual values for individual bending (see eq. (6.76)), global bending (see eq. (6.77)) and racking shear (see eq. (6.78)) are substituted into eq. (6.72) the critical load is now conservative (see eq. (6.79)), because the overall bending buckling shape (see fig. 6.26a) is not identical to the racking shear buckling shape (see fig. 6.26b).

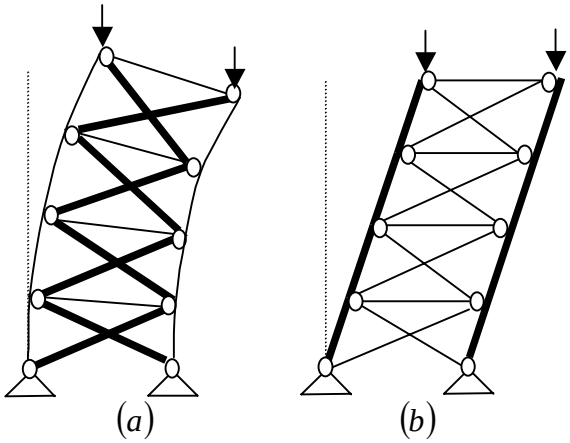

Figure 6.26 Buckling shapes for loadcase P.

6.4.2 Uniformly distributed vertical loads

In fig. 6.27a a braced frame with continous columns is subjected to vertical point loads F_v accept for the point loads at the roof and at the bottom of the frame which are $0.5F_v$.
In a similar way a stick-spring model can be used here to obtain an approximate solution for the overall critical load of a braced frame. First a braced frame subjected to vertical point loads is transformed into a shear-flexure cantilever subjected to a vertical UDL f (see fig. 6.27b), which then can be transformed into a stick-spring model (see fig. 6.27c).

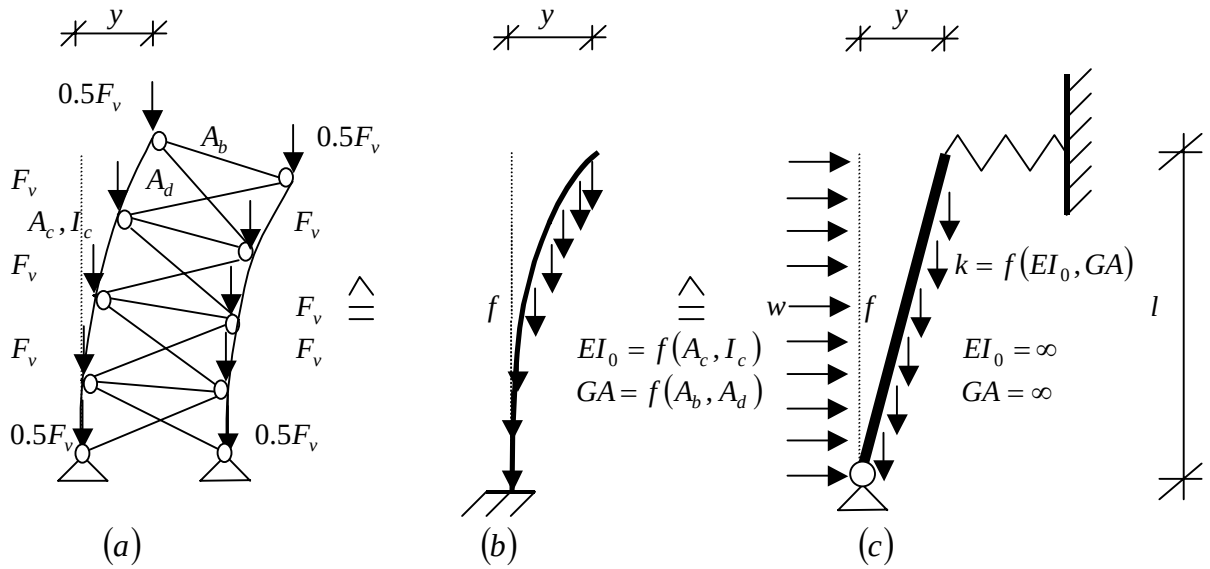

Figure 6.27 Transformation braced frame (continous) into stick-spring model (vertical UDL).

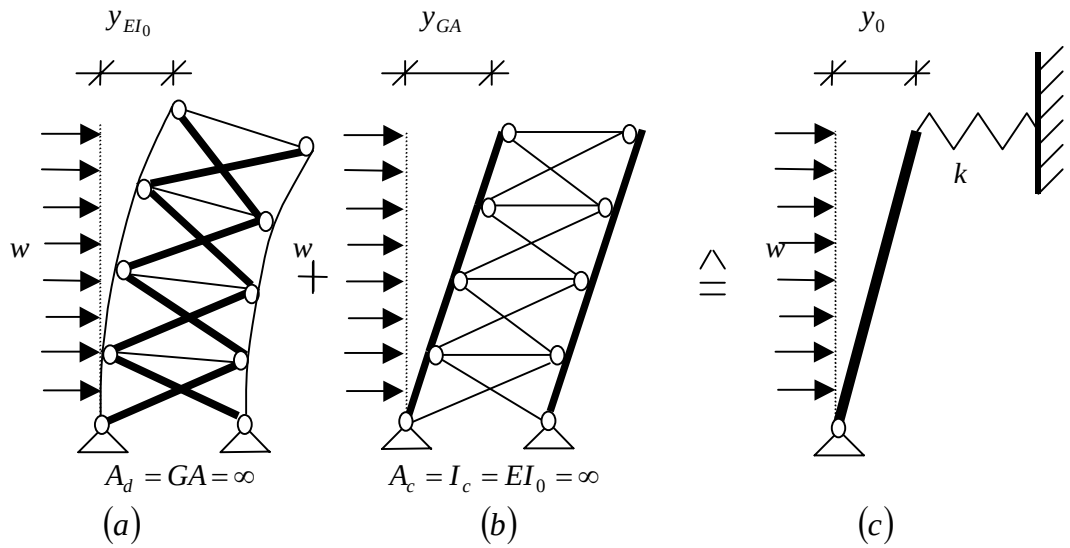

Figure 6.28 Deformations X-braced frame (continous) caused by horizontal UDL w.

The first-order deformation at the top of a braced frame is (see fig. 6.28a/b):

$$y_0 = y_{EI_0} + y_{GA} = \frac{wl^4}{8EI_0} + \frac{wl^2}{2GA} \tag{6.80}$$

The overall bending stiffness is [5]:

$$EI_0 = EAc^2 + EI \tag{6.81}$$

After substituting eq. (6.81) into eq. (6.80) the first-order deformation can be rearranged into:

$$y_0 = \frac{Ql^3}{8EI + 8EAc^2} + \frac{Ql}{2GA} \tag{6.82}$$

The first-order deformation at the top of the stick-spring model is (see fig. 6.28c):

$$y_0 = \frac{wl}{2k} \tag{6.83}$$

Both deformations are the same yielding the horizontal translational spring stiffness k:

$$\frac{1}{k} = \frac{l^3}{4EI + 4EAc^2} + \frac{l}{GA} \tag{6.84}$$

It has been shown that the critical load of the stick-spring model is (see eq. (4.12)):

$$F_{cr} = 2kl \tag{6.85}$$

After substituting eq. (6.84) into eq. (6.85) the critical load of the stick-spring model is:

$$\frac{1}{F_{cr}} = \frac{1}{2kl} = \frac{l^2}{8EI + 8EAc^2} + \frac{1}{2GA} \tag{6.86}$$

In general, the critical load of eq. (6.86) can be written as:

$$\frac{1}{F_{cr}} = \frac{1}{F_{cr;EI} + F_{cr;EAc^2}} + \frac{1}{F_{cr;GA}} \tag{6.87}$$

Where the critical loads obtained from the stick-spring model are for:

- Individual bending [1, 2]

$$F_{cr;EI} = \frac{8EI}{l^2} \tag{6.88}$$

- Global bending [1, 2]:

$$F_{cr;EAc^2} = \frac{8EAc^2}{l^2} \tag{6.89}$$

- Racking shear:

$$F_{cr;GA} = 2GA \tag{6.90}$$

But the actual critical loads are for:

- Individual bending [5]:

$$F_{cr;EI} = \frac{7.837EI}{l^2} \tag{6.91}$$

- Global bending [5]:

$$F_{cr;EAc^2} = \frac{7.837EAc^2}{l^2} \tag{6.92}$$

- Racking shear:

$$F_{cr;GA} = 2GA \tag{6.93}$$

The racking shear critical load of the stick-spring model (see eq. (6.90)) is equal to the actual racking shear critical load of a braced frame (see eq. (6.93)), because the racking shear deflection shape of a braced frame (see fig. 6.29a) is identical to the racking shear buckling shape of a braced frame (see fig. 6.29b). The racking shear buckling shape of a braced has a definite buckling shape, which means the racking shear buckling shape can assume only one form. Therefore the racking shear buckling shape has one eigenvalue and one critical load.

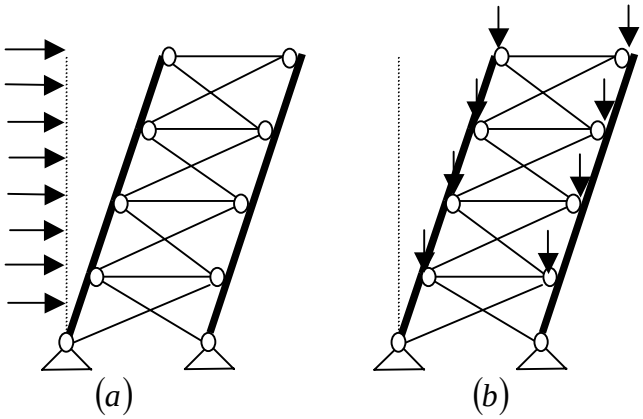

Figure 6.29 Racking shear shapes braced frame (continous) caused by UDL.

If the actual values for individual bending (see eq. (6.91)), global bending (see eq. (6.92)) and racking shear (see eq. (6.93)) are substituted into eq. (6.87) the critical load of a braced frame is:

$$\frac{1}{F_{cr}} = \frac{l^2}{7.837EI + 7.837EAc^2} + \frac{1}{2GA} \tag{6.94}$$

Eq. (6.86) gives in most cases an overestimated critical load, because the individual bending critical load (see eq. (6.88)) and the global bending critical load (see eq. (6.89)) are overestimated by 2.1% in the stick-spring model. If the actual values for individual bending (see eq. (6.91)), global bending (see eq. (6.92)) and racking shear (see eq. (6.93)) are substituted into eq. (6.87) the critical load is now conservative (see eq. (6.94)), because the overall bending buckling shape (see fig. 6.30a) is not identical to the racking shear buckling shape (see fig. 6.30b).

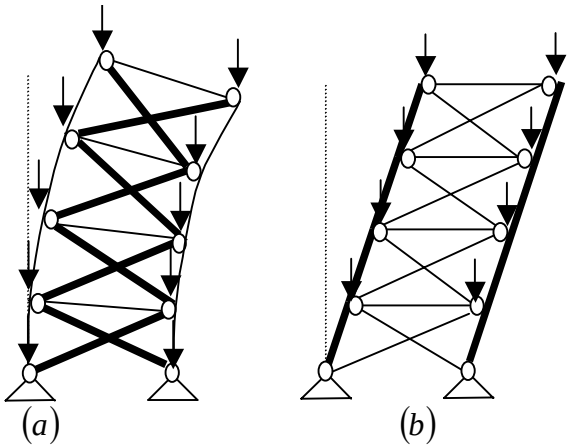

Figure 6.30 Buckling shapes for loadcase F .

6.4.3 Load combinations

In fig. 6.31a a braced frame with continous columns is subjected to vertical point loads F_v accept for the point load at the roof, which is F_d and the load at the bottom, which is $0.5F_v$.
In a similar way a stick-spring model can be used here to obtain an approximate solution for the overall critical load of a braced frame. First a braced frame subjected to vertical point loads is transformed into a shear-flexure cantilever subjected to a vertical top load P and a UDL f (see fig. 6.31b), which then can be transformed into a stick-spring model (see fig. 6.31c).

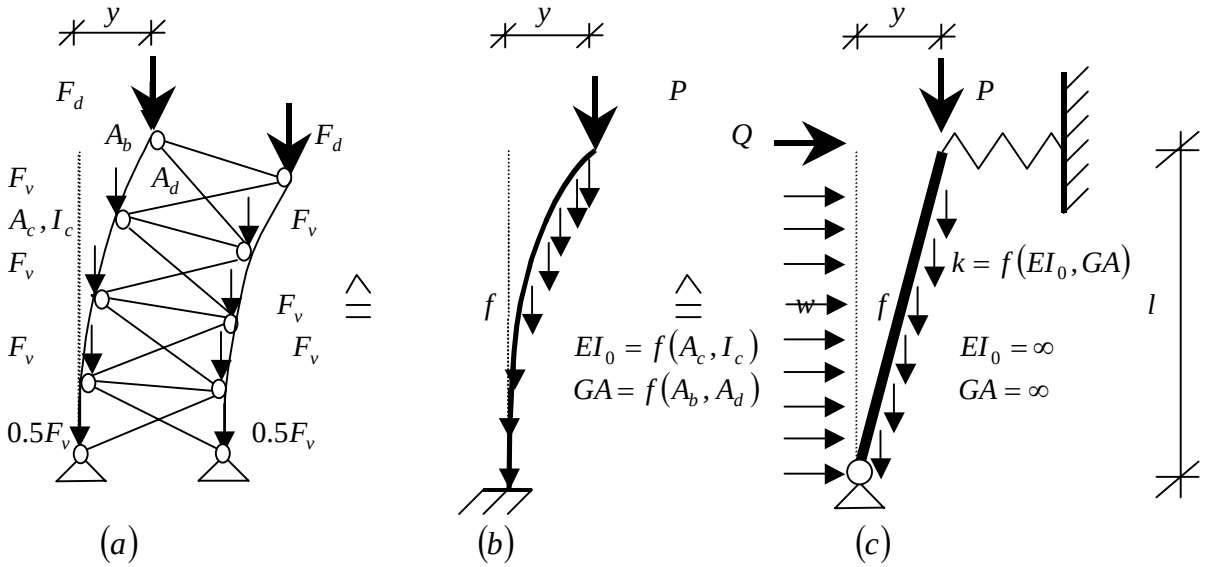

Figure 6.31 Transformation braced frame (continous) into stick-spring model (load combination).

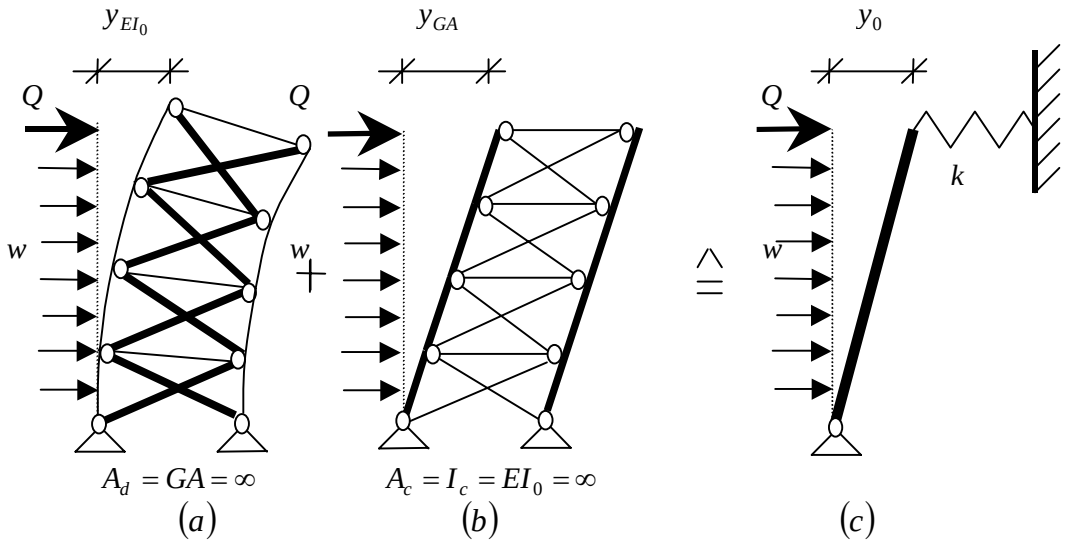

Figure 6.32 Deformations X-braced frame (continous) caused by load combination.

The first-order deformation at the top of the braced frame is (see fig. 6.32a/b):

$$y_0 = y_{EI_0} + y_{GA} = \frac{Ql^3}{3EI_0} + \frac{wl^4}{8EI_0} + \frac{Ql}{GA} + \frac{wl^2}{2GA} \tag{6.95}$$

The overall bending stiffness is [5]:

$$EI_0 = EAc^2 + EI \tag{6.96}$$

By substituting eq. (4.9), eq. (4.25) and eq. (6.96) into eq. (6.95) the first-order deformation at the top of he braced frame can be rearranged into:

$$y_0 = \frac{Wl^3}{3EI + 3EAc^2}\left(\frac{\gamma - 0.5}{s}\right) + \frac{Wl^3}{8EI + 8EAc^2} + \frac{Wl}{GA}\left(\frac{\gamma - 0.5}{s}\right) + \frac{Wl}{2GA} \tag{6.97}$$

It has been shown that the first-order deformation at the top of the stick-spring model is (see eq. (4.30) and fig. 6.32c):

$$y_0 = \frac{W}{2\omega k} \tag{6.98}$$

Both deformations are the same yielding the horizontal translational spring stiffness k:

$$\frac{1}{2\omega k} = \frac{l^3}{3EI + 3EAc^2}\left(\frac{\gamma - 0.5}{s}\right) + \frac{l^3}{8EI + 8EAc^2} + \frac{l}{GA}\left(\frac{\gamma - 0.5}{s}\right) + \frac{l}{2GA} \tag{6.99}$$

It has been shown that the critical load of the stick-spring model is (see eq. (4.28)):

$$F'_{cr} = 2\omega k l \tag{6.100}$$

After substituting eq. (6.99) into eq. (6.100) the critical load of the stick-spring model is:

$$\frac{1}{F'_{cr}} = \frac{1}{2\omega k l} = \frac{l^2}{3EI + 3EAc^2}\left(\frac{\gamma - 0.5}{s}\right) + \frac{l^2}{8EI + 8EAc^2} + \frac{1}{GA}\left(\frac{\gamma - 0.5}{s}\right) + \frac{1}{2GA} \tag{6.101}$$

In general, the critical load in eq. (6.101) can be written as:

$$\frac{1}{F'_{cr}} = \frac{1}{P_{cr;EI} + P_{cr;EAc^2}}\left(\frac{\gamma - 0.5}{s}\right) + \frac{1}{F_{cr;EI} + F_{cr;EAc^2}} + \frac{1}{P_{cr;GA}}\left(\frac{\gamma - 0.5}{s}\right) + \frac{1}{F_{cr;GA}} \tag{6.102}$$

Where the critical loads obtained from the stick-spring model are for:

- Individual bending for loadcase P [1, 2]

$$P_{cr;EI} = \frac{3EI}{l^2} \tag{6.103}$$

- Individual bending for loadcase P [1, 2]

$$P_{cr;EI} = \frac{3EI}{l^2} \tag{6.104}$$

- Global bending for loadcase F [1, 2]:

$$F_{cr;EAc^2} = \frac{8EAc^2}{l^2} \tag{6.105}$$

- Global bending for loadcase P [1, 2]:

$$F_{cr;EAc^2} = \frac{8EAc^2}{l^2} \tag{6.106}$$

- Racking shear for loadcase P [5]:

$$P_{cr;GA} = GA \tag{6.107}$$

- Racking shear for loadcase F :

$$F_{cr;GA} = 2GA \tag{6.108}$$

But the actual critical loads are for:

- Individual bending for loadcase P [4]:

$$P_{cr;EI} = \frac{\pi^2 EI}{4l^2} \tag{6.109}$$

- Individual bending critical load for loadcase F [5]:

$$F_{cr;EI} = \frac{7.837EI}{l^2} \tag{6.110}$$

- The actual global bending critical load for loadcase P [4]:

$$P_{cr;EAc^2} = \frac{\pi^2 EAc^2}{4l^2} \tag{6.111}$$

- The actual global bending critical load for loadcase F [5]:

$$F_{cr;EAc^2} = \frac{7.837EAc^2}{l^2} \tag{6.112}$$

- Racking shear for loadcase P [5]:

$$P_{cr;GA} = GA \tag{6.113}$$

- Racking shear for loadcase F :

$$F_{cr;GA} = 2GA \tag{6.114}$$

Eq. (6.101) gives an overestimated critical load, because the individual bending critical loads (see eq. (6.103) and eq. (6.104)) and the global bending critical loads (see eq. (6.105) and eq. (6.106)) are overestimated in the stick-spring-model. If the actual values for individual bending (see eq. (6.109) and eq. (6.110)), global bending (see eq. (6.111) and eq. (6.112)) and racking shear (see eq. (6.113) and eq. (6.114)) are substituted into eq. (6.102) the critical load can be rearranged into:

$$\frac{1}{F'_{cr}} = \frac{4l^2}{\pi^2 EI + \pi^2 EAc^2}\left(\frac{\gamma - 0.5}{s}\right) + \frac{l^2}{7.837EI + 7.837EAc^2} + \frac{1}{GA}\left(\frac{\gamma - 0.5}{s}\right) + \frac{1}{2GA} \tag{6.115}$$

The ratio for the individual bending critical loads is:

$$\frac{F_{cr;EI}}{P_{cr;EI}} = \frac{7.837EI}{l^2}\frac{4l^2}{\pi^2 EI} = 3.176 \tag{6.116}$$

The ratio for the global bending critical loads is:

$$\frac{F_{cr;EAc^2}}{P_{cr;EAc^2}} = \frac{7.837EAc^2}{l^2}\frac{4l^2}{\pi^2 EAc^2} = 3.176 \tag{6.117}$$

The ratio for the racking shear critical loads is:

$$\frac{F_{cr;GA}}{P_{cr;GA}} = \frac{2GA}{GA} \tag{6.118}$$

By substituting eq. (6.116), eq. (6.117) and eq. (6.118) into eq. (6.115) the critical load is:

$$\frac{1}{F'_{cr}} = \frac{1}{F_{cr;EAc^2}}\left[3.176\left(\frac{\gamma - 0.5}{s}\right)+1\right] + \frac{1}{F_{cr;GA}}\left[2\left(\frac{\gamma - 0.5}{s}\right)+1\right] = \frac{1}{\alpha F_{cr;EAc^2}} + \frac{1}{\beta' F_{cr;GA}} \tag{6.119}$$

In general, the critical load of eq. (6.119) can be written as:

$$\frac{1}{F'_{cr}} = \frac{1}{F'_{cr;EI} + F'_{cr;EAc^2}} + \frac{1}{F'_{cr;GA}} \tag{6.120}$$

Where the actual critical loads are for:

- Individual bending [17]:

$$F'_{cr;EI} = \alpha F_{cr;EI} = \frac{7.837\alpha EI}{l^2} \tag{6.121}$$

- Global bending [17]:

$$F'_{cr;EAc^2} = \alpha F_{cr;EAc^2} = \frac{7.837\alpha EAc^2}{l^2} \tag{6.122}$$

, where α is a reduction factor for the bending critical load, which takes the influence of the vertical top load P into account is:

$$\alpha = \frac{s}{s + 3.176(\gamma - 0.5)} \tag{6.123}$$

- Racking shear:

$$F'_{cr;GA} = 2\beta' GA \tag{6.124}$$

, where β' is a reduction factor for the racking shear critical load, which takes the influence of the vertical top load P into account is:

$$\beta' = \frac{1}{2\left(\frac{\gamma - 0.5}{s}\right) + 1} = \frac{1}{\frac{(2\gamma - 1) + s}{s}} = \frac{s}{s + 2\gamma - 1} \tag{6.125}$$

The racking shear critical load of eq. (6.124) is mathematically exact, because the racking shear buckling for loadcase P (see fig. 6.26b) is identical to the racking shear buckling shape for loadcase F (see fig. 6.30b).

If the actual values for individual bending (see eq. (6.121)), global bending (see eq. (6.122)) and racking shear (see eq. (6.124)) are substituted into eq. (6.120) the critical load of a braced frame is:

$$\frac{1}{F'_{cr}} = \frac{l^2}{7.837\alpha EI + 7.837\alpha EAc^2} + \frac{1}{2\beta' GA} \tag{6.126}$$

Formula (6.126) gives now a conservative critical load, because the overall bending buckling shape (see fig. 6.33a) is not identical to the racking shear buckling shape (see fig. 6.33b).

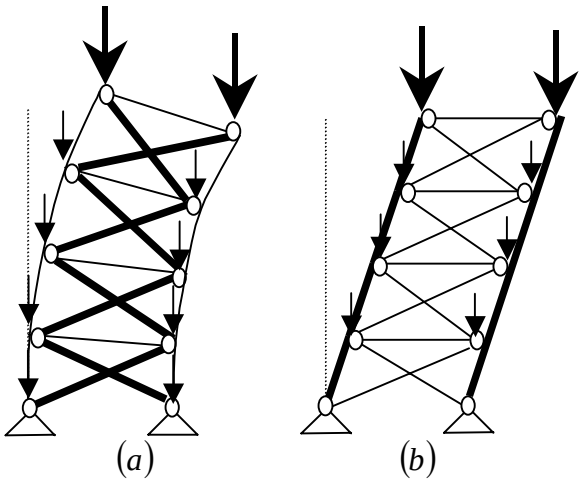

Figure 6.33 Buckling shapes for loadcase $P + F$.

6.5 Lateral stiffnesses of braced frame with continous columns

6.5.1 Individual bending stiffness

The individual bending stiffness caused by individual single curvature bending of the individual columns is (see fig. 6.34):

$$EI = \sum EI_{ci} \tag{6.127}$$

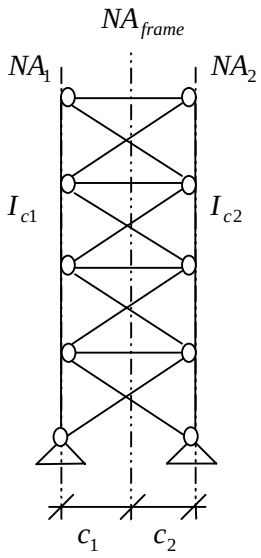

Figure 6.34 Individual bending stiffness braced frame with continous columns.

6.6 Accuracy

To establish the accuracy of the stick-spring model, critical loads of a number of one-bay X-braced frames were estimated using the stick-spring model and a finite element analyses. Finite element program ANSYS was used to obtain the eigenvalues of the braced frames. The braced frames have continous columns and pinned supports and the height of the frames varied from eight to forty stories. The X-braced frames are subjected to three different loadcases (see fig. 1.5):

- Vertical top loads (see fig. 1.5a).
- Uniformly distributed vertical loads (see fig. 1.5b).
- Load combinations (see fig. 1.5c).

Three different cases will be investigated for one-bay X-braced frames:

- Overall bending deformation only (see fig. 6.35a).
- Racking shear deformation only (see fig. 6.35b).
- All deformations together (see fig. 6.35a/b).

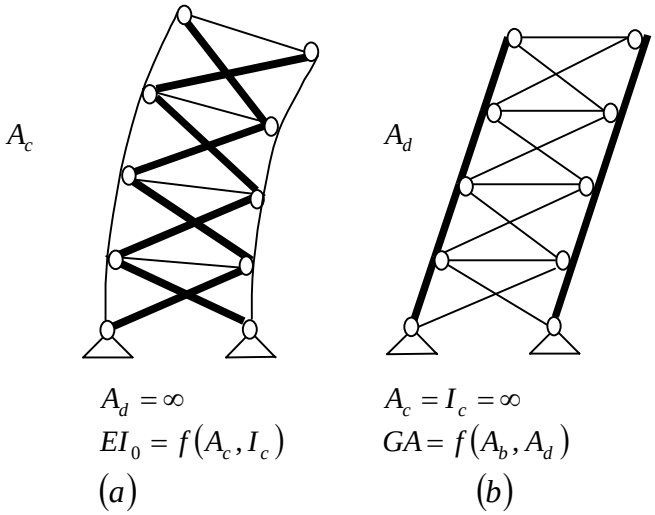

Fig 6.35 Cases to investigate for braced frames with non-continous columns.

The first two cases only represent theoretical cases, but the inclusion of them is very important to make a well-based judgement on the accuracy of the stick-spring model.
The critical loads found with the finite element method are assumed to be exact.

The errors are calculated as follows $\Delta = \dfrac{P_{cr} - P_{cr(ANSYS)}}{P_{cr(ANSYS)}} \times 100\%$.

If the error is negative the stick-spring model gives a conservative value for the critical load.

6.6.1 Numerical model

The numerical model is built up from LINK1 and BEAM3 elements (see fig. 6.36). LINK1 elements can only sustain normal forces and BEAM3 elements can sustain normal forces, bending moments and shear forces. The continous columns are BEAM3 elements with a cross-sectional area A_c and a second moment of area I_c. The beams and diagonals are LINK1 elements with only a cross-sectional area A_d and A_b. The connections between the BEAM3 and LINK1 elements are hinged.
The columns are pin-connected to the base. In this investigation it is assumed that the braced frame has an uniform cross-sectional area of the columns A_c, of the diagonals A_d and of the beams A_b up the height and an uniform second moment of area of the columns up the height I_c.

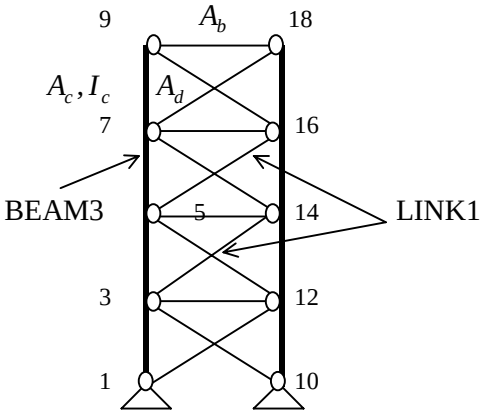

Figure 6.36 Numerical model for a braced frame with continous columns.

6.6.2 Example

An example is given for the three loadcases to demonstrate the simplicity and the accuracy of the stick-spring model. An eight storey high one bay X-braced frame with continous columns (see fig. 6.37) has an individual bending stiffness EI, a global bending stiffness EAc^2, a racking shear stiffness GA and is subjected to three different loadcases.
The characteristics of the braced frame can be found in table 6.1.

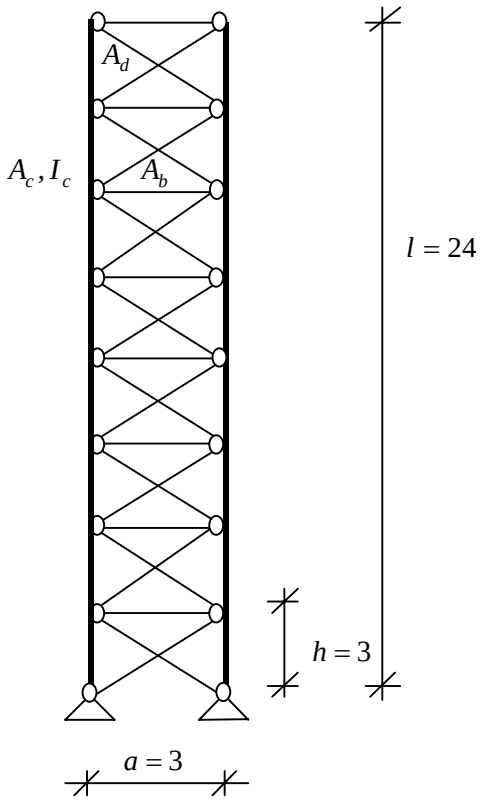

Figure 6.37 Example of braced frame with continous columns.

6.6.2.1 Stiffness parameters

The individual bending stiffness is (see eq. (6.127)):

$$EI = \sum EI_{ci} = 2EI_{ci} = 2 \times 2 \times 10^5 \times 3.281 \times 10^{-4} = 131.2MN$$

The global bending stiffness is (see eq. (6.60)):

$$EAc^2 = \sum EA_{ci}c_i^{\ 2} = 2EA_c c_i^{\ 2} = 2 \times 2 \times 10^5 \times 1.744 \cdot 10^{-2} \times 1.5^2 = 15696MN$$

The ratio between the bending stiffnesses:

$$\frac{EI}{EAc^2} \approx \frac{1}{120}$$

The racking shear stiffness is (see eq. (6.61)):

$$GA_X = \frac{2a^2 hEA_d}{d^3} = \frac{2 \times 3^2 \times 3 \times 2 \times 10^5 \times 3.75 \times 10^{-3}}{\left(3\sqrt{2}\right)^3} = 530.3MN$$

6.6.2.2 Vertical top load

The individual bending critical load is (see eq. (6.76)):

$$P_{cr;EI} = \frac{\pi^2 EI}{4l^2} = \frac{\pi^2 \times 131.2}{4 \times 24^2} = 0.56MN\ .$$

The global bending critical load is (see eq. (6.77)):

$$P_{cr;EAc^2} = \frac{\pi^2 EAc^2}{4l^2} = \frac{\pi^2 \times 15696}{4 \times 24^2} = 67.24MN$$

The overall bending critical load is:

$$P_{cr;EI_0} = \frac{\pi^2 EI_0}{4l^2} = \frac{\pi^2 \times \left(131.2 + 15696\right)}{4 \times 24^2} = 67.80MN$$

The racking shear critical load is (see eq. (6.78)):

$$P_{cr;GA} = GA = 530.3MN$$

The critical load is (see eq. (6.72)):

$$P_{cr} = \left[\frac{1}{P_{cr;EI} + P_{cr;EAc^2}} + \frac{1}{P_{cr;GA}}\right]^{-1} = \left[\frac{1}{0.56 + 67.24} + \frac{1}{530.3}\right]^{-1} = 60.11MN$$

6.6.2.3 Vertical UDL

The individual bending critical load is (see eq. (6.91)):

$$F_{cr;EI} = \frac{7.837EI}{l^2} = \frac{7.837 \times 131.2}{24^2} = 1.79MN$$

The global bending critical load is (see eq. (6.92)):

$$F_{cr;EAc^2} = \frac{7.837EAc^2}{l^2} = \frac{7.837 \times 15696}{24^2} = 213.6MN$$

The overall bending critical load is:

$$F_{cr;EI_0} = \frac{7.837EI_0}{l^2} = \frac{7.837 \times (131.2 + 15696)}{24^2} = 215.3MN$$

The racking shear critical load is (see eq. (6.93)):

$$F_{cr;GA} = 2GA = 2 \times 530.3 = 1060.6MN$$

The critical load is (see eq. (6.87)):

$$F_{cr} = \left[\frac{1}{F_{cr;EI} + F_{cr;EAc^2}} + \frac{1}{F_{cr;GA}} \right]^{-1} = \left[\frac{1}{1.79 + 213.6} + \frac{1}{565.7} \right]^{-1} = 179.0MN$$

6.6.2.4 Load combinations

Assume the vertical top load is 4 times the floorloading.
Factor γ is (see eq. (4.18)):

$$\gamma = \frac{F_d}{F_v} = 4$$

Reduction factor α is (see eq. (6.123)):

$$\alpha = \frac{s}{s + 3.176(\gamma - 0.5)} = \frac{8}{8 + 3.176(4 - 0.5)} = 0.4185$$

The individual bending critical load is (see eq. (6.121)):

$$F'_{cr;EI} = \frac{7.837\alpha EI}{l^2} = \alpha F_{cr;EI} = 0.4185 \times 1.79 = 0.75MN \text{ .}$$

The global bending critical load is (see eq. (6.122)):

$$F'_{cr;EAc^2} = \frac{7.837\alpha EAc^2}{l^2} = \alpha F_{cr;EAc^2} = 0.4185 \times 179.0 = 74.91MN \text{ .}$$

The overall bending critical load is:

$$F'_{cr;EI_0} = \frac{7.837\alpha EI_0}{l^2} = \frac{7.837 \times 0.4185 \times (131.2 + 15696)}{24^2} = 90.12MN \quad \text{(see table 16).}$$

Reduction factor β' is (see eq. (6.125)):

$$\beta' = \frac{s}{s + 2\gamma - 1} = \frac{8}{8 + 2 \times 4 - 1} = 0.5333$$

The racking shear critical load is (see eq. (6.124)):

$$F'_{cr;GA} = 2\beta' GA = 2 \times 0.5333 \times 530.3 = 565.7MN$$

The critical load is (see eq. (6.120)):

$$F'_{cr} = \left[\frac{1}{F'_{cr;EI} + F'_{cr;EAc^2}} + \frac{1}{F'_{cr;GA}} \right]^{-1} = \left[\frac{1}{0.75 + 89.37} + \frac{1}{565.7} \right]^{-1} = 77.74MN$$

All critical loads in this example calculated by the stick-spring model are in bold type and can be found in tables 6.12-6.17.

6.6.3 Results

The figures and tables below present the results of the critical loads obtained from the stick-spring model and the numerical analysis. Table 6.12 shows the accurracy of the global bending critical loads $P_{cr;EI_0}$ and $F_{cr;EI_0}$ and table 6.13 of the racking shear critical loads $P_{cr;GA}$ and $F_{cr;GA}$ and table 6.14 of the critical loads P_{cr} and F_{cr}. Table 6.15 shows the accuraccy of the global bending critical load $F'_{cr;EI_0}$, table 6.16 of the racking shear critical load $F'_{cr;GA}$ and table 6.17 of the critical load F'_{cr}.

Table 6.12. Critical loads for braced frames with continous columns, overall bending deformation only.

Number of storeys s [-]	Vertical top load P with $P_{cr;EI_0} = \frac{\pi^2 EI_0}{4l^2}$			UDL $F(\gamma = 0.5)$ $F_{cr;EI_0} = \frac{7.837 EI_0}{l^2}$		
	Critical loads P_{cr} [MN]			Critical loads F_{cr} [MN]		
	Stick-spring model	ANSYS	Error Δ [%]	Stick-spring model	ANSYS	Error Δ [%]
8	**67.80**	68.14	-0.5	**215.3**	216.4	-0.5
16	16.95	16.97	-0.1	53.84	53.87	-0.1
24	7.53	7.54	0.0	23.93	23.93	0.0
32	4.24	4.24	0.0	13.46	13.46	0.0
40	2.71	2.71	0.0	8.61	8.61	0.0

Table 6.13. Critical loads for braced frames with continous columns, racking shear deformation only.

Number of storeys s [-]	Vertical top load P with $P_{cr;GA} = GA$ (see eq. (6.78))			UDL $F(\gamma = 0.5)$ with $F_{cr;GA} = 2GA$ (see eq. (6.93))		
	Critical loads P_{cr} [MN]			Critical loads F_{cr} [MN]		
	Stick-spring model	ANSYS	Error Δ [%]	Stick-spring model	ANSYS	Error Δ [%]
8	**530.3**	530.3	0.0	**1060.7**	1060.6	0.0
16	530.3	530.2	0.0	1060.6	1060.5	0.0
24	530.3	530.3	0.0	1060.6	1060.3	0.0
32	530.2	530.2	0.0	1060.5	1060.0	0.0
40	530.2	530.2	0.0	1060.4	1059.7	0.1

Table 6.14. Critical loads for braced frames with continous columns, all deformations together.

Number of storeys s [-]	Vertical top load P (see eq. (6.72))			UDL $F(\gamma = 0.5)$ (see eq. (6.87))		
	Critical loads P_{cr} [MN]			Critical loads F_{cr} [MN]		
	Stick-spring model	ANSYS	Error Δ [%]	Stick-spring model	ANSYS	Error Δ [%]
8	**60.11**	60.41	-0.5	**179.0**	180.0	-0.6
16	16.43	16.44	-0.1	51.24	51.37	-0.3
24	7.43	7.43	0.0	23.40	23.43	-0.1
32	4.20	4.20	0.0	13.29	13.30	-0.1
40	2.70	2.70	0.0	8.54	8.55	0.0

Table 6.15. Critical loads for braced frames with continous columns, $P+F$, overall bending deformation only.

Number of storeys s [-]	Load combination $P+F$ with $F'_{cr;EI_0}=\frac{7.837\alpha EI_0}{l^2}$											
	Critical loads F'_{cr} [MN]											
	$\gamma=1$			$\gamma=4$			$\gamma=16$			$\gamma=64$		
	Stick-spring model	ANSYS	Error Δ [%]	Stick-spring model	ANSYS	Error Δ [%]	Stick-spring model	ANSYS	Error Δ [%]	Stick-spring model	ANSYS	Error Δ [%]
8	179.7	181.9	-1.2	**90.12**	91.73	-1.8	30.10	30.44	-1.1	8.22	8.27	-0.7
16	48.98	49.23	-0.5	31.77	32.22	-1.4	13.21	13.35	-1.1	3.96	3.98	-0.5
24	22.44	22.52	-0.3	16.35	16.56	-1.2	7.84	7.94	-1.3	2.55	2.56	-0.5
32	12.82	12.86	-0.3	9.99	10.10	-1.1	5.30	5.37	-1.4	1.84	1.86	-0.7
40	8.29	8.30	-0.2	6.74	6.81	-0.9	3.86	3.92	-1.4	1.43	1.44	-0.8

Table 6.16. Critical loads for braced frames with continous columns, $P+F$, racking shear deformation only.

Number of storeys s [-]	Load combination $P+F$ with $F'_{cr;GA}=2\beta' GA$ (see eq. (6.124))											
	Critical loads F'_{cr} [MN]											
	$\gamma=1$			$\gamma=4$			$\gamma=16$			$\gamma=64$		
	Stick-spring model	ANSYS	Error Δ [%]	Stick-spring model	ANSYS	Error Δ [%]	Stick-spring model	ANSYS	Error Δ [%]	Stick-spring model	ANSYS	Error Δ [%]
8	942.8	942.8	0.0	**565.7**	565.7	0.0	217.6	217.6	0.0	62.85	62.85	0.0
16	998.2	998.1	0.0	737.8	737.8	0.0	361.1	361.1	0.0	118.7	118.7	0.0
24	1018.2	1017.9	0.0	821.1	821.0	0.0	462.8	462.8	0.0	168.6	168.6	0.0
32	1028.4	1027.9	0.0	870.2	869.9	0.0	538.7	538.6	0.0	213.4	213.4	0.0
40	1034.6	1033.9	0.1	902.5	902.0	0.1	597.4	597.3	0.0	254.0	254.0	0.0

Table 6.17. Critical loads for braced frames with continous columns, all deformations together.

Number of storeys s [-]	Load combination $P+F$											
	Critical loads F'_{cr} [MN] (see eq. (6.120))											
	$\gamma=1$			$\gamma=4$			$\gamma=16$			$\gamma=64$		
	Stick-spring model	ANSYS	Error Δ [%]	Stick-spring model	ANSYS	Error Δ [%]	Stick-spring model	ANSYS	Error Δ [%]	Stick-spring model	ANSYS	Error Δ [%]
8	150.9	154.0	-2.0	**77.74**	80.31	-3.2	26.44	26.94	-1.9	26.44	26.94	-0.9
16	46.69	47.06	-0.8	30.46	31.04	-1.9	12.74	12.93	-1.5	12.74	12.93	-0.6
24	21.96	22.06	-0.5	16.03	16.27	-1.4	7.71	7.82	-1.5	7.71	7.82	-0.6
32	12.67	12.71	-0.3	9.88	9.99	-1.0	5.25	5.33	-1.5	5.25	5.33	-0.7
40	8.22	8.24	-0.3	6.69	6.76	-0.7	3.84	3.89	-1.5	3.84	3.89	-0.8

Observations

- **The buckling behavior of a braced frame with non-continous columns can be divided into individual bending, global bending and racking shear.**

- **The dominant buckling shape for highrise braced frames is global bending.**

- **The racking shear buckling shape of a braced with continous columns for loadcase P, F and $P+F$ has a definite buckling shape, which means the racking shear buckling shape can assume only one form.** Therefore the racking shear buckling shape has one eigenvalue and one critical load.

- **The overall bending critical loads $P_{cr;EI_0} = \frac{\pi^2 EI_0}{4l^2}$, $F_{cr;EI_0} = \frac{7.837EI_0}{l^2}$ and $F'_{cr;EI_0} = \frac{7.837\alpha EI_0}{l^2}$ are conservative,** because all errors are negative (see table 6.12 and 6.15).

- **The racking shear critical loads are $P_{cr;GA} = GA$, $F_{cr;GA} = 2GA$ and $F'_{cr;GA} = 2\beta' GA$,** because the errors are zero (see table 6.13 and 6.16). This is because the racking shear deflection shape of the braced frame is identical to the racking shear buckling shape of the braced frame.

- **The critical loads $P_{cr} = \left[\frac{4l^2}{\pi^2 EI + \pi^2 EAc^2} + \frac{1}{GA}\right]^{-1}$, $F_{cr} = \left[\frac{l^2}{7.837EI + 7.837EAc^2} + \frac{1}{2GA}\right]^{-1}$ and $F'_{cr} = \left[\frac{l^2}{7.837\alpha EI + 7.837\alpha EAc^2} + \frac{1}{2\beta' GA}\right]^{-1}$ are conservative,** because the errors are negative (see table 6.12-6.17). This because the overall bending buckling shape is not identical to the racking shear buckling shape.

- **The stick-spring model compares very well to the numerical results for the three loadcases (see table 6.12-6.17).**
  The highest conservative error for loadcase P is -0.5 %.
  The highest conservative error for loadcase F is -0.6 %.
  The highest conservative error for loadcase $P+F$ is: -3.2 %.

- **All suggested formula give good results for the preliminary design of highrise braced frames with continous columns within a maximum error of 3.2%.**

- **All observations are only valid for X-braced frames of eight till forty stories pin-connected to the base with continous columns.**

- **All observations are only valid for the investigated cases in this parameterstudy.**

6.7 Comparison between the two investigated braced frames

This section compares a braced frame with non-continous and continous columns (see table 6.18).

Table 6.18. Comparison between braced frames with continous columns and non-continous columns.

	Non-continous	**Continous**
Columns	non-continous	continous
Lateral stiffnesses	EAc^2, GA	EI, EAc^2 and GA
Individual bending critical load for loadcase P	$P_{cr;EI} = 0$	$P_{cr;EI} = \frac{\pi^2 EI}{4l^2}$
Global bending critical load for loadcase P	$P_{cr;EAc^2} = \frac{\pi^2 EAc^2}{4l^2}$	$P_{cr;EAc^2} = \frac{\pi^2 EAc^2}{4l^2}$
Racking shear critical load for loadcase P	$P_{cr;GA} = GA$	$P_{cr;GA} = GA$
Racking shear buckling shape for loadcase P	can assume any form	assumes one form
Critical load for loadcase P	$\frac{1}{P_{cr}} = \frac{1}{P_{cr;EAc^2}} + \frac{1}{P_{cr;GA}}$	$\frac{1}{P_{cr}} = \frac{1}{P_{cr;EI} + P_{cr;EAc^2}} + \frac{1}{P_{cr;GA}}$
Individual bending critical load for loadcase F	$F_{cr;EI} = 0$	$F_{cr;EI} = \frac{7.837EI}{l^2}$
Global bending critical load for loadcase F	$F_{cr;EAc^2} = \frac{7.837EAc^2}{l^2}$	$F_{cr;EAc^2} = \frac{7.837EAc^2}{l^2}$
Racking shear critical load for loadcase F	$F_{cr;GA} = \eta GA$	$F_{cr;GA} = 2GA$
Racking shear buckling shape for loadcase F	assumes one form	assumes one form
Critical load for loadcase F	$\frac{1}{F_{cr}} = \frac{1}{F_{cr;EAc^2}} + \frac{1}{F_{cr;GA}}$	$\frac{1}{F_{cr}} = \frac{1}{F_{cr;EI} + F_{cr;EAc^2}} + \frac{1}{F_{cr;GA}}$
Individual bending critical load for loadcase $P + F$	$F'_{cr;EI} = 0$	$F'_{cr;EI} = \frac{7.837\alpha EI}{l^2}$
Global bending critical load for loadcase $P + F$	$F'_{cr;EAc^2} = \frac{7.837\alpha EAc^2}{l^2}$	$F'_{cr;EAc^2} = \frac{7.837\alpha EAc^2}{l^2}$
Racking shear critical load for loadcase $P + F$	$F'_{cr;GA} = \eta'\beta GA$	$F_{cr;GA} = 2\beta' GA$
Reduction factor for racking shear critical load	$\beta = \frac{s}{s + \gamma - 0.5}$	$\beta' = \frac{s}{s + 2\gamma - 1}$
Racking shear buckling shape for loadcase $P + F$	assumes one form	assumes one form
Critical load for loadcase $P + F$	$\frac{1}{F'_{cr}} = \frac{1}{F'_{cr;EAc^2}} + \frac{1}{F'_{cr;GA}}$	$\frac{1}{F'_{cr}} = \frac{1}{F'_{cr;EI} + F'_{cr;EAc^2}} + \frac{1}{F'_{cr;GA}}$

Conclusions:

- **The errors of a braced frames with continous columns are lower then of braced frames with non-continous columns for loadcase** F and $P+F$, because the global bending and racking shear buckling shapes of a braced frame with continous columns (see fig. 6.38a/b) are more identical to each other then the global bending and racking shear buckling shapes of a braced frame with non-continous columns (see fig. 6.38c/d).

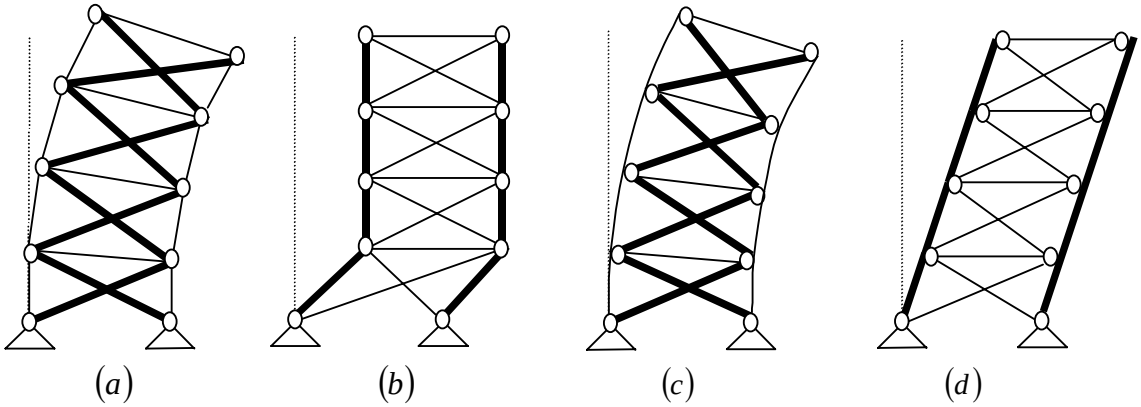

Figure 6.38 Buckling shapes of braced frames for loadcase F *and* $P+F$.

7 One bay rigid frames

7.1 Fixed rigid frames

A rigid frame is a structure which consists of columns and beams (see fig. 7.1). The joints of a rigid frame are moment resistant. The boundary conditions at the base of a rigid frame can be pinned, fixed or flexible. In this investigation the boundary conditions are fixed (see fig. 7.1). This fixed connection at the base introduces a new mode of deformation to the buckling behavior, which is individual bending.

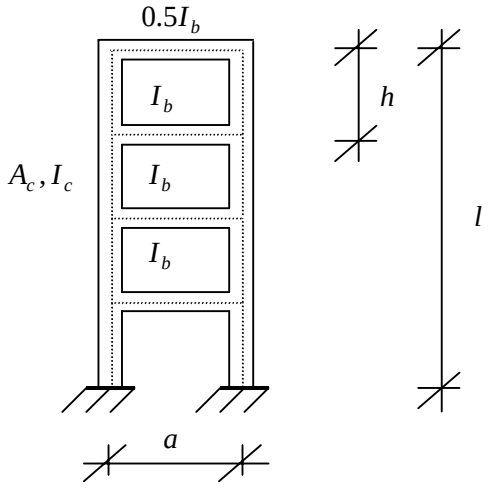

Figure 7.1 Fixed rigid frame.

The buckling behaviour of a fixed rigid frame can be divided into 4 modes of deformation:

- Individual bending of the columns (EI): single curvature bending of the vertical members (see fig. 7.2a).
- Global bending (EAc^2): axial deformation in the columns (shortening of the columns at one side of the rigid frame and lengthening at the other side) (see fig. 7.2b).
- Racking shear of the columns (GA_c): double curvature bending in the columns (see fig. 7.2c).
- Racking shear of the beams (GA_b): double curvature bending in the beams (see fig. 7.2d).

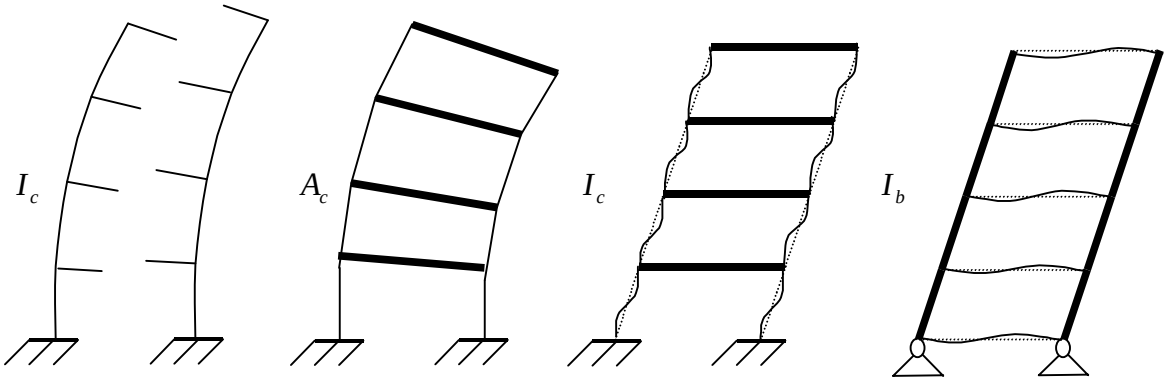

$I_b = 0$	$I_b = \infty$	$A_c = I_b = \infty$	$A_c = I_c = \infty$
$EI = f(I_c)$	$EAc^2 = f(A_c)$	$GA_c = f(I_c)$	$GA_b = f(I_b)$
(a)	(b)	(c)	(d)

Fig 7.2 Modes of behavior of a fixed rigid frame.

Assumptions:

- The column-beam connections are fully moment resistant.
- The rigid frame is fixed to the base.
- The columns are continuous up the total height of the structure.
- The fixed rigid frame has four lateral stiffness parameters $EI = f(I_c)$, $EAc^2 = f(A_c)$, $GA_b = f(I_b)$ and $GA_c = f(I_c)$.
- For the racking shear buckling shape of the beams it is assumed that the column-base connections are pinned (see fig. 7.2d).
- The cross-section of the beams is infinite $A_b = \infty$ for all modes of behaviour.
- Shear deformations in the beams and columns are neglected, which means $A_{b;shear} = A_{c;shear} = \infty$.

7.1.1 Vertical top loads

A stick-spring model is introduced here to obtain an approximate solution for the overall critical load of a one-bay fixed rigid frame (see fig. 7.3a). It is first suggested to transform a rigid frame subjected to vertical top loads into a multiple stick model (see fig. 7.3b).
In a multiple stick model a pinned column is supported by a flexural cantilever with individual bending stiffness EI and by a shear-flexure cantilever with global bending stiffness EAc^2, racking shear stiffness of the columns GA_c and racking shear stiffness of the beams GA_b.
The flexural cantilever can be transformed into a stick-spring model with horizontal translational spring stiffness $k_1 = f(EI)$ and the shear-flexure cantilever can be transformed into a stick-spring model with horizontal translational spring stiffness $k_2 = f(EAc^2, GA_c, GA_b)$. The multiple stick model can then be transformed into a stick-spring model, where the horizontal translation spring $k = f(k_1, k_2)$ (see fig. 7.3c).
The justification for this suggestion is that the shear-flexure cantilever can be seen as a quasi-braced frame with the flexural cantilever adding an individual bending stiffness EI of the rigid frame.
If the beams of a rigid frame are cut through it can still develop individual bending (see fig. 7.2a), because of the fixed connection at the bottom and the continuous columns.

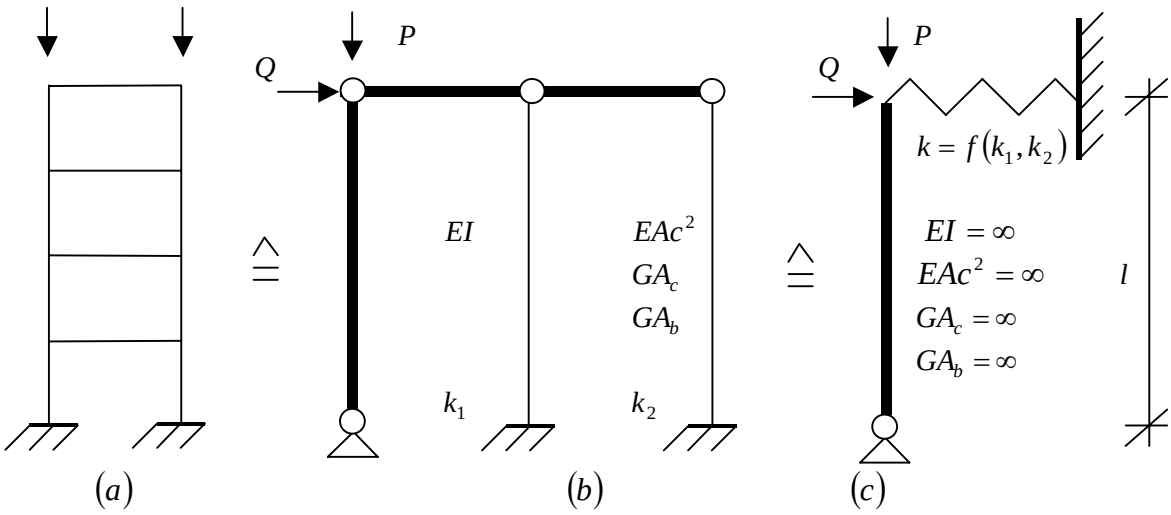

Figure 7.3 Transformation of fixed rigid frame into stick-spring model (vertical top loads).

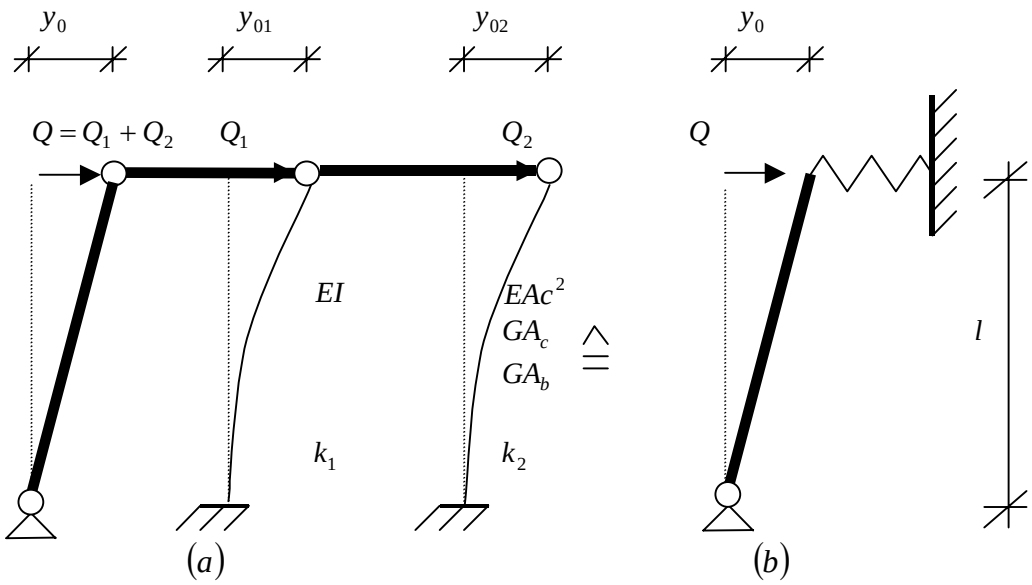

Figure 7.4 Deformations caused by load Q .

The horizontal beams are rigid links and therefore the first-order deformation at the top of the multiple stick model is (see fig. 7.4a):

$$y_0 = y_{01} = y_{02} \tag{7.1}$$

The horizontal load Q at the top of the multiple stick-model is (see fig. 7.4a):

$$Q = Q_1 + Q_2 \tag{7.2}$$

The first-order deformations at the top of the stick-spring models are

$$y_0 = \frac{Q}{k} \tag{7.3}$$

$$y_{01} = \frac{Q_1}{k_1} \tag{7.4}$$

and

$$y_{02} = \frac{Q_2}{k_2} \tag{7.5}$$

Substituting eq. (7.3), eq. (7.4) and eq. (7.5) into eq. (7.2) leads to:

$$ky_0 = k_1 y_{01} + k_2 y_{02} \tag{7.6}$$

Sustituting eq. (7.1) into eq. (7.6) yields the horizontal translational spring stiffness k :

$$k = k_1 + k_2 = \sum k_i \tag{7.7}$$

The critical load of the stick-spring model for the rigid frame is (see eq. (4.3)):

$$P_{cr} = kl \tag{7.8}$$

The critical loads $P_{cr;1}$ and $P_{cr;2}$ of the stick-spring models shown in fig. 7.5b and 7.6b for the separate cantilevers can similarly be obtained from:

$$P_{cr;1} = k_1 l \tag{7.9}$$

and

$$P_{cr;2} = k_2 l \tag{7.10}$$

Substituting eq. (7.7) into eq. (7.8) leads to:

$$P_{cr} = k_1 l + k_2 l \tag{7.11}$$

Substituting eq. (7.9) and eq. (7.10) into eq. (7.11) leads to:

$$P_{cr} = P_{cr;1} + P_{cr;2} = \sum P_{cr;i} \tag{7.12}$$

The flexural cantilever, with individual bending EI, is assumed to be standing alone so $k_2 = 0$ (see fig. 7.5a). This can be modelled into a stick-spring model with horizontal translation spring stiffness $k_1 = f(EI)$ (see fig. 7.5b).

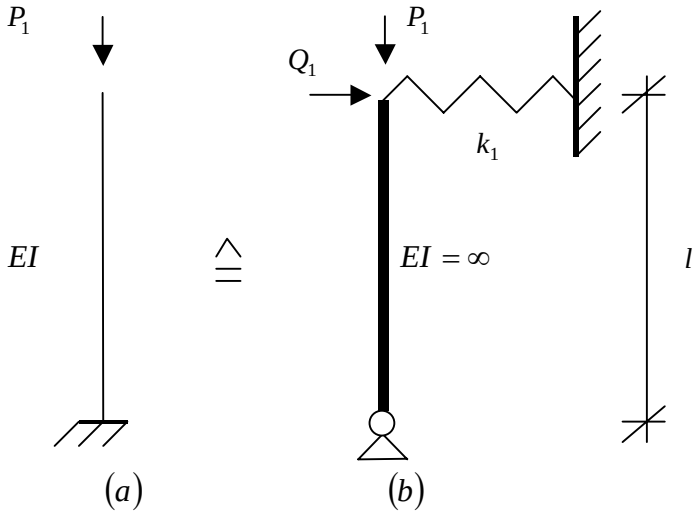

Figure 7.5 Flexural cantilever subjected to top loads.

The first-order deformation at the top of the flexural cantilever is (see fig. 7.5a):

$$y_{01} = y_{EI} = \frac{Q_1 l^3}{3EI} \tag{7.13}$$

The first-order deformation at the top of the stick-spring model is (see fig. 7.5b):

$$y_{01} = \frac{Q_1}{k_1} \tag{7.14}$$

Both deformations are the same yielding the horizontal translational spring stiffness k_1:

$$k_1 = \frac{3EI}{l^3} \tag{7.15}$$

After substituting eq. (7.15) into eq. (7.9) the critical load of the stick-spring model is:

$$P_{cr;1} = \frac{3EI}{l^2} \tag{7.16}$$

In general, the critical load of eq. (7.16) can be written as:

$$P_{cr;1} = P_{cr;EI} \tag{7.17}$$

The shear-flexure cantilever, with global bending stiffness EAc^2, racking shear stiffness of the columns GA_c and racking shear stiffness of the beams GA_b is assumed to be standing alone so $k_1 = 0$ (see fig. 7.6a). This can be modelled into a stick-spring model with horizontal translation spring stiffness $k_2 = f\left(EAc^2, GA_c, GA_b\right)$ (see fig. 7.6b).

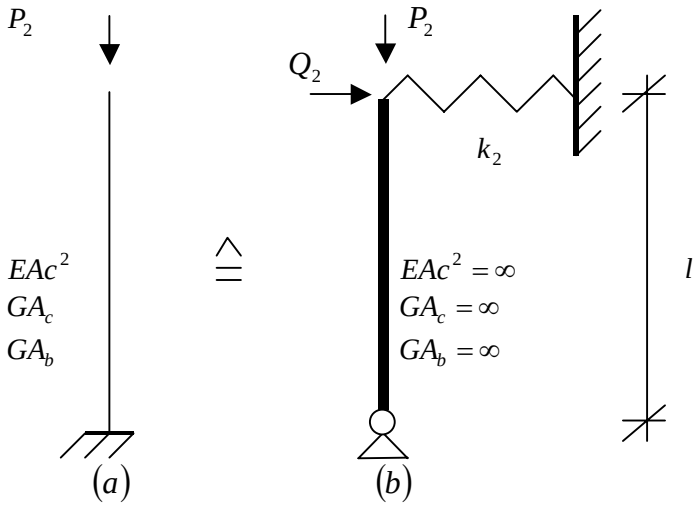

Figure 7.6 Shear-flexure cantilever subjected to top loads.

The first-order deformation at the top of the spring-flexure cantilever is:

$$y_{02} = y_{EAc^2} + y_{GA_c} + y_{GA_b} = \frac{Q_2 l^3}{3EAc^2} + \frac{Q_2 l}{GA_c} + \frac{Q_2 l}{GA_b} \tag{7.18}$$

The first-order deformation at the top of the stick-spring model is:

$$y_{02} = \frac{Q_2}{k_2} \tag{7.19}$$

Both deformations are the same yielding the horizontal translational spring stiffness k_2:

$$\frac{1}{k_2} = \frac{l^3}{3EAc^2} + \frac{l}{GA_c} + \frac{l}{GA_b} \tag{7.20}$$

After substituting eq. (7.20) into eq. (7.10) the critical load of the stick-spring model is:

$$\frac{1}{P_{cr;2}} = \frac{1}{k_2 l} = \frac{l^2}{3EAc^2} + \frac{1}{GA_c} + \frac{1}{GA_b} \tag{7.21}$$

In general, the critical load of eq. (7.21) can be written as:

$$P_{cr;2} = \left[\frac{1}{P_{cr;EAc^2}} + \frac{1}{P_{cr;GA_c}} + \frac{1}{P_{cr;GA_b}} \right]^{-1} \tag{7.22}$$

After substituting eq. (7.17) and eq. (7.22) into eq. (7.12) the critical load of a rigid frame is:

$$P_{cr} = P_{cr;EI} + \left[\frac{1}{P_{cr;EAc^2}} + \frac{1}{P_{cr;GA_c}} + \frac{1}{P_{cr;GA_b}} \right]^{-1} \tag{7.23}$$

Where the critical loads obtained from the stick spring model are for:

- Individual bending [1, 2]:

$$P_{cr;EI} = \frac{3EI}{l^2} \tag{7.24}$$

- Global bending [1, 2]:

$$P_{cr;EAc^2} = \frac{3EAc^2}{l^2} \tag{7.25}$$

- Racking shear of the columns [5]:

$$P_{cr;GA_c} = GA_c' = \frac{24EI_c}{h^2} \tag{7.26}$$

- Racking shear of the beams [5]:

$$P_{cr;GA_b} = GA_b = \frac{12EI_b}{ah} \tag{7.27}$$

The actual critical loads are for:

- Individual bending [4]:

$$P_{cr;EI} = \frac{\pi^2 EI}{4l^2} \tag{7.28}$$

- Global bending [4]:

$$P_{cr;EAc^2} = \frac{\pi^2 EAc^2}{4l^2} \tag{7.29}$$

- Racking shear of the columns [27]:

$$P_{cr;GA_c} = GA_c = \frac{2\pi^2 EI_c}{h^2} \tag{7.30}$$

- Racking shear of the beams [5]:

$$P_{cr;GA_b} = GA_b = \frac{12EI_b}{ah} \tag{7.31}$$

The individual bending critical load of the stick-spring model (see eq. (7.24)) is 21.6% larger then the actual individual bending critical load of a rigid frame (see eq. (7.28)), because the individual bending deflection shape of a rigid frame is not identical to the individual bending buckling shape of a rigid frame. The deflection shape of a rigid frame is a third order function and the buckling shape of a rigid frame is a cosine function.

Similar reasoning can be done for the global bending critical load (compare eq. (7.25) and eq. (7.29)).

The racking shear critical load of the columns of the stick-spring model (see eq. (7.26)) is 21.6% larger then the actual racking shear critical load of the columns of a rigid frame (see eq. (7.30)), because the racking shear deflection shape of the columns of a rigid frame (see fig. 7.7a) is not identical to the racking shear buckling shape of the columns of a rigid frame (see fig. 7.7b). The deflection shape of a rigid frame is a third order function and the buckling shape of a rigid frame is a cosine function.

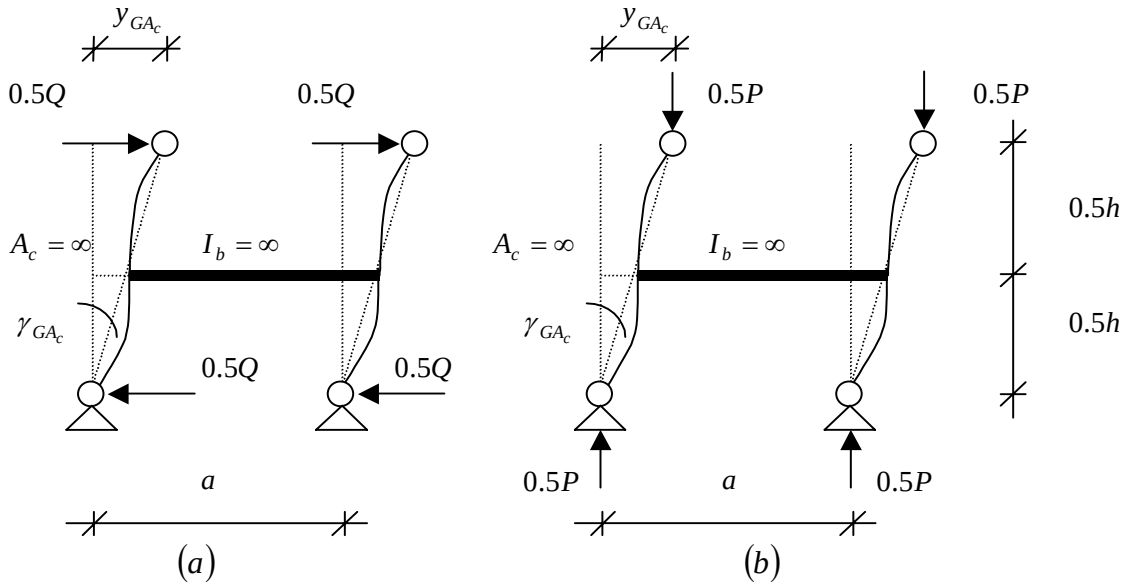

Figure 7.7 Double curvature bending of the columns.

The racking shear critical load of the beams of a fixed rigid (see eq. (7.31)) is assumed to be the same as the racking shear critical load of the beams of a flexible rigid frame (see eq. (7.84)).

If the actual values for individual bending (see eq. (7.28)), global bending (see eq. (7.29)), racking shear of the columns (see eq. (7.30)) and racking shear of the beams (see eq. (7.31)) are substituted into eq. (7.23) the critical load of a rigid frame becomes:

$$P_{cr} = \frac{\pi^2 EI}{4l^2} + \left[\frac{4l^2}{\pi^2 EAc^2} + \frac{h^2}{2\pi^2 EI_c} + \frac{ah}{12EI_b} \right]^{-1} \tag{7.32}$$

7.1.2 Uniformly distributed vertical loads

In fig. 7.8a a rigid frame is subjected to vertical point loads F_v accept for the point loads at the roof and at the bottom of the frame which are $0.5F_v$. In a similar way a stick-spring model can be used to obtain an approximate solution for the overall critical load of a rigid frame. First a rigid frame subjected to vertical point loads is transformed into a multiple stick model subjected to a horizontal UDL w and a vertical UDL f (see fig. 7.8b). The multiple stick model is then transformed into the stick-spring model (see fig. 7.8c).

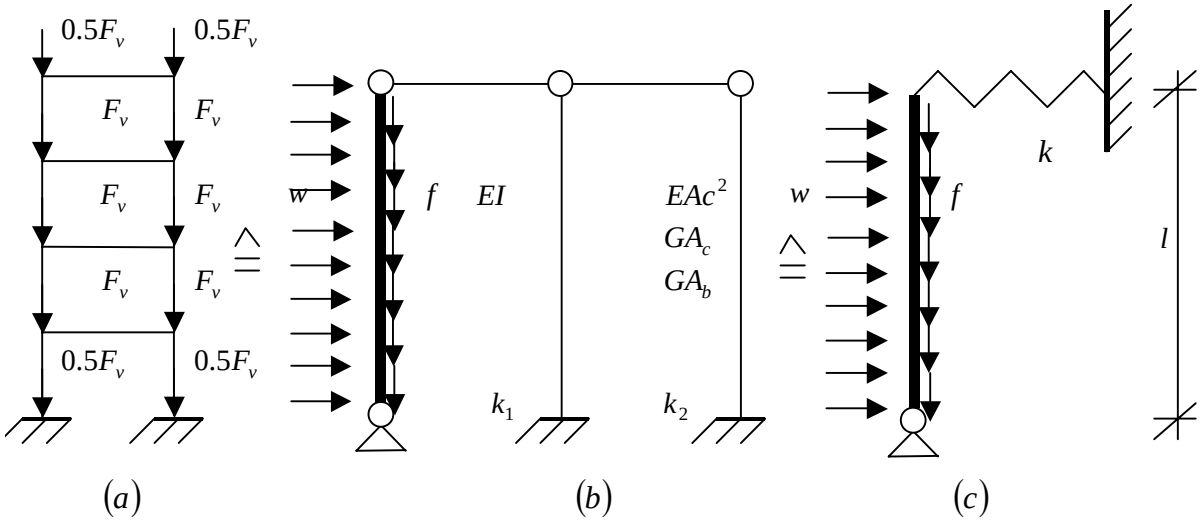

Figure 7.8 Transformation of fixed rigid frame into stick-spring model (UDL).

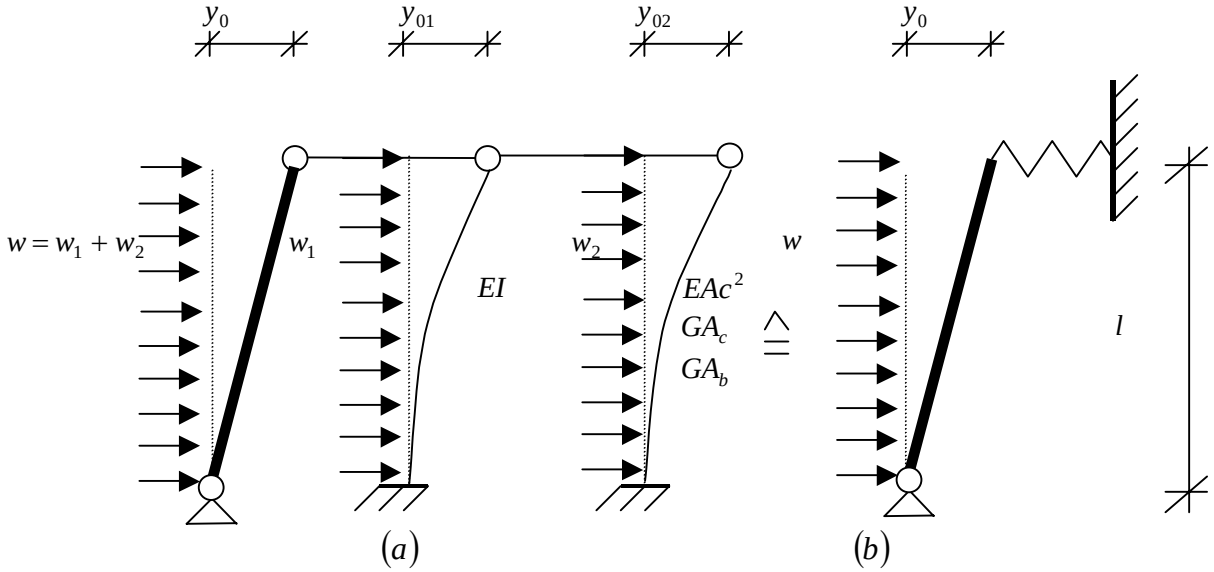

Figure 7.9 Deformations multiple stick model caused by load w.

The horizontal beams are rigid links and therefore the first-order deformation at the top of the multiple stick model is (see fig. 7.9a):

$$y_0 = y_{01} = y_{02} \tag{7.33}$$

The horizontal UDL w on the multiple stick model is (see fig. 7.9a):

$$w = w_1 + w_2 \tag{7.34}$$

The first-order deformations at the top of the stick-spring models are

$$y_0 = \frac{wl}{2k} \tag{7.35}$$

$$y_{01} = \frac{w_1 l}{2k_1} \tag{7.36}$$

and

$$y_{02} = \frac{w_2 l}{2k_2} \tag{7.37}$$

Substituting eq. (7.35), eq. (7.36) and eq. (7.37) into eq. (7.34) leads to:

$$2k\frac{y_0}{l} = 2k_1\frac{y_{01}}{l} + 2k_2\frac{y_{02}}{l} \tag{7.38}$$

Substituting eq. (7.33) into (7.38) yields the horizontal translational spring stiffness k:

$$2k = 2k_1 + 2k_2 = 2\sum k_i \tag{7.39}$$

The critical load of the stick-spring model for a rigid frame is (see eq. (4.12)):

$$F_{cr} = 2kl \tag{7.40}$$

The critical loads $F_{cr;1}$ and $F_{cr;2}$ of the stick-spring models shown in fig. 7.10b and 7.11b for the separate cantilevers can similarly be obtained from:

$$F_{cr;1} = 2k_1 l \tag{7.41}$$

and

$$F_{cr;2} = 2k_2 l \tag{7.42}$$

Substituting eq. (7.39) into eq. (7.40) leads to:

$$F_{cr} = 2k_1 l + 2k_2 l \tag{7.43}$$

Substituting eq. (7.41) and eq. (7.42) into eq. (7.43) leads to:

$$F_{cr} = F_{cr;1} + F_{cr;2} = \sum F_{cr;i} \tag{7.44}$$

The flexural cantilever, with individual bending EI, is assumed to be standing alone so $k_2 = 0$ (see fig. 7.10a). This can be modelled into a stick-spring model with horizontal translation spring stiffnes $k_1 = f(EI)$ (see fig. 7.10b).

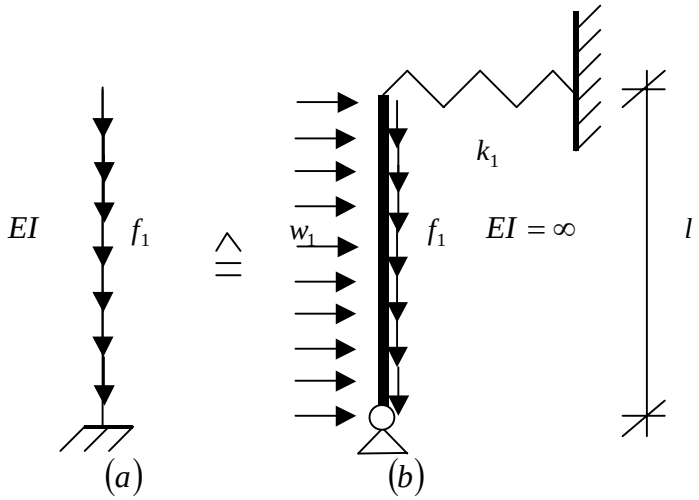

Figure 7.10 Flexure cantilever subjected to UDL.

The first-order deformation at the top of the flexural cantilever is:

$$y_{01} = y_{EI} = \frac{w_1 l^4}{8EI} \tag{7.45}$$

The first-order deformation at the top of the stick-spring model is:

$$y_{01} = \frac{2w_1 l}{k_1} \tag{7.46}$$

Both deformations are the same yielding the horizontal translational spring stiffness k_1:

$$k_1 = \frac{4EI}{l^3} \tag{7.47}$$

After substituting eq. (7.47) into eq. (7.41) the critical load of the stick-spring model is:

$$F_{cr;1} = \frac{8EI}{l^2} \tag{7.48}$$

In general, the critical load of eq. (7.48) can be written as:

$$F_{cr;1} = F_{cr;EI} \tag{7.49}$$

The shear-flexure cantilever, with global bending stiffness EAc^2, racking shear stiffness of the columns GA_c and racking shear stiffness of the beams GA_b, is assumed to be standing alone so $k_1 = 0$ (see fig. 7.11a). This can be modelled into a stick-spring model with horizontal translation spring stiffness $k_2 = f\left(EAc^2, GA_c, GA_b\right)$ (see fig. 7.11b).

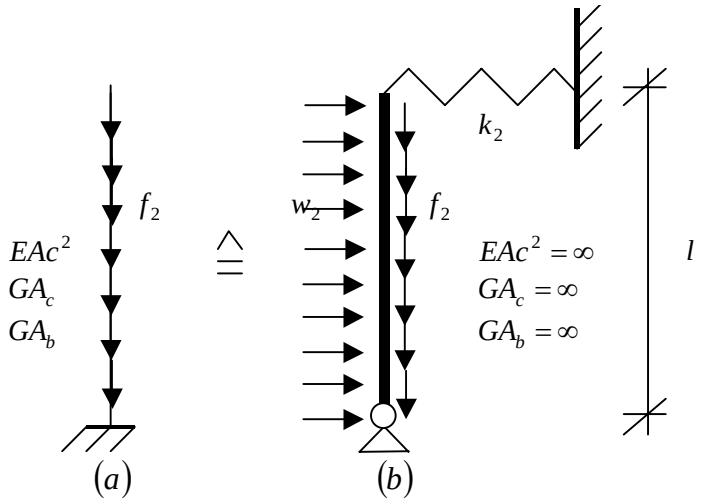

Figure 7.11 Shear-flexure cantilever subjected to UDL.

The first-order deformation at the top of the spring-flexure cantilever is:

$$y_{02} = y_{EAc^2} + y_{GA_c} + y_{GA_b} = \frac{w_2 l^4}{8EAc^2} + \frac{w_2 l}{2GA_c} + \frac{w_2 l}{2GA_b} \tag{7.50}$$

The first-order deformation at the top of the stick-spring model is:

$$y_{02} = \frac{w_2 l}{2k_2} \tag{7.51}$$

Both deformations are the same yielding the horizontal translational spring stiffness k_2:

$$\frac{1}{k_2} = \frac{l^3}{4EAc^2} + \frac{l}{GA_c} + \frac{l}{GA_b} \tag{7.52}$$

After substituting eq. (7.52) into eq. (7.42) the critical load of the stick-spring model is:

$$\frac{1}{F_{cr;2}} = \frac{1}{2k_2 l} = \frac{l^2}{8EAc^2} + \frac{1}{2GA_c} + \frac{1}{2GA_b} \tag{7.53}$$

In general, the critical load of eq. (7.53) can be written as:

$$F_{cr;2} = \left[\frac{1}{F_{cr;EAc^2}} + \frac{1}{F_{cr;GA_c}} + \frac{1}{F_{cr;GA_b}} \right]^{-1} \tag{7.54}$$

After substituting eq. (7.49) and eq. (7.54) into eq. (7.44) the critical load of a rigid frame is:

$$F_{cr} = F_{cr;EI} + \left[\frac{1}{F_{cr;EAc^2}} + \frac{1}{F_{cr;GA_c}} + \frac{1}{F_{cr;GA_b}} \right]^{-1} \tag{7.55}$$

Where the critical loads obtained from the stick spring model are for:

- Individual bending [1, 2]:

$$F_{cr;EI} = \frac{8EI}{l^2} \tag{7.56}$$

- Global bending [1, 2]:

$$F_{cr;EAc^2} = \frac{8EAc^2}{l^2} \tag{7.57}$$

- Racking shear of the columns:

$$F_{cr;GA_c} = 2GA_c' = \frac{48EI_c}{h^2} \tag{7.58}$$

- Racking shear of the beams:

$$F_{cr;GA_b} = 2GA_b = \frac{24EI_b}{ah} \tag{7.59}$$

The actual critical loads are for:

- Individual bending [5]:

$$F_{cr;EI} = \frac{7.837EI}{l^2} \tag{7.60}$$

- Global bending [5]:

$$F_{cr;EAc^2} = \frac{7.837EAc^2}{l^2} \tag{7.61}$$

- Racking shear of the columns (see eq. (6.21)):

$$F_{cr;GA_c} = \eta GA_c = \eta \frac{2\pi^2 EI_c}{h^2} \tag{7.62}$$

Where factor η is (see eq. (6.22)):

$$\eta = \frac{s}{s - 0.5} \tag{7.63}$$

- Racking shear of the beams:

$$F_{cr;GA_b} = 2GA_b = \frac{24EI_b}{ah} \tag{7.64}$$

The individual bending critical load of the stick-spring model (see eq. (7.56)) is 2.1% larger then the actual individual bending critical load of a rigid frame (see eq. (7.60)), because the individual bending deflection shape of a rigid frame is not identical to the individual bending buckling shape of a rigid frame. The deflection shape of a rigid frame is a fourth order function and the buckling shape of a rigid frame can be approximated by a cosine function.

Similar reasoning can be done for the global bending critical load (compare eq. (7.57) and eq. (7.61)).

The racking shear critical load of the columns of the stick-spring model (see eq. (7.58)) is 143% larger then the actual racking shear critical load of the columns of a rigid frame (see eq. (7.62), because the racking shear deflection shape of the columns of a rigid frame (see fig. 7.12a) is not identical to the racking shear buckling shape of the columns of a rigid frame (see fig. 7.12b).

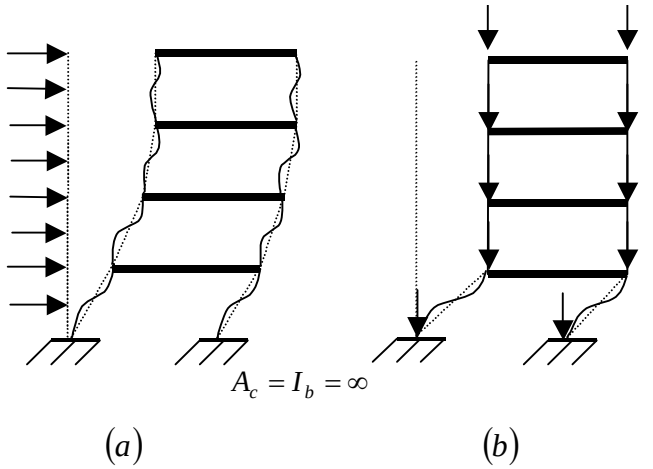

Figure 7.12 Racking shear shapes of the columns caused by UDL.

The racking shear critical load of the beams of a fixed rigid (see eq. (7.59)) is assumed to be the same as the racking shear critical load of the beams of a flexible rigid frame (see eq. (7.105)).

If the actual values for individual bending (see eq. (7.60)), global bending (see eq. (7.61)), racking shear of the columns (see eq. (7.62)) and racking shear of the beams (see eq. (7.64)) are substituted into eq. (7.55) the critical load of a rigid frame becomes:

$$F_{cr} = \frac{7.837EI}{l^2} + \left[\frac{l^2}{7.837EAc^2} + \frac{h^2}{\eta 2\pi^2 EI_c} + \frac{ah}{24EI_b} \right]^{-1} \tag{7.65}$$

7.2 Accuracy

To establish the accuracy of the stick-spring model, critical loads of a number of one-bay rigid frames were estimated using the stick-spring model and a finite element analyses. Finite element program ANSYS was used to obtain the eigenvalues of the rigid frames. The rigid frames have fixed supports and the height of the frames varied from eight to forty stories. The rigid frames are subjected to two different loadcases (see fig. 1.5):

- Vertical top loads (see fig. 1.5a).
- Uniformly distributed vertical loads (see fig. 1.5b).

Six different cases will be investigated for one-bay rigid frames:

- Individual bending deformation only (see fig. 7.13a)
- Global bending deformation dominates (see fig. 7.13b).
- Racking shear deformation of the columns dominates (see fig. 7.13c).
- Global racking shear deformation dominates (7.13c/d).
- All deformations together (see fig. 7.13a/b/c/d).
- Influence individual bending stiffness on the critical load.

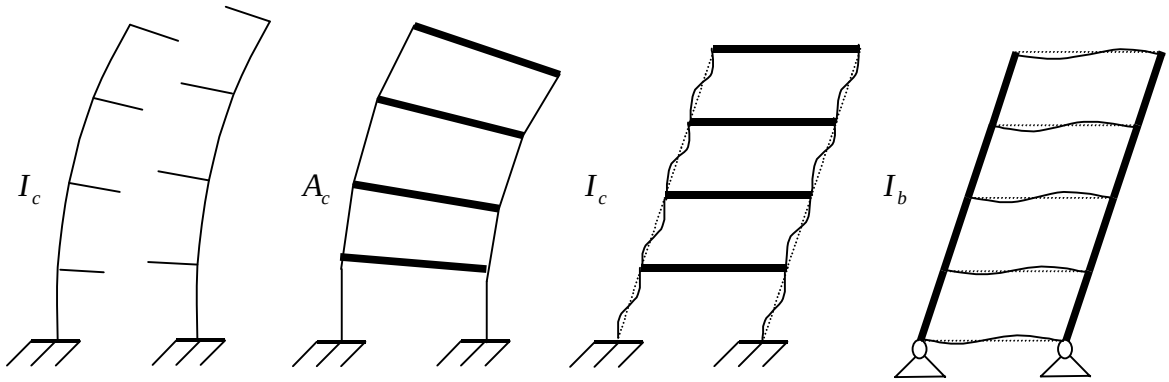

Figure 7.13 Cases to investigate for fixed rigid frames.

The first four cases only represent theoretical cases, but the inclusion of them is very important to make a well-based judgement on the accuracy of the stick-spring model.
The critical loads found with the finite element method are assumed to be exact.

The errors are calculated as follows $\Delta = \dfrac{P_{cr} - P_{cr(ANSYS)}}{P_{cr(ANSYS)}} \times 100\%$.

If the error is negative the stick-spring model gives a conservative value for the critical load.

7.2.1 Numerical model

The numerical model shown in figure 7.14 is built up from BEAM3 elements. BEAM3 elements can sustain normal forces, bending moments and shear forces. All the connections at each node are moment resistant. The columns and beams are divided into three BEAM3 elements.
In this investigation it is assumed that the columns have an uniform cross-sectional area A_c and an uniform second moment of area I_c up the height and the beams have a uniform second moment of area I_b up the height except for the roof beam, which has a second moment of area $0.5I_b$.
The rigid frame has no uniform racking shear stiffness of the columns GA_c up the height, because of a discontinuity at the bottom caused by the fixed connection at the base.
This discontinuity can`t be solved and causes a larger racking shear stiffness at the bottom of the rigid frame. If the number of stories increases the influence of this discontinuity decreases.
The cross-section of the beams is assumed to be infinite $A_b = \infty$.
Shear deformations in the beams and columns are neglected, i.e. $A_{b;shear} = A_{c;shear} = \infty$.

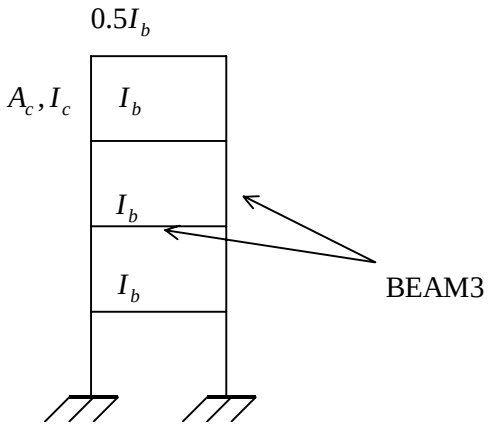

Figure 7.14 Numerical model for a rigid frame fix-connected to the base.

7.2.2 Example

An eight storey high one bay fixed rigid frame (see fig. 7.15) has an individual bending stiffness EI, global bending stiffness EAc^2, racking shear stiffness of the columns GA_c, a racking shear stiffness of the beams GA_b and is subjected to two different loadcases. The characteristics of the rigid frame can be found in table 6.1.

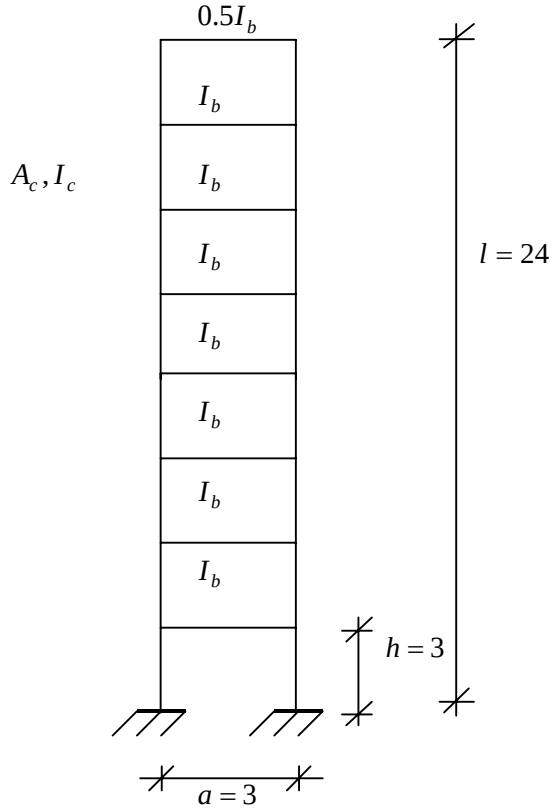

Figure 7.15. Example of fixed rigid frames.

7.2.2.1 Stiffness parameters

The individual bending stiffness is (see eq. (6.127)):

$$EI = \sum EI_{ci} = 2EI_{ci} = 2 \times 2 \times 10^5 \times 3.281 \times 10^{-4} = 131.2MN$$

The global bending stiffness is (see eq. (6.60)):

$$EAc^2 = \sum EA_{ci}c_i^{\,2} = 2EA_c c_i^{\,2} = 2 \times 2 \times 10^5 \times 1.744 \cdot 10^{-2} \times 1.5^2 = 15696MN$$

Ratio between the bending stiffnesses:

$$\frac{EI}{EAc^2} = \frac{131.2}{15696} \approx \frac{1}{120}$$

7.2.2.2 Vertical top load

The individual bending critical load is (see eq. (7.28)):

$$P_{cr;EI} = \frac{\pi^2 EI}{4l^2} = \frac{\pi^2 \times 131.2}{4 \times 24^2} = 0.562MN\,.$$

The global bending critical load is (see eq. (7.29)):

$$P_{cr;EAc^2} = \frac{\pi^2 EAc^2}{4l^2} = \frac{\pi^2 \times 15696}{4 \times 24^2} = 67.24MN$$

The racking shear critical load of the columns is (see eq. (7.30)):

$$P_{cr;GA_c} = \frac{2\pi^2 EI_c}{h^2} = \frac{2 \times \pi^2 \times 2 \times 10^5 \times 3.281 \times 10^{-4}}{3^2} = 143.9MN$$

The racking shear critical load of the beams is (see eq. (7.31)):

$$P_{cr;GA_b} = \frac{12EI_b}{ah} = \frac{12 \times 2 \times 10^5 \times 1.207 \times 10^{-4}}{3 \times 3} = 32.19MN$$

The critical load is (see eq. (7.23)):

$$P_{cr} = P_{cr;EI} + \left[\frac{1}{P_{cr;EAc^2}} + \frac{1}{P_{cr;GA_c}} + \frac{1}{P_{cr;GA_b}} \right]^{-1} = 0.562 + \left[\frac{1}{67.24} + \frac{1}{143.9} + \frac{1}{32.19} \right]^{-1} = 19.47MN$$

7.2.2.3 Vertical UDL

The individual bending critical load is (see eq. (7.60)):

$$F_{cr;EI} = \frac{7.837EI}{l^2} = \frac{7.837 \times 131.2}{24^2} = 1.786MN$$

The global bending critical load is (see eq. (7.61)):

$$F_{cr;EAc^2} = \frac{7.837EAc^2}{l^2} = \frac{7.837 \times 15696}{24^2} = 213.6MN$$

Factor η is (see eq. (7.63)):

$$\eta = \frac{s}{s - 0.5} = \frac{8}{8 - 0.5} = \frac{16}{15} = 1.0666$$

The racking shear critical load of the columns is (see eq. (7.62)):

$$F_{cr;GA_c} = \eta \frac{2\pi^2 EI_c}{h^2} = 1.0666 \times 143.9 = 153.5MN$$

The racking shear critical load of the beams is (see eq. (7.64)):

$$F_{cr;GA_b} = \frac{24EI_b}{ah} = \frac{24 \times 2 \times 10^5 \times 1.207 \times 10^{-4}}{3 \times 3} = 64.37MN$$

The critical load is (see eq. (7.55)):

$$F_{cr} = F_{cr;EI} + \left[\frac{1}{F_{cr;EAc^2}} + \frac{1}{F_{cr;GA_c}} + \frac{1}{F_{cr;GA_b}} \right]^{-1} = 1.786 + \left[\frac{1}{213.6} + \frac{1}{153.5} + \frac{1}{64.37} \right]^{-1} = 39.20MN$$

All critical loads in this example calculated by the stick-spring model are in bold type and can be found in tables 7.1-7.7.

7.2.3 Results

The figures and tables below present the results of the critical loads obtained from the stick-spring model and the numerical analysis.

7.2.3.1 Individual bending deformation only

The second moment of area of the beams is assumed to be zero $I_b = 0$, which leads to a zero racking shear critical load of the beams $P_{cr;GA_b} = 0$. The structure no longer behaves as a rigid frame, but as two independent flexural cantilevers, which develop single curvature bending deformation only. Therefore the rigid frame cannot develop double curvature bending of the columns, which leads to a zero racking shear critical load of the columns $P_{cr;GA_c} = 0$ and the rigid frame cannot develop global bending, which leads to a zero global bending critical load $P_{cr;EAc^2} = 0$.

Substituting $P_{cr;GA_b} = 0$, $P_{cr;GA_c} = 0$ and $P_{cr;EAc^2} = 0$ into eq. (7.23) leads to:

$$P_{cr} = P_{cr;EI} + \left[\frac{1}{0} + \frac{1}{0} + \frac{1}{0}\right]^{-1} = P_{cr;EI} + 0 = P_{cr;EI}\,.$$

Now the rigid frame can develop individual bending deformation only.
Table 7.1 shows the accurracy of the individual bending critical loads $P_{cr;EI}$ and $F_{cr;EI}$.

Table 7.1. Critical loads for fixed rigid frames, individual bending deformation only.

Number of storeys s [-]	Vertical top load P with $P_{cr;EI} = \frac{\pi^2 EI}{4l^2}$			UDL $F(\gamma = 0.5)$ with $F_{cr;EI} = \frac{7.837EI}{l^2}$		
	Critical loads P_{cr} [MN]			Critical loads F_{cr} [MN]		
	Stick-spring model	ANSYS	Error Δ [%]	Stick-spring model	ANSYS	Error Δ [%]
8	**0.562**	0.562	0.0	**1.786**	1.774	0.6
16	0.141	0.141	0.0	0.446	0.446	0.2
24	0.062	0.062	0.0	0.198	0.198	0.0
32	0.035	0.035	0.0	0.112	0.112	0.0
40	0.023	0.023	0.0	0.071	0.071	0.0

Observations

- **The rigid frame develops one mode of deformation: individual bending only (see fig 7.13a).**

- **The individual bending critical loads can very well be predicted by $P_{cr;EI} = \frac{\pi^2 EI}{4l^2}$ and $F_{cr;EI} = \frac{7.837EI}{l^2}$,** because all errors are nearly zero (see table 7.1).

7.2.3.2 Global bending deformation dominates

The second moment of area of the beams is assumed to be infinite $I_b = \infty$, which leads to an infinite racking shear critical load of the beams $P_{cr;GA_b} = \infty$.

Substituting $P_{cr;GA_b} = \infty$ into eq. (7.23) leads to:

$$P_{cr} = P_{cr;EI} + \left[\frac{1}{P_{cr;EAc^2}} + \frac{1}{P_{cr;GA_c}} + \frac{1}{\infty} \right]^{-1} = P_{cr;EI} + \left[\frac{1}{P_{cr;EAc^2}} + \frac{1}{P_{cr;GA_c}} \right]^{-1}.$$

Now the rigid frame can develop individual bending, global bending and racking shear deformation of the columns. Global bending dominates, because $P_{cr;GA_c} > P_{cr;EAc^2}$ and $P_{cr;EAc^2} > P_{cr;EI}$.

Table 7.2 shows the accurracy of the global bending critical loads $P_{cr;EAc^2}$ and $F_{cr;EAc^2}$.

Alternative 1 is introduced to show that more identical buckling shapes lead to lower errors.

Table 7.2. Critical loads for fixed rigid frames, global bending deformation dominates.

Number of storeys s [-]	Vertical top load P			**UDL** $F(\gamma = 0.5)$			UDL $F(\gamma = 0.5)$		
	Critical loads P_{cr} [MN]			**Critical loads F_{cr} [MN]** with $F_{cr;GA_c} = \eta GA_c$ and $F_{cr;GA_b} = 2GA_b$			Alternative 1 Critical loads F_{cr} [MN] with $F_{cr;GA_c} = 2GA_c$ and $F_{cr;GA_b} = 2GA_b$		
	Stick-spring model	ANSYS	Error Δ [%]	**Stick-spring model**	**ANSYS**	**Error Δ [%]**	Stick-spring model	ANSYS	Error Δ [%]
8	46.39	48.20	-3.8	**91.10**	**124.3**	**-27**	124.4	124.3	+0.1
16	15.19	15.44	-1.6	**39.72**	**46.61**	**-15**	45.48	46.61	-2.4
24	7.16	7.22	-0.8	**20.63**	**22.43**	**-8.0**	22.12	22.43	-1.4
32	4.12	4.14	-0.5	**12.34**	**12.98**	**-4.9**	12.87	12.98	-0.9
40	2.66	2.67	-0.3	**8.14**	**8.42**	**-3.3**	8.37	8.42	-0.6

Observations

- **The rigid frame develops three modes of deformation: individual bending (see fig. 7.13a), global bending (see fig. 7.13b) and racking shear of the columns (see fig. 7.13c).**
- **Global bending dominates the buckling behavior.**
- **Rigid frames subjected to vertical top loads P give lower errors then rigid frames subjected to vertical UDL`s F (see table 7.2),** because the buckling shapes of the first (see fig. 7.16) are more identical to each other then the buckling shapes of the second (see fig. 7.17).
- **Rigid frames subjected to vertical UDL`s F give lower errors if the buckling shapes are more identical (compare fig. 7.17/7.18 and table 7.2)**.
- **The global bending critical loads $P_{cr;EAc^2} = \frac{\pi^2 EAc^2}{4l^2}$ and $F_{cr;EAc^2} = \frac{7.837 EAc^2}{l^2}$ are conservative,** because all errors are negative (see table 7.2).

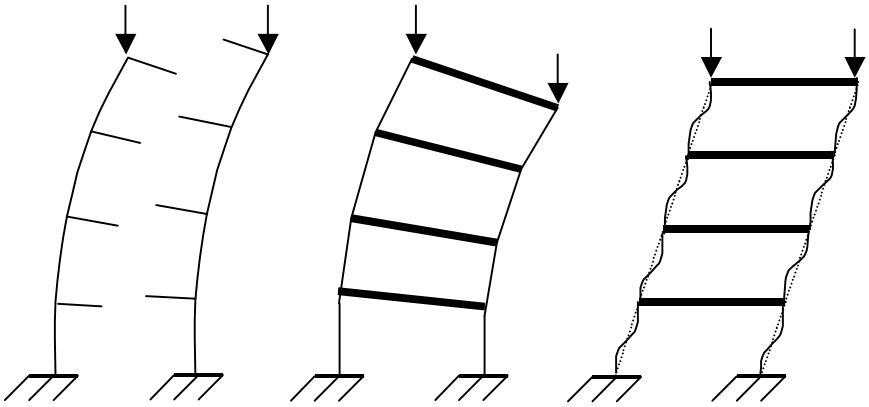

(a) (b) (c)

Fig 7.16 Modes of behavior of a fixed rigid frame subjected to top loads.

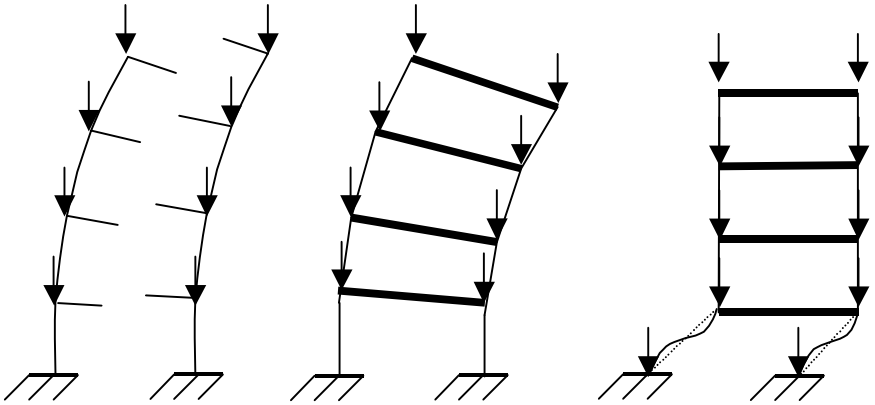

(a) (b) (c)

Fig 7.17 Modes of behavior of a fixed rigid frame subjected to UDL`s.

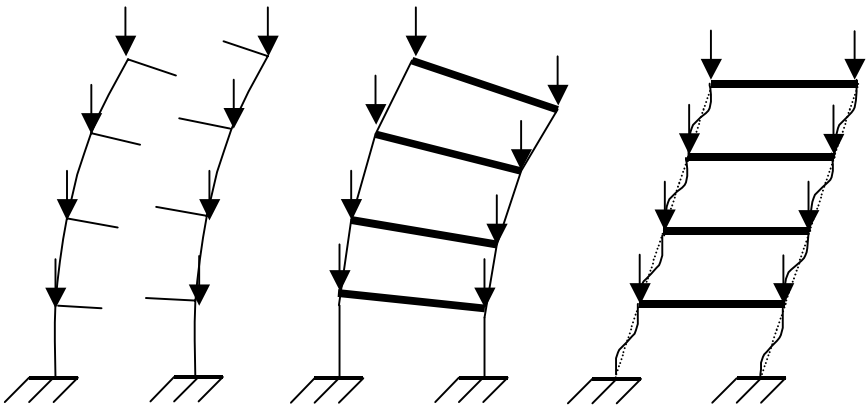

(a) (b) (c)

Fig 7.18 Modes of behavior of a fixed rigid frame subjected to UDL`s (alternative 1).

7.2.3.3 Racking shear deformation of the columns dominates

The cross-sectional area of the columns is assumed to be infinite $A_c = \infty$ and the second moment of area of the beams is assumed to be infinite $I_b = \infty$. The first leads to an infinite global bending critical load $P_{cr;EAc^2} = \infty$. The second leads to an infinite racking shear critical load of the beams $P_{cr;GA_b} = \infty$. Substituting $P_{cr;EAc^2} = \infty$ and $P_{cr;GA_b} = \infty$ into eq. (7.23) leads to:

$$P_{cr} = P_{cr;EI} + \left[\frac{1}{\infty} + \frac{1}{P_{cr;GA_c}} + \frac{1}{\infty}\right]^{-1} = P_{cr;EI} + P_{cr;GA_c} \approx P_{cr;GA_c}.$$

Now the rigid frame can develop individual bending and racking shear deformation of the columns. Racking shear of the columns dominates, because $P_{cr;GA_c} > P_{cr;EI}$.

Table 7.3 shows the accurracy of the racking shear critical loads of the columns $P_{cr;GA_c}$ and $F_{cr;GA_c}$.

Table 7.3. Critical loads for fixed rigid frames, racking shear deformation of the columns dominates.

Number of storeys s [-]	Vertical top load P			UDL $F(\gamma = 0.5)$		
	Critical loads P_{cr} [MN]			Critical loads F_{cr} [MN]		
	Stick-spring model	ANSYS	Error Δ [%]	Stick-spring model	ANSYS	Error Δ [%]
8	144.5	144.2	+0.2	155.3	153.8	+1.0
16	144.1	144.2	-0.1	149.0	148.8	+0.1
24	144.0	144.1	-0.1	147.2	147.2	0.0
32	144.0	144.1	-0.1	146.3	146.4	-0.1
40	143.9	144.1	-0.1	145.8	146.0	-0.1

Observations

- **The rigid frame develops two modes of deformation: individual bending of the columns (see fig. 7.13a) and racking shear of the columns (see fig 7.13c).**
- **Racking shear of columns dominates the buckling behavior.**
- **The stick spring model gives good results (see table 7.3).**
- **The racking shear critical loads of the columns can very well be predicted by** $P_{cr;GA_c} = \frac{2\pi^2 EI_c}{h^2}$ **and** $F_{cr;GA_c} = \eta \frac{2\pi^2 EI_c}{h^2}$**,** because the errors are very low (see table 7.3). This is because the racking shear buckling shape of a cantilever is identical to the racking shear buckling shape of the columns of a rigid frame.
- **If the number of stories increases to infinite the reduction factor** $\eta = \frac{s}{s - 0.5}$ **decreases to 1 and the racking shear critical load of the columns becomes** $F_{cr;GA_c} = \frac{2\pi^2 EI_c}{h^2}$ **(see table 7.3).**

7.2.3.4 Global racking shear dominates

The area of the columns $A_c = \infty$ is assumed to be infinite, which leads to an infinite global bending critical load $P_{cr;EAc^2} = \infty$. Substituting $P_{cr;EAc^2} = \infty$ into eq. (7.23) leads to:

$$P_{cr} = P_{cr;EI} + \left[\frac{1}{\infty} + \frac{1}{P_{cr;GA_c}} + \frac{1}{P_{cr;GA_b}} \right]^{-1} = P_{cr;EI} + P_{cr;GA} \approx P_{cr;GA}.$$

where

$$P_{cr;GA} = \left[\frac{1}{P_{cr;GA_c}} + \frac{1}{P_{cr;GA_b}} \right]^{-1}$$

Now the rigid frame can develop individual bending deformation and global racking shear deformation. Global racking shear dominates, because $P_{cr;GA} > P_{cr;EI}$. Table 7.4 shows the accuracy of the global racking shear critical load $P_{cr;GA}$ and $F_{cr;GA}$. For rigid frames subjected to UDL two other alternatives will be presented here. Alternative 1 and 2 are introduced to find upper and lower bound solutions for the actual global racking shear critical load.

Table 7.4 Critical loads for rigid frames fix-connected to the base, global racking shear deformation dominates.

Number of storeys s [-]	Vertical top load P			**UDL** $F(\gamma = 0.5)$			UDL $F(\gamma = 0.5)$			UDL $F(\gamma = 0.5)$		
	Critical loads P_{cr} [MN]			**Critical loads F_{cr} [MN]** with $F_{cr;GA_c} = \eta GA_c$ and $F_{cr;GA_b} = 2GA_b$			Alternative 1 Critical loads F_{cr} [MN] with $F_{cr;GA_c} = 2GA_c$ and $F_{cr;GA_b} = 2GA_b$			Alternative 2 Critical loads F_{cr} [MN] with $F_{cr;GA_c} = \eta GA_c$ and $F_{cr;GA_b} = \eta GA_b$		
	Stick-spring model	ANSYS	Error Δ [%]	**Stick-spring model**	**ANSYS**	**Error Δ [%]**	Stick-spring model	ANSYS	Error Δ [%]	Stick-spring model	ANSYS	Error Δ [%]
8	26.87	27.60	-2.7	**47.14**	**44.95**	**+4.9**	54.39	44.95	+21	29.84	44.95	-38
16	26.44	27.19	-2.7	**45.36**	**36.95**	**+23**	53.05	36.95	+44	27.60	36.95	-27
24	26.37	27.11	-2.8	**44.96**	**34.23**	**+31**	52.80	34.23	+54	27.06	34.23	-22
32	26.34	27.08	-2.8	**44.80**	**32.82**	**+37**	52.72	32.82	+61	26.83	32.82	-19
40	26.33	27.07	-2.8	**44.72**	**31.93**	**+40**	52.68	31.93	+65	26.71	31.93	-17

Observations

- **The rigid frame develops three modes of deformation: individual bending of the columns (see fig. 7.13a), racking shear of the columns (see fig 7.13c) and racking shear of the beams (see fig. 7.13d).**

- **Global racking shear (racking shear of columns and beams) dominates the buckling behavior.**

- **The actual global racking critical load lays between:**
  $\eta GA < F_{cr;GA;actual} < 2GA$ (see tabel 7.4 and fig. 7.19).

$F_{cr;GA} = 2GA$ (alternative 1)

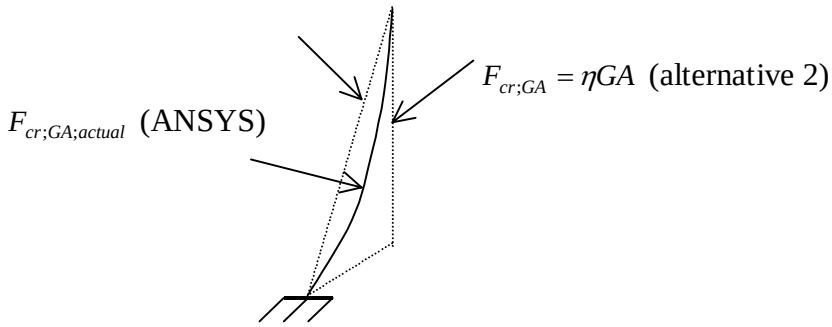

Figure 7.19 Global racking shear buckling shapes for load case F .

- **The global racking shear critical load** $P_{cr;GA} = \left[\frac{h^2}{2\pi^2 EI_c} + \frac{ah}{12EI_b} \right]^{-1}$
  is conservative, because all errors are negative (see table 7.4).

- **The global racking shear critical load** $F_{cr;GA} = \left[\frac{h^2}{\eta 2\pi^2 EI_c} + \frac{ah}{24EI_b} \right]^{-1}$
  is unconservative, because all errors are positive (see table 7.4).

- **If global racking shear is dominant, which is the case if** $F_{cr;GA} < F_{cr;EAc^2}$ **, formula**
  $F_{cr} = \frac{7.837EI}{l^2} + \left[\frac{l^2}{7.837EAc^2} + \frac{h^2}{\eta 2\pi^2 EI_c} + \frac{ah}{24EI_b} \right]^{-1}$ **gives unconservative critical loads (see table 7.4).**

7.2.3.5 All deformations together

Table 7.5 shows the accuracy of the critical loads P_{cr} and F_{cr} .

Table 7.5. Critical loads for fixed rigid frames, all deformations together.

Number of storeys s [-]	Vertical top load P			UDL $F(\gamma = 0.5)$		
	Critical loads P_{cr} [MN]			Critical loads F_{cr} [MN]		
	Stick-spring model	ANSYS	Error Δ [%]	Stick-spring model	ANSYS	Error Δ [%]
8	**19.47**	19.85	**-1.9**	**39.20**	40.34	**-2.9**
16	10.40	10.51	**-1.1**	24.84	26.15	**-5.0**
24	5.88	5.92	**-0.7**	15.71	16.60	**-5.4**
32	3.66	3.67	**-0.4**	10.39	10.84	**-4.2**
40	2.46	2.47	**-0.3**	7.24	7.48	**-3.1**

Observations

- **The buckling behavior of a fixed rigid frame can be divided into individual bending, global bending, racking shear of columns and racking shear of beams (see fig. 7.13).**

- **The critical loads P_{cr} and F_{cr} are conservative,** because the errors are negative (see table 7.5).

- **Formula** $F_{cr} = \frac{7.837EI}{l^2} + \left[\frac{l^2}{7.837EAc^2} + \frac{h^2}{\eta 2\pi^2 EI_c} + \frac{ah}{24EI_b} \right]^{-1}$ **can only be used for tall rigid frames dominated by global bending, which is the case if** $F_{cr;EAc^2} < F_{cr;GA}$ **(see table 7.5),** because it then gives conservative critical loads.

- **The maximum errors for the theoretical tall building structures are (see table 7.1-7.7).**
  The highest conservative error for loadcase P is: -3.8 %.
  The highest conservative error for loadcase F is: -27 %.
  The highest unconservative error for loadcase P is: +0.2 %.
  The highest unconservative error for loadcase F is: +40 %.

- **The extreme cases (see table 7.1-7.4 and table 7.6-7.7) are normally of theoritical interest,** because there is always a combination between individual bending, individual rotation, global bending, racking shear of the columns and racking shear of the beams. For practical tall building structures, therefore only table 7.5 is important.

- **The maximum errors for the practical tall building structures are (see table 7.5 in red).**
  The highest conservative error for loadcase P is: -1.9 %.
  The highest conservative error for loadcase F is: -5.4 %.

- **All suggested formula give good results for the preliminary design of practical highrise fixed rigid frames of 8 till 40 stories within a maximum error of 5.4% .**

- **All observations are only valid for one-bay fixed rigid frames of eight till forty stories.**

- **All observations are only valid for the investigated cases in this parameterstudy.**

7.2.3.6 Influence of the individual bending stiffness on the critical load

The influence of the individual bending stiffness EI on the overall critical will be investigated. This will be done by increasing the second moment of area of the columns. Therefore the individual bending stiffness EI and the racking shear stiffness of columns GA_c will also increase. All other parameters remain constant. The global bending stiffness is $EAc^2 = 15696 MNm^2$ and the racking shear stiffness of the beams is $GA_b = 32.19 MN$. Very important in this matter is the $\frac{EI}{EAc^2}$ ratio. First the practical limits of the $\frac{EI}{EAc^2}$ ratio will be defined.

A lower bound can be found by assuming a rigid frame with weak columns (see fig. 7.20a):

$$\frac{EI}{EAc^2} = \frac{2EI_c}{2EA_c{c_i}^2} = \frac{I_c}{A_c{c_i}^2} = \frac{0.000003492}{0.002124 \times 1.5^2} \approx \frac{1}{1369}$$

An upper bound can be found by assuming a coupled wall with very stiff columns (see fig. 7.20b):

$$\frac{EI}{EAc^2} = \frac{I_c}{A_c{c_i}^2} = \frac{0.007223}{0.04442 \times 1.5^2} \approx \frac{1}{14}$$

Practical limits:

$$\frac{1}{1369} \le \frac{EI}{EAc^2} \le \frac{1}{14}$$

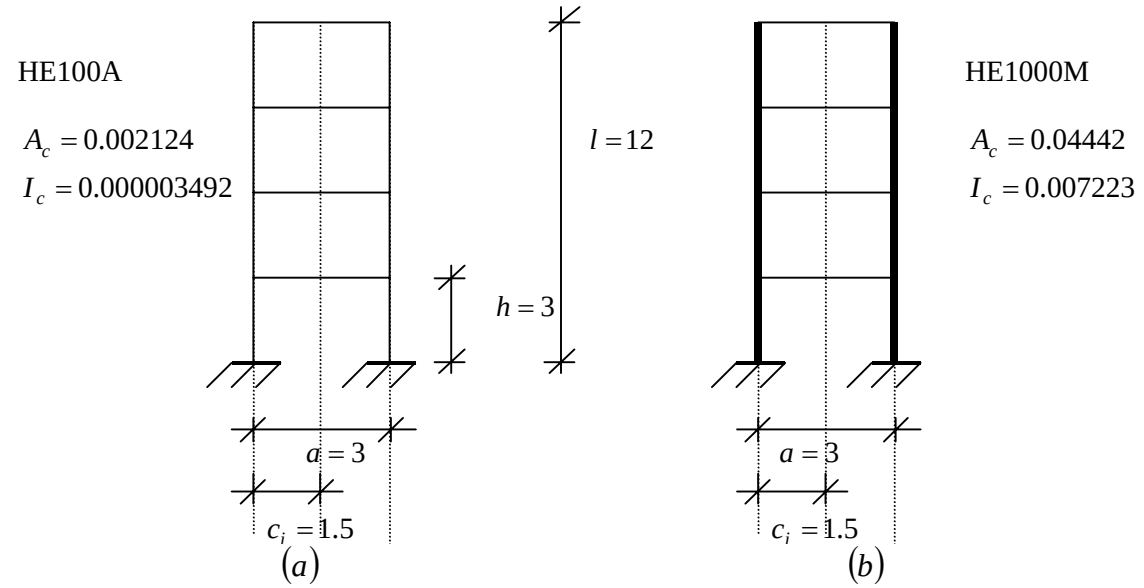

Figure 7.20 Practical limits.

Table 7.6 shows the influence of the individual bending critical load on the overall critical load by varying ratio $\frac{EI}{EAc^2}$ with $s = 8$. Table 7.7 shows the influence of individual bending stiffness EI on the critical loads P_{cr} and F_{cr}.

Table 7.6. Influence individual bending critical load on the overall critical load by varying $\frac{EI}{EAc^2}$ *ratio,* $s = 8$.

Critical loads [MN]			
$\frac{EI}{EAc^2}$ [-]	$P_{cr;EI;ANSYS}$	$P_{cr;ANSYS}$	$\frac{P_{cr;EI;ANSYS}}{P_{cr;ANSYS}}$ [%]
0.001	0.13447	14.08	1
0.01	1.3447	22.00	6
0.1	13.447	35.08	38
1	134.47	156.21	86

Table 7.7. Critical loads for fixed rigid frames, influence of the individual bending stiffness EI *on the critical loads* P_{cr} *and* F_{cr}, $s = 24$.

$\frac{EI}{EAc^2}$ [-]	Vertical top load P			UDL $F(\gamma = 0.5)$		
	Critical loads P_{cr} [MN]			Critical loads F_{cr} [MN]		
	Stick-spring model	ANSYS	Error Δ [%]	Stick-spring model	ANSYS	Error Δ [%]
0.001	5.17	5.29	-2.3	11.66	13.90	-16
0.01	6.11	6.12	-0.3	17.00	17.44	-2.5
0.1	7.55	7.55	0.0	22.00	22.48	-2.1
1	21.00	21.00	0.0	64.79	65.78	-1.5

Observations

- **If the ratio** $\frac{EI}{EAc^2}$ **is higher the influence of the individual bending critical load on the overall critical load is larger (see table 7.6).**

- **The individual bending stiffness** EI **can have a big influence on the critical load and therefore can`t be neglected (see table 7.7).**

7.3 Rigid frames flexibly connected to the base

A rigid frame is a structure which consists of columns and beams (see fig. 7.21). The joints of a rigid frame are moment resistant. The boundary conditions at the base of a rigid frame can be pinned, fixed or flexible. In this investigation the boundary conditions are flexible (see fig. 7.21). This flexible connection at the base introduces a new mode of deformation to the buckling behavior, which is individual rotation of the columns.

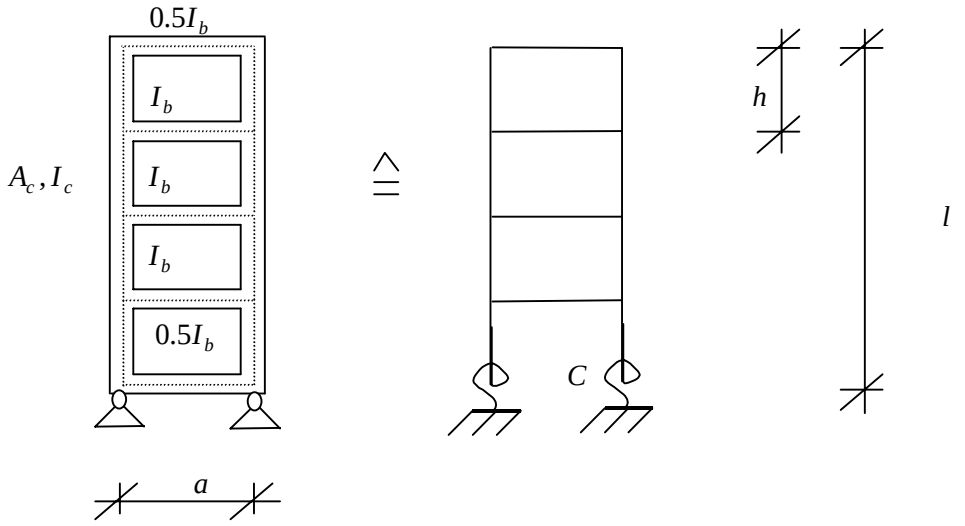

Figure 7.21 Flexible rigid frames.

The buckling behaviour of a flexible rigid frame can be divided into 5 modes of deformation:

- Individual bending (EI): single curvature bending of the vertical members (see fig. 7.22a).
- Individual rotation (C): caused by double curvature bending of a groundfloor beam (see fig. 7.22b).
- Global bending (EAc^2): axial deformation in the columns (see fig. 7.22c).
- Racking shear of the columns (GA_c): double curvature bending in the columns (see fig. 7.22d).
- Racking shear of the beams (GA_b): double curvature bending in the beams (see fig. 7.22e).

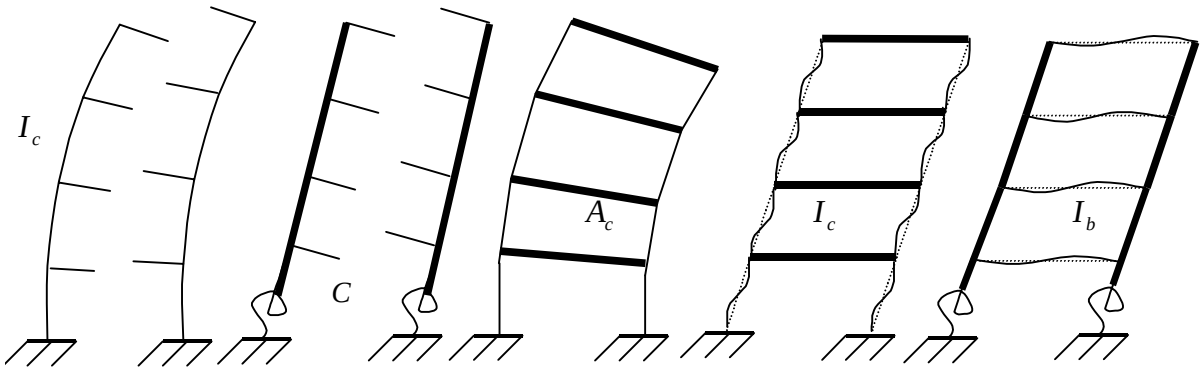

$I_b = 0,\ C = \infty$	$I_b = 0, I_c = \infty$	$I_b = C = \infty$	$A_b = I_b = C = \infty$	$A_c = I_c = \infty$
$EI = f(I_c)$	$C = f(I_b)$	$EAc^2 = f(A_c)$	$GA_c = f(I_c)$	$GA_b = f(I_b)$
(a)	(b)	(c)	(d)	(e)

Fig 7.22 Modes of behavior of a flexible rigid frame.

Assumptions:

- The column-beam connections are fully moment resistant.
- The rigid frame is flexibly connected to the base.
- The columns are continuous up the total height of the structure.
- The flexible rigid frame has five lateral stiffness parameters $EI = f(I_c)$, $C = f(I_b)$, $EAc^2 = f(A_c)$, $GA_b = f(I_b)$ and $GA_c = f(I_c)$.
- The cross-section of the beams is infinite $A_b = \infty$ for all modes of behavior.
- Shear deformations in the beams and columns are neglected, which means $A_{b;shear} = A_{c;shear} = \infty$.

7.3.1 Vertical top loads

A stick-spring model is introduced here to obtain an approximate solution for the overall critical load of a one-bay flexible rigid frame (see fig. 7.23a). It is first suggested to transform a rigid frame subjected to vertical top loads into a multiple stick model (see fig. 7.23b).
In a multiple stick model a pinned column is supported by a spring-flexure cantilever with individual bending stiffness EI, individual rotational spring stiffness C and by a shear-flexure cantilever with global bending stiffness EAc^2, racking shear stiffness of the columns GA_c and racking shear stiffness of the beams GA_b. The spring-flexure cantilever can be transformed into a stick-spring model with horizontal translational spring stiffness $k_1 = f(EI, C)$ and the shear-flexure cantilever can be transformed into a stick-spring model with horizontal translational spring stiffness $k_2 = f(EAc^2, GA_c, GA_b)$. The multiple stick model can then be transformed into a stick-spring model, where the horizontal translation spring $k = f(k_1, k_2)$ (see fig. 7.23c).
The justification for this suggestion is that the shear-flexure cantilever can be seen as a quasi-braced frame and the spring-flexure cantilever can be seen as a flexible column adding the individual bending stiffness EI and rotational spring stiffness C of the rigid frame. If the beams of a rigid frame are cut through it can still develop individual bending (see fig. 7.22a) and individual rotation of the columns (see fig. 7.22b), because of the flexible connection at the bottom and the continuous columns.

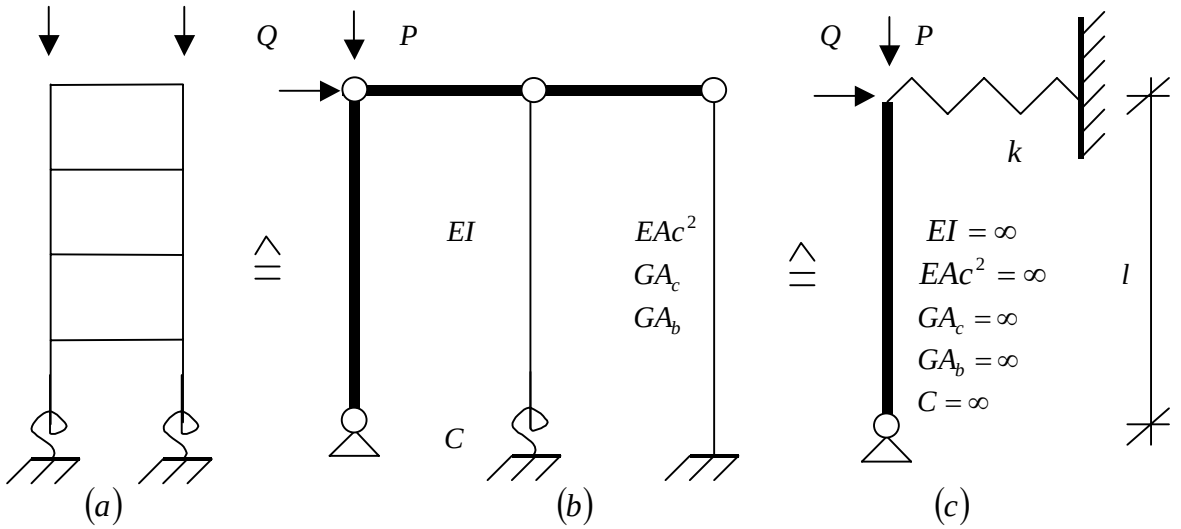

Figure 7.23 Transformation of flexible rigid frame into stick-spring model for loadcase P.

It has been shown that (see eq. (7.12)):

$$P_{cr} = P_{cr;1} + P_{cr;2} \tag{7.66}$$

The spring-flexure cantilever, with individual bending EI and individual rotational spring stiffness C, is assumed to be standing alone so $k_2 = 0$ (see fig. 7.24a). This can be modelled into the stick-spring model with translation spring $k_1 = f(EI, C)$ (see fig. 7.24b).

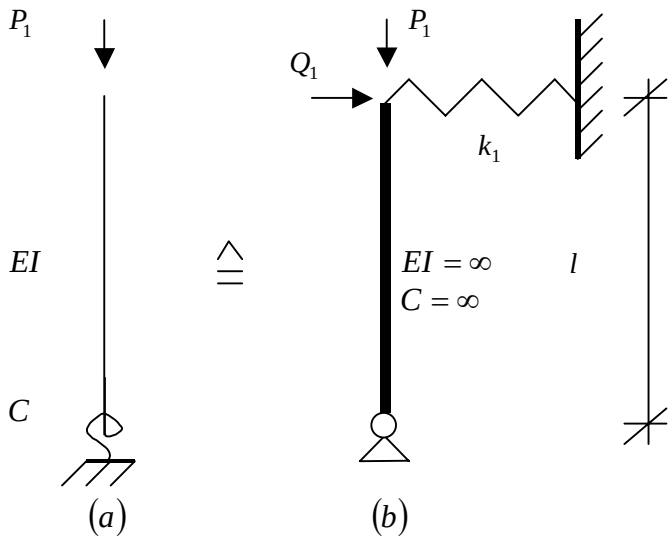

Figure 7.24 Spring-flexure cantilever subjected to top loads.

The first-order deformation at the top of the spring-flexure cantilever is:

$$y_{01} = y_{EI} + y_C = \frac{Q_1 l^3}{3EI} + \frac{Q_1 l}{C} \tag{7.67}$$

The first-order deformation at the top of the stick-spring model is:

$$y_{01} = \frac{Q_1}{k_1} \tag{7.68}$$

Both deformations are the same yielding the horizontal translational spring stiffness k_1:

$$\frac{1}{k_1} = \frac{l^3}{3EI} + \frac{l}{C} \tag{7.69}$$

The critical load of the stick-spring model is:

$$P_{cr;1} = k_1 l \tag{7.70}$$

After substituting eq. (7.69) into eq. (7.70) the critical load of the stick-spring model is:

$$\frac{1}{P_{cr;1}} = \frac{1}{k_1 l} = \frac{l^2}{3EI} + \frac{1}{C} \tag{7.71}$$

In general, the critical load of eq. (7.71) can be written as:

$$P_{cr;1} = \left[\frac{1}{P_{cr;EI}} + \frac{1}{P_{cr;C}} \right]^{-1} \tag{7.72}$$

It has been shown that the critical load of the shear-flexure cantilever is (see eq. (7.22)):

$$P_{cr;2} = \left[\frac{1}{P_{cr;EAc^2}} + \frac{1}{P_{cr;GA_c}} + \frac{1}{P_{cr;GA_b}} \right]^{-1} \tag{7.73}$$

After substituting eq. (7.72) and eq. (7.73) into eq. (7.66) the critical load of a rigid frame is:

$$P_{cr} = \left[\frac{1}{P_{cr;EI}} + \frac{1}{P_{cr;C}} \right]^{-1} + \left[\frac{1}{P_{cr;EAc^2}} + \frac{1}{P_{cr;GA_c}} + \frac{1}{P_{cr;GA_b}} \right]^{-1} \tag{7.74}$$

Where the critical loads obtained from the stick spring model are for:

- Individual bending [1, 2]:

$$P_{cr;EI} = \frac{3EI}{l^2} \tag{7.75}$$

- Individual rotation [1, 2]:

$$P_{cr;C} = \frac{C}{l} \tag{7.76}$$

- Global bending [1, 2]:

$$P_{cr;EAc^2} = \frac{3EAc^2}{l^2} \tag{7.77}$$

- Racking shear of the columns [5]:

$$P_{cr;GA_c} = GA'_c = \frac{24EI_c}{h^2} \tag{7.78}$$

- Racking shear of the beams [5]:

$$P_{cr;GA_b} = GA_b = \frac{12EI_b}{ah} \tag{7.79}$$

The actual critical loads are for:

- Individual bending [4]:

$$P_{cr;EI} = \frac{\pi^2 EI}{4l^2} \tag{7.80}$$

- Individual rotation [1, 2]:

$$P_{cr;C} = \frac{C}{l} \tag{7.81}$$

- Global bending [4]:

$$P_{cr;EAc^2} = \frac{\pi^2 EAc^2}{4l^2} \tag{7.82}$$

- Racking shear of the columns [27]:

$$P_{cr;GA_c} = GA_c = \frac{2\pi^2 EI_c}{h^2} \tag{7.83}$$

- Racking shear of the beams [5]:

$$P_{cr;GA_b} = GA_b = \frac{12EI_b}{ah} \tag{7.84}$$

The individual rotational spring critical load of the stick-spring model (see eq. (7.76)) is equal to the actual individual rotational spring critical load of a rigid frame (see eq. (7.81)), because the individual rotation deflection shape of a rigid frame (see fig. 7.25a) is identical to the individual rotation buckling shape of a rigid frame (see fig. 7.25b).

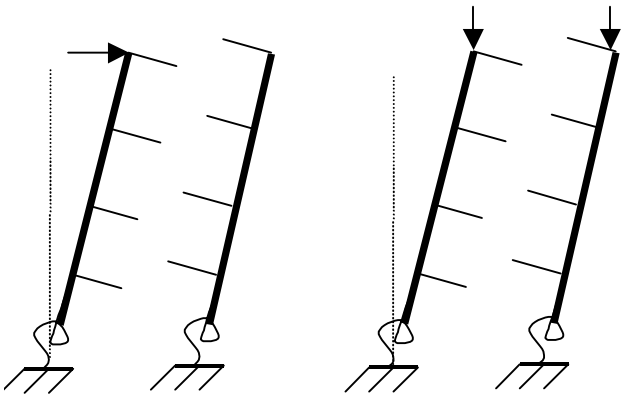

Figure 7.25 Individual rotational spring shapes for top loads.

The racking shear critical load of the beams of the stick-spring model (see eq. (7.79)) is equal to the actual racking shear critical load of the beams of a rigid frame (see eq. (7.84)), because the racking shear deflection shape of the beams of a rigid frame (see fig. 7.26a) is identical to the racking shear buckling shape of the beams of a rigid frame (see fig. 7.26b).

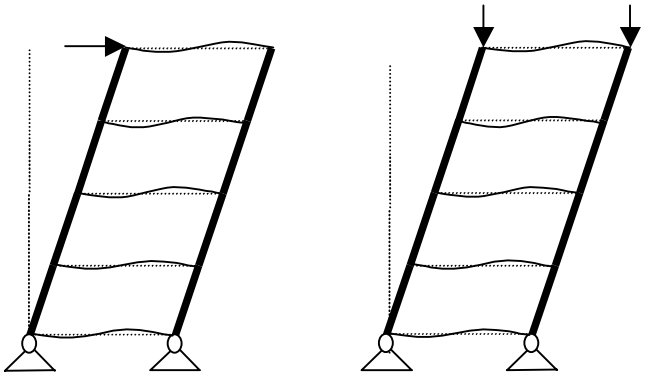

Figure 7.26 Racking shear shapes of the beams caused by top loads.

If the actual values for individual bending (see eq. (7.80)), individual rotation (see eq. (7.81)), global bending (see eq. (7.82)), racking shear of the columns (see eq. (7.83)) and racking shear of the beams (see eq. (7.84)) are substituted into eq. (7.74) the critical load of a rigid frame becomes:

$$P_{cr} = \left[\frac{4l^2}{\pi^2 EI} + \frac{l}{C} \right]^{-1} + \left[\frac{4l^2}{\pi^2 EAc^2} + \frac{h^2}{2\pi^2 EI_c} + \frac{ah}{12EI_b} \right]^{-1} \tag{7.85}$$

7.3.2 Uniformly distributed vertical loads

In fig. 7.27a a rigid frame is subjected to vertical point loads F_v accept for the point loads at the roof and at the bottom of the frame which are $0.5F_v$. In a similar way a stick-spring model can be used to obtain an approximate solution for the overall critical load of a rigid frame
First a rigid frame subjected to vertical point loads is transformed into a multiple stick model subjected to a horizontal UDL w and a vertical UDL f (see fig. 7.27b).
The multiple stick model is then transformed into the stick-spring model (see fig. 7.27c).

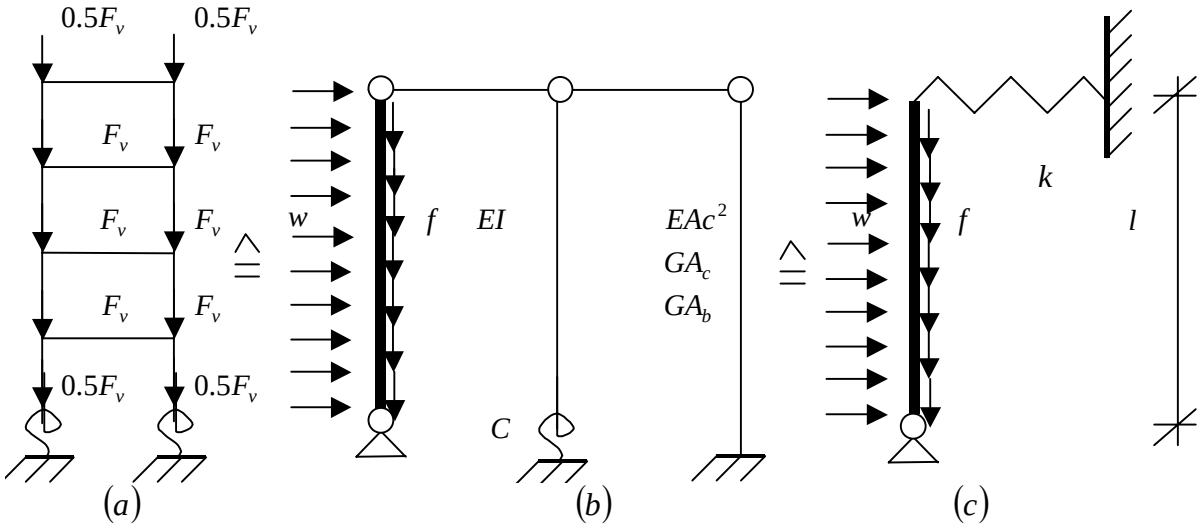

Figure 7.27 Transformation of flexible rigid frame into stick-spring model (UDL).

It has been shown that (see eq. (7.44)):

$$F_{cr} = F_{cr;1} + F_{cr;2} \tag{7.86}$$

The spring-flexure cantilever, with individual bending EI and individual rotational spring stiffness C, is assumed to be standing alone so $k_2 = 0$ (see fig. 7.28a). This can be modelled into the stick-spring model with translation spring $k_1 = f(EI, C)$ (see fig. 7.28b).

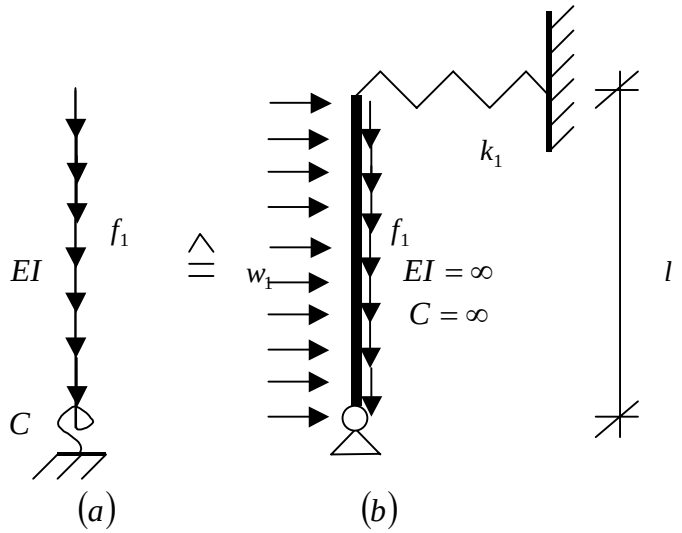

Figure 7.28 Spring-flexure cantilever subjected to UDL.

The first-order deformation at the top of the spring-flexure cantilever is:

$$y_{01} = y_{EI} + y_C = \frac{w_1 l^4}{8EI} + \frac{w_1 l^2}{2C} \tag{7.87}$$

The first-order deformation at the top of the stick-spring model is:

$$y_{01} = \frac{2w_1 l}{k_1} \tag{7.88}$$

Both deformations are the same yielding the horizontal translational spring stiffness k_1:

$$\frac{1}{k_1} = \frac{l^3}{4EI} + \frac{l}{C} \tag{7.89}$$

It has been shown that the critical load of the stick-spring model is:

$$F_{cr;1} = 2k_1 l \tag{7.90}$$

After substituting eq. (7.89) into eq. (7.90) the critical load of the stick-spring model is:

$$\frac{1}{F_{cr;1}} = \frac{1}{2k_1 l} = \frac{l^2}{8EI} + \frac{1}{2C} \tag{7.91}$$

In general, the critical load of eq. (7.91) can be written as:

$$F_{cr;1} = \left[\frac{1}{F_{cr;EI}} + \frac{1}{F_{cr;C}} \right]^{-1} \tag{7.92}$$

It has been shown that the critical load of the shear-flexure cantilever is (see eq. (7.54)):

$$F_{cr;2} = \left[\frac{1}{F_{cr;EAc^2}} + \frac{1}{F_{cr;GA_c}} + \frac{1}{F_{cr;GA_b}} \right]^{-1} \tag{7.93}$$

After substituting eq. (7.92) and eq. (7.93) into eq. (7.86) leads to the critical load of a rigid frame:

$$F_{cr} = \left[\frac{1}{F_{cr;EI}} + \frac{1}{F_{cr;C}} \right]^{-1} + \left[\frac{1}{F_{cr;EAc^2}} + \frac{1}{F_{cr;GA_c}} + \frac{1}{F_{cr;GA_b}} \right]^{-1} \tag{7.94}$$

Where the critical loads obtained from the stick spring model are for:

- Individual bending [1, 2]:

$$F_{cr;EI} = \frac{8EI}{l^2} \tag{7.95}$$

- Individual rotation [1, 2]:

$$F_{cr;C} = \frac{2C}{l} \tag{7.96}$$

- Global bending [1, 2]:

$$F_{cr;EAc^2} = \frac{8EAc^2}{l^2} \tag{7.97}$$

- Racking shear of the columns [5]:

$$F_{cr;GA_c} = 2GA_c' = \frac{48EI_c}{h^2} \tag{7.98}$$

- Racking shear of the beams [5]:

$$F_{cr;GA_b} = 2GA_b = \frac{24EI_b}{ah} \tag{7.99}$$

The actual critical loads are for:

- Individual bending [5]:

$$F_{cr;EI} = \frac{7.837EI}{l^2} \tag{7.100}$$

- Individual rotation [1, 2]:

$$F_{cr;C} = \frac{2C}{l} \tag{7.101}$$

- Global bending [5]:

$$F_{cr;EAc^2} = \frac{7.837EAc^2}{l^2} \tag{7.102}$$

- Racking shear of the columns (see eq. (6.21)):

$$F_{cr;GA_c} = \eta GA_c = \eta \frac{2\pi^2 EI_c}{h^2} \tag{7.103}$$

Where factor η is (see eq. (6.22)):

$$\eta = \frac{s}{s - 0.5} \tag{7.104}$$

- Racking shear of the beams:

$$F_{cr;GA_b} = 2GA_b = \frac{24EI_b}{ah} \tag{7.105}$$

The individual rotational spring critical load of the stick-spring model (see eq. (7.96)) is equal to the actual individual rotational spring critical load of a rigid frame (see eq. (7.101)), because the individual rotation deflection shape of a rigid frame (see fig. 7.29a) is identical to the individual rotation buckling shape of a rigid frame (see fig. 7.29b).

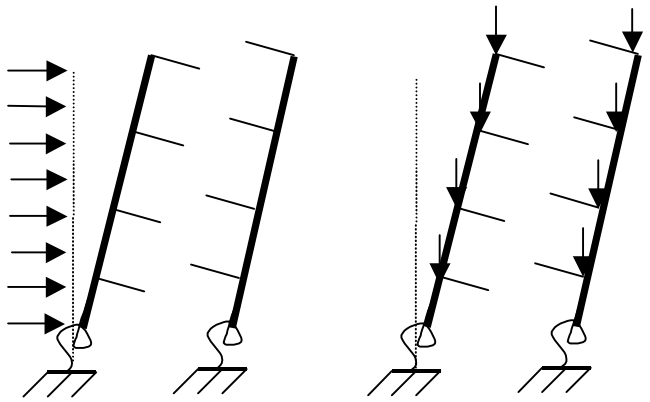

$I_b = 0\,,\ I_c = \infty$

(a) (b)

Figure 7.29 Individual rotational spring shapes for top UDl.

The racking shear critical load of the beams of the stick-spring model (see eq. (7.99)) is equal to the actual racking shear critical load of the beams of a rigid frame (see eq. (7.105)), because the racking shear deflection shape of the beams of a rigid frame (see fig. 7.30a) is identical to the racking shear buckling shape of the beams of a rigid frame (see fig. 7.30b).

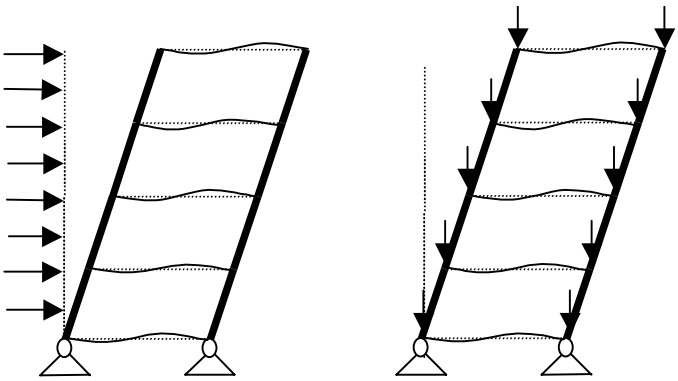

$A_c = I_c = \infty$

(a) (b)

Figure 7.30 Racking shear shapes of the beams of rigid frames caused by UDL`s.

If the actual values for individual bending (see eq. (7.100)), individual rotation (see eq. (7.101)), global bending (see eq. (7.102)), racking shear of the columns (see eq. (7.103)) and racking shear of the beams (see eq. (7.105)) are substituted into eq. (7.94) the critical load of a rigid frame becomes:

$$F_{cr} = \left[\frac{l^2}{7.837EI} + \frac{l}{2C}\right]^{-1} + \left[\frac{l^2}{7.837EAc^2} + \frac{h^2}{\eta 2\pi^2 EI_c} + \frac{ah}{24EI_b}\right]^{-1} \qquad (7.106)$$

7.4 Lateral stiffnesses of a flexible rigid frame

7.4.1 Individual rotational spring stiffness

The individual rotational spring stiffness C of the columns caused by double curvature bending of the groundfloor beam can be obtained from (see fig. 7.31).

$$C = 2c' = 2\frac{M}{\phi} = 2\frac{M}{\frac{M \times 0.5a}{3 \times 0.5EI_b}} = \frac{6EI_b}{a} \tag{7.107}$$

where E is the elastic modulus, I_b is the second moment of area of the groundfloor beam and a is the distance between the neutral axis of the columns.

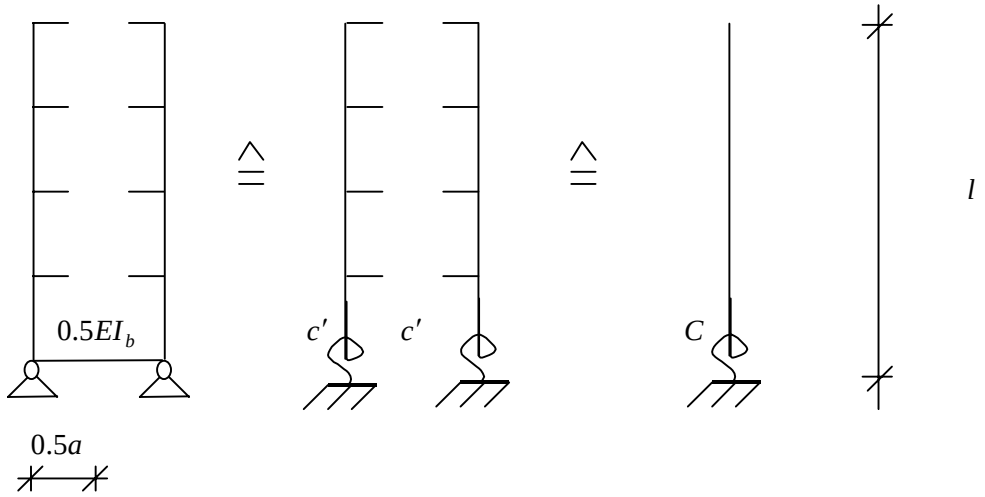

Figure 7.31 Individual rotational spring stiffness of a flexibe rigid frame.

7.5 Accuracy

To establish the accuracy of the stick-spring model, critical loads of a number of one-bay rigid frames were estimated using the stick-spring model and a finite element analyses. Finite element program ANSYS was used to obtain the eigenvalues of the rigid frames. The rigid frames have flexible supports and the height of the frames varied from eight to forty stories. The rigid frames are subjected to two different loadcases (see fig. 1.5):

- Vertical top loads (see fig. 1.5a).
- Uniformly distributed vertical loads (see fig. 1.5b).

Eight different cases will be investigated for one-bay rigid frames:

- Individual bending deformation only (see fig. 7.32a)
- Individual rotational spring deformation only (see fig. 7.32b).
- Global bending deformation dominates (see fig. 7.32c).
- Racking shear deformation of the columns only (see fig. 7.32d).
- Racking shear deformation of the beams only (see fig. 7.32e).
- Global racking shear deformation dominates (7.32d/e).
- Individual bending and individual rotational spring deformation (see fig. 7.32a/b).
- All deformations together (see fig. 7.32a/b/c/d/e).

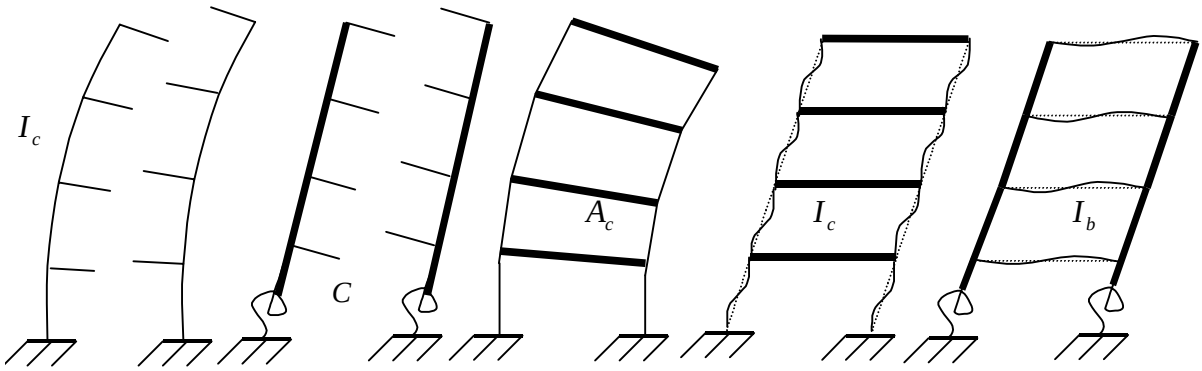

Figure 7.32 Cases to investigate for flexibly rigid frames.

The first seven cases only represent theoretical cases, but the inclusion of them is very important to make a well-based judgement on the accuracy of the stick-spring model.
The critical loads found with the finite element method are assumed to be exact.

The errors are calculated as follows $\Delta = \dfrac{P_{cr} - P_{cr(ANSYS)}}{P_{cr(ANSYS)}} \times 100\%$.

If the error is negative the stick-spring model gives a conservative value for the critical load.

7.5.1 Introduction numerical model

The numerical model shown in figure 7.33 is built up from BEAM3 elements. BEAM3 elements can sustain normal forces, bending moments and shear forces. All the connections at each node are moment resistant. The columns and beams are divided into three BEAM3 elements.
In this investigation it is assumed that the columns have an uniform cross-sectional area A_c and an uniform second moment of area I_c up the height and the beams have a uniform second moment of area I_b up the height except for the groundfloor- and roof beam., which has a second moment of area $0.5I_b$. The cross-section of the beams is assumed to be infinite $A_b = \infty$.
Shear deformations in the beams and columns are neglected, which means $A_{b;shear} = A_{c;shear} = \infty$.

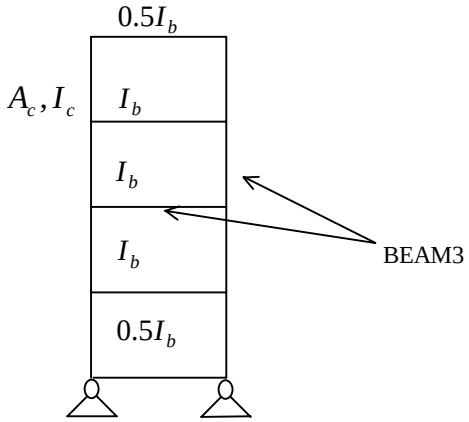

Figure 7.33 Numerical model for a rigid frame flexibly connected to the base.

7.5.2 Example

An eight storey high one bay flexible rigid frame (see fig. 7.34) has an individual bending stiffness EI, individual rotational spring stiffness C, global bending stiffness EAc^2, racking shear stiffness of the columns GA_c, racking shear stiffness of the beams GA_b and is subjected to two different loadcases. The characteristics of the rigid frame can be found in table 6.1.

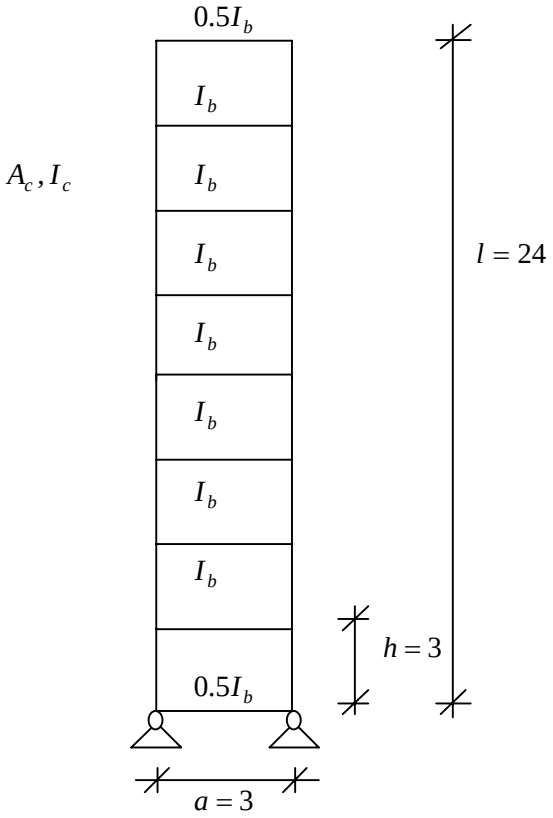

Figure 7.34. Example of flexible rigid frames.

7.5.2.1 Stiffness parameters

The individual bending stiffness is (see eq. (6.127)):

$$EI = \sum EI_{ci} = 2EI_{ci} = 2 \times 2 \times 10^5 \times 3.281 \times 10^{-4} = 131.2MN$$

The individual rotational spring stiffness is (see eq. (7.107)):

$$C = \frac{6EI_b}{a} = \frac{6 \times 2 \times 10^5 \times 1.207 \times 10^{-4}}{3} = 48.28MNm$$

The global bending stiffness is (see eq. (6.60)):

$$EAc^2 = \sum EA_{ci}c_i^{\,2} = 2EA_c c_i^{\,2} = 2 \times 2 \times 10^5 \times 1.744 \cdot 10^{-2} \times 1.5^2 = 15696MN$$

Ratio between the bending stiffnesses:

$$\frac{EI}{EAc^2} = \frac{131.2}{15696} \approx \frac{1}{120}$$

7.5.2.2 Vertical top load

The individual bending critical load is (see eq. (7.80)):

$$P_{cr;EI} = \frac{\pi^2 EI}{4l^2} = \frac{\pi^2 \times 131.2}{4 \times 24^2} = 0.562MN\,.$$

The individual rotational spring critical load is (see eq. (7.81)):

$$P_{cr;C} = \frac{C}{l} = \frac{48.28}{24} = 2.01MN$$

The global bending critical load is (see eq. (7.82)):

$$P_{cr;EAc^2} = \frac{\pi^2 EAc^2}{4l^2} = \frac{\pi^2 \times 15696}{4 \times 24^2} = 67.24MN$$

The racking shear critical load of the columns is (see eq. (7.83)):

$$P_{cr;GA_c} = \frac{2\pi^2 EI_c}{h^2} = \frac{2 \times \pi^2 \times 2 \times 10^5 \times 3.281 \times 10^{-4}}{3^2} = 143.9MN$$

The racking shear critical load of the beams is (see eq. (7.84)):

$$P_{cr;GA_b} = \frac{12EI_b}{ah} = \frac{12 \times 2 \times 10^5 \times 1.207 \times 10^{-4}}{3 \times 3} = 32.19MN$$

The critical load is (see eq. (7.74)):

$$P_{cr} = \left[\frac{1}{P_{cr;EI}} + \frac{1}{P_{cr;C}}\right]^{-1} + \left[\frac{1}{P_{cr;EAc^2}} + \frac{1}{P_{cr;GA_c}} + \frac{1}{P_{cr;GA_b}}\right]^{-1} = \left[\frac{1}{0.562} + \frac{1}{2.01}\right]^{-1} + \left[\frac{1}{67.24} + \frac{1}{143.9} + \frac{1}{32.19}\right]^{-1}$$

$$P_{cr} = 19.35MN$$

7.5.2.3 Vertical UDL

The individual bending critical load is (see eq. (7.100)):

$$F_{cr;EI} = \frac{7.837EI}{l^2} = \frac{7.837 \times 131.2}{24^2} = 1.786MN$$

The individual rotational spring critical load is(see eq. (7.101):

$$F_{cr;C} = \frac{2C}{l} = \frac{2 \times 48.28}{24} = 4.02MN$$

The global bending critical load is (see eq. (7.102)):

$$F_{cr;EAc^2} = \frac{7.837EAc^2}{l^2} = \frac{7.837 \times 15696}{24^2} = 213.56MN$$

Reduction factor η is (see eq. (7.104)):

$$\eta = \frac{s}{s-0.5} = \frac{8}{8-0.5} = \frac{16}{15} = 1.0666$$

The racking shear critical load of the columns is (see eq. (7.103)):

$$F_{cr;GA_c} = \eta \frac{2\pi^2 EI_c}{h^2} = 1.0666 \times \frac{2 \times \pi^2 \times 2 \times 10^5 \times 3.281 \times 10^{-4}}{3^2} = 153.5MN$$

The racking shear critical load of the beams is (see eq. (7.105)):

$$F_{cr;GA_b} = \frac{24EI_b}{ah} = \frac{24 \times 2 \times 10^5 \times 1.207 \times 10^{-4}}{3 \times 3} = 64.37MN$$

The critical load is (see eq. (7.94)):

$$F_{cr} = \left[\frac{1}{F_{cr;EI}} + \frac{1}{F_{cr;C}}\right]^{-1} + \left[\frac{1}{F_{cr;EAc^2}} + \frac{1}{F_{cr;GA_c}} + \frac{1}{F_{cr;GA_b}}\right]^{-1} = \left[\frac{1}{1.786} + \frac{1}{4.02}\right]^{-1} + \left[\frac{1}{213.6} + \frac{1}{153.5} + \frac{1}{64.37}\right]^{-1}$$

$$F_{cr} = 38.65MN$$

All critical loads in this example calculated by the stick-spring model are in bold type and can be found in tables 7.8-7.12.

7.5.3 Results

The figures and tables below present the results of the critical loads obtained from the stick-spring model and the numerical analysis.

7.5.3.1 Individual bending deformation only

For results and observations see section 7.3.3.1.

7.5.3.2 Individual rotational spring deformation only

The second moment of area of the beams is assumed to be zero $I_b = 0$ and the second moment of area is assumed to be infinite $I_c = \infty$. The first leads to a zero racking shear critical load of the beams $P_{cr;GA_b} = 0$. The second leads to an infinite individual bending critical load $P_{cr;EI} = \infty$ and an infinite racking shear critical load of the columns $P_{cr;GA_c} = \infty$. The structure no longer behaves as a rigid frame, but as two independent spring-cantilevers, which develop individual rotational spring deformation only only. Therefore the rigid frame cannot develop global bending, which leads to a zero global bending critical load $P_{cr;EAc^2} = 0$. Substituting $P_{cr;GA_b} = 0$, $P_{cr;GA_c} = \infty$ and $P_{cr;EAc^2} = 0$ into eq. (7.74) leads to:

$$P_{cr} = \left[\frac{1}{\infty} + \frac{1}{P_{cr;C}}\right]^{-1} + \left[\frac{1}{0} + \frac{1}{\infty} + \frac{1}{0}\right]^{-1} = P_{cr;C} + 0 = P_{cr;C}.$$

Now the rigid frame can develop individual rotational spring deformation only.
Table 7.8 shows the accurracy of the individual rotational spring critical loads $P_{cr;C}$ and $F_{cr;C}$.

Table 7.8. Critical loads for flexible rigid frames, individual rotational spring deformation only.

Number of storeys s [-]	Vertical top load P with $P_{cr;C} = \frac{C}{l}$			UDL $F(\gamma = 0.5)$ with $F_{cr;C} = \frac{2C}{l}$		
	Critical loads P_{cr} [MN]			Critical loads F_{cr} [MN]		
	Stick-spring model	ANSYS	Error Δ [%]	Stick-spring model	ANSYS	Error Δ [%]
8	**2.01**	2.01	0.0	**4.02**	4.02	0.0
16	1.01	1.01	0.0	2.01	2.01	0.0
24	0.67	0.67	0.0	1.34	1.34	0.0
32	0.50	0.50	0.0	1.01	1.01	0.0
40	0.40	0.40	0.0	0.80	0.80	0.0

Observations

- **The rigid frame develops individual rotational spring deformation only (see fig 7.32a).**

- **The individual rotational spring critical loads are equal to $P_{cr;C} = \frac{C}{l}$ and $F_{cr;C} = \frac{2C}{l}$,** because all errors are zero (see table 7.8). This is because the rotational spring deflection shape of the rigid frame is identical to rotational spring buckling shape of the rigid frame.

7.5.3.3 Global bending deformation dominates

For results and observations see section 7.3.3.2.

7.5.3.4 Racking shear deformation of the columns dominates

For results and observations see section 7.3.3.3.

7.5.3.5 Racking shear deformation of the beams dominates

The cross-sectional area of the columns is assumed to be infinite $A_c = \infty$ and the second moment of area of the columns is assumed to be infinite $I_c = \infty$. The first leads to an infinite global bending critical load $P_{cr;EAc^2} = \infty$. The second leads to an infinite individual bending critical load $P_{cr;EI} = \infty$ and an infinite racking shear critical load of the columns $P_{cr;GA_c} = \infty$. Substituting $P_{cr;EI} = \infty$, $P_{cr;EAc^2} = \infty$ and $P_{cr;GA_c} = \infty$ into eq. (7.74) leads to:

$$P_{cr} = \left[\frac{1}{\infty} + \frac{1}{P_{cr;C}}\right]^{-1} + \left[\frac{1}{\infty} + \frac{1}{\infty} + \frac{1}{P_{cr;GA_b}}\right]^{-1} = P_{cr;C} + P_{cr;GA_b} \approx P_{cr;GA_b}.$$

Now the rigid frame can develop individual rotational spring and racking shear deformation of the beams. Racking shear deformation of the beams dominates, because $P_{cr;GA_b} > P_{cr;C}$. Table 7.9 shows the accurracy of the racking shear critical loads of the beams $P_{cr;GA_b}$ and $F_{cr;GA_b}$.

Table 7.9. Critical loads for flexible rigid frames, racking shear deformation of the beams dominates.

Number of storeys s [-]	Vertical top load P			UDL $F(\gamma = 0.5)$		
	Critical loads P_{cr} [MN]			Critical loads F_{cr} [MN]		
	Stick-spring model	ANSYS	Error Δ [%]	Stick-spring model	ANSYS	Error Δ [%]
8	**34.20**	32.19	+6.3	**68.40**	64.37	+6.3
16	33.19	32.19	+3.1	66.38	64.37	+3.1
24	32.86	32.19	+2.1	65.71	64.37	+2.1
32	32.69	32.19	+1.6	65.38	64.37	+1.6
40	32.59	32.19	+1.3	65.18	64.37	+1.3

Observations

- **The rigid frame develops two modes of deformation: individual rotation (see fig. 7.32b) and racking shear of the beams (see fig 7.32e).**
- **Racking shear of beams dominates the buckling behavior.**
- **The stick spring model gives good results (see table 7.9).**
- **The racking shear critical load of the beams are very well be predicted by** $P_{cr;GA_b} = \frac{12EI_b}{ah}$ **and** $F_{cr;GA_b} = \frac{24EI_b}{ah}$**,** because the errors are very low (see table 7.9).

7.5.3.6 Global racking shear deformation dominates

The cross-sectional area of the columns is assumed to be infinite $A_c = \infty$, which leads to an infinite global bending critical load $P_{cr;EAc^2} = \infty$. Substituting $P_{cr;EAc^2} = \infty$ into eq. (7.74) leads to:

$$P_{cr} = \left[\frac{1}{P_{cr;EI}} + \frac{1}{P_{cr;C}}\right]^{-1} + \left[\frac{1}{\infty} + \frac{1}{P_{cr;GA_c}} + \frac{1}{P_{cr;GA_b}}\right]^{-1} = P_{cr;1} + P_{cr;GA}.$$

where $$P_{cr;1} = \left[\frac{1}{P_{cr;EI}} + \frac{1}{P_{cr;C}}\right]^{-1}$$ and $$P_{cr;GA} = \left[\frac{1}{P_{cr;GA_c}} + \frac{1}{P_{cr;GA_b}}\right]^{-1}$$

Now the rigid frame can develop individual bending, individual rotational spring and global racking shear deformation. Global racking shear dominates, because $P_{cr;GA} > P_{cr;1}$. Table 7.10 shows the accurracy of the global racking shear critical loads $P_{cr;GA}$ and $F_{cr;GA}$.

Table 7.10. Critical loads for flexible rigid frames, global racking shear deformation dominates.

Number of storeys S [-]	Vertical top load P			UDL $F(\gamma = 0.5)$		
	Critical loads P_{cr} [MN]			Critical loads F_{cr} [MN]		
	Stick-spring model	ANSYS	Error Δ [%]	Stick-spring model	ANSYS	Error Δ [%]
8	26.74	27.05	-1.1	46.59	33.69	+38
16	26.43	27.05	-2.3	45.28	30.96	+46
24	26.36	27.05	-2.6	44.94	29.95	+50
32	26.34	27.05	-2.6	44.79	29.41	+52
40	26.32	27.06	-2.7	44.72	29.07	+54

Observations

- **The rigid frame develops four modes of deformation: individual bending (see fig. 7.32a), individual rotation (see fig. 7.32b), racking shear of the columns (see fig 7.32c) and racking shear of the beams (see fig. 7.32d).**

- **Global racking shear (racking shear of columns and beams) dominates the buckling behavior.**

- **The global racking shear critical load** $P_{cr;GA} = \left[\frac{h^2}{2\pi^2 EI_c} + \frac{ah}{12EI_b}\right]^{-1}$ **is conservative,** because all errors are negative (see table 7.10).

- **The global racking shear critical load** $F_{cr;GA} = \left[\frac{h^2}{\eta 2\pi^2 EI_c} + \frac{ah}{24EI_b}\right]^{-1}$ **is unconservative,** because all errors are positive (see table 7.10).

- **If global racking shear is dominant, which is the case if** $P_{cr;GA} < P_{cr;EAc^2}$ **, formula** $F_{cr} = \left[\frac{l^2}{7.837EI} + \frac{l}{2C}\right]^{-1} + \left[\frac{l^2}{7.837EAc^2} + \frac{h^2}{\eta 2\pi^2 EI_c} + \frac{ah}{24EI_b}\right]^{-1}$ **gives unconservative critical loads (see table 7.10).**

7.5.3.7 Individual bending and individual rotational spring deformation

The second moment of area of the beams is assumed to be zero $I_b = 0$, which leads to a zero racking shear critical load of the beams $P_{cr;GA_b} = 0$. The structure no longer behaves as a rigid frame, but as two independent spring-flexure cantilevers, which develop individual bending and individual rotational spring deformation only. Therefore the rigid frame cannot develop double curvature bending of the columns, which leads to a zero racking shear critical load of the columns $P_{cr;GA_c} = 0$ and the rigid frame cannot develop global bending, which leads to a zero global bending critical load $P_{cr;EAc^2} = 0$. Substituting $P_{cr;GA_b} = 0$, $P_{cr;GA_c} = 0$ and $P_{cr;EAc^2} = 0$ into eq. (7.74) leads to:

$$P_{cr} = \left[\frac{1}{P_{cr;EI}} + \frac{1}{P_{cr;C}}\right]^{-1} + \left[\frac{1}{0} + \frac{1}{0} + \frac{1}{0}\right]^{-1} = \left[\frac{1}{P_{cr;EI}} + \frac{1}{P_{cr;C}}\right]^{-1} + 0 = P_{cr;1} + 0 = P_{cr;1}.$$

where

$$P_{cr;1} = \left[\frac{1}{P_{cr;EI}} + \frac{1}{P_{cr;C}}\right]^{-1}$$

Now the rigid frame can develop individual bending and individual rotational spring deformation. Table 7.11 shows the accurracy of the critical loads $P_{cr;1}$ and $F_{cr;1}$.

Table 7.11. Critical loads for flexible rigid frames, individual bending and individual rotational spring def.

Number of storeys s [-]	Vertical top load P			UDL $F(\gamma = 0.5)$		
	Critical loads P_{cr} [MN]			Critical loads F_{cr} [MN]		
	Stick-spring model	ANSYS	Error Δ [%]	Stick-spring model	ANSYS	Error Δ [%]
8	0.439	0.454	-3.3	1.237	1.297	-4.7
16	0.123	0.126	-2.1	0.365	0.378	-3.4
24	0.057	0.058	-1.5	0.172	0.178	-2.6
32	0.033	0.033	-1.2	0.100	0.103	-2.1
40	0.021	0.022	-1.0	0.066	0.067	-1.8

Observations

- **The rigid frame develops two modes of deformation: individual bending (see fig. 7.32a) and individual rotation (see fig. 7.32b).**
- **The stick spring model gives good results (see table 7.11).**
- **The critical loads** $P_{cr;1} = \left[\frac{1}{P_{cr;EI}} + \frac{1}{P_{cr;C}}\right]^{-1}$ **and** $F_{cr;1} = \left[\frac{1}{F_{cr;EI}} + \frac{1}{F_{cr;C}}\right]^{-1}$ **are conservative,** because all errors are negative (see table 7.11). This because the individual bending buckling shape is not identical to the individual rotational spring buckling shape.

7.5.3.8 All deformations together

Table 7.12 shows the accuracy of the critical loads P_{cr} and F_{cr}.

Table 7.12. Critical loads for flexible rigid frames, all deformations together.

Number of storeys s [-]	Vertical top load P			UDL $F(\gamma = 0.5)$		
	Critical loads P_{cr} [MN]			Critical loads F_{cr} [MN]		
	Stick-spring model	ANSYS	Error Δ [%]	Stick-spring model	ANSYS	Error Δ [%]
8	**19.35**	19.67	-1.7	**38.65**	32.12	+20
16	10.38	10.50	**-1.2**	24.76	25.32	**-2.2**
24	5.88	5.92	**-0.7**	15.68	16.54	**-5.2**
32	3.66	3.67	**-0.4**	10.38	10.83	**-4.2**
40	2.46	2.47	**-0.3**	7.24	7.47	**-3.2**

Observations

- **The buckling behavior of a fixed rigid frame can be divided into individual bending, individual rotation, global bending, racking shear of the columns and racking shear of the beams (see fig. 7.32).**

- **The critical loads P_{cr} and F_{cr} are conservative,** because the errors are negative with $s \geq 16$ (see table 7.12).

- **Formula** $F_{cr} = \left[\frac{l^2}{7.837EI} + \frac{l}{2C}\right]^{-1} + \left[\frac{l^2}{7.837EAc^2} + \frac{h^2}{\eta 2\pi^2 EI_c} + \frac{ah}{24EI_b}\right]^{-1}$ **can only be used for tall rigid frames dominated by global bending, which is the case if** $F_{cr;EAc^2} < F_{cr;GA}$ **(see table 7.12),** because it then gives conservative critical loads.

- **The maximum errors for the theoretical tall building structures are (see table 7.8-7.12).**
  The highest conservative error for loadcase P is: -3.8 %.
  The highest conservative error for loadcase F is: -27 %.
  The highest unconservative error for loadcase P is: +6.3 %.
  The highest unconservative error for loadcase F is: +54 %.

- **The extreme cases (see table 7.8-7.11) are normally of theoritical interest,** because there is always a combination between individual bending, individual rotation, global bending, racking shear of the columns and racking shear of the beams. For practical tall building structures, therefore only table 7.12 is important.

- **The maximum errors for the practical tall building structures are (see table 7.12 in red).**
  The highest conservative error for loadcase P is: -1.2 %.
  The highest conservative error for loadcase F is: -5.2 %.

- **All suggested formula give good results for the preliminary design of practical highrise flexible rigid frames of 16 till 40 stories within a maximum error of 5.2% .**

- **All observations are only valid for one-bay flexible rigid frames of eight till forty stories.**

- **All observations are only valid for the investigated cases in this parameterstudy.**

8 Discussion and conclusions

8.1 Comparison between suggested formulae and existing formulae

In the literature several formulae can be found for estimating the critical loads of braced and rigid frames. In this section some existing formulae will be compared to the formulae derived with the stick-spring model to make a comparison. Only frames subjected to uniformly distributed loads will be compared, because this loadcase is only interesting for tall building structures.
The characteristics of the frames can be found in table 6.1.

8.1.1 Braced frames

8.1.1.1 Uniformly distributed loads

Zalka
In 1999 Zalka [24] modelled a braced frame subjected to a vertical UDL by a sandwich column with thin faces and obtained a mathematically exact formula for the critical load by making use of a table or graph in which a critical load parameter $\overline{\lambda}$ is a function of a stiffness parameter $\overline{\beta}$

$$F_{cr} = \overline{\lambda} F_{cr;GA} \tag{8.1}$$

Where:

- The stiffness parameter $\overline{\beta}$ is:

$$\overline{\beta} = \frac{F_{cr;GA}}{F_{cr;EAc^2}} \tag{8.2}$$

- Global bending critical load is:

$$F_{cr;EAc^2} = \frac{7.837 \alpha EAc^2}{l^2} \tag{8.3}$$

- Reduction factor α_s is:

$$\alpha_s = \frac{s}{s + 1.588} \tag{8.4}$$

- Global racking shear critical load is:

$$F_{cr;GA} = \left[\frac{h^2}{2\pi^2 EI_c} + \frac{ah}{12EI_b} \right]^{-1} \tag{8.5}$$

Hoenderkamp [18-21]

In 2002 [18-21] Hoenderkamp modelled a braced frame subjected to a vertical UDL by a stick-spring model and suggested an approximate formula for the critical load

$$\frac{1}{F_{cr}} = \frac{l^2}{7.837EAc^2} + \frac{1}{2GA} \tag{8.6}$$

Stick-spring model

The critical load for a braced frame subjected to a vertical UDL in this project has been derived from a stick-spring model and can be written as

$$\frac{1}{F_{cr}} = \frac{l^2}{7.837EAc^2} + \frac{1}{\eta GA} \tag{8.7}$$

where reduction factor η is

$$\eta = \frac{s}{s - 0.5} \tag{8.8}$$

In tabel 8.1 Zalka`s formula (see eq. (8.1)), Hoenderkamp`s formula (see eq. (8.6)) and the stick-spring model (see eq. (8.7)) are compared. Formulae which are based on tables and graphs are given with capital letter T and approximate formula with capital letter A in table 8.1.

Table 8.1. Comparison of Zalka, Hoenderkamp and stick-spring model.

Number of storeys s [-]	Vertical UDL F						
	Critical loads F_{cr} [MN]				Error Δ [%]		
	Zalka (sandwich column with thin faces) T	Hoenderkamp A	Stick-spring model A	ANSYS	Zalka (sandwich column with thin faces) T	Hoenderkamp A	Stick-spring model A
8	153.4	177.8	155.0	179.7	-15	-1.1	-14
16	46.89	50.83	48.65	51.04	-8.1	-0.4	-4.7
24	22.02	23.21	22.73	23.26	-5.3	-0.2	-2.2
32	12.63	13.18	13.03	13.20	-4.3	-0.1	-1.3
40	8.16	8.47	8.41	8.48	-3.8	-0.1	-0.8

Conclusions:

- **If the approximate methods are compared to the FE method Hoenderkamps formula gives more accurate results then the stick-spring model (see table 8.1) if the buckling behavior is dominated by global bending which is the case if** $F_{cr;EAc^2} < F_{cr;GA}$**,**

  because the global bending and racking shear buckling shapes of Hoenderkamp (see fig. 8.1a/b) are more identical to each other then the global bending and racking shear buckling shapes of the stick-spring model (see fig. 8.1c/d).

- **The stick-spring model gives always conservative critical loads, but Hoenderkamp`s approximate method does not.** If the buckling behavior is dominated by global bending $F_{cr;EAc^2} < F_{cr;GA}$ Hoenderkamps formula gives conservative critical loads, but if the buckling behavior is dominated by global shear $F_{cr;EAc^2} > F_{cr;GA}$ Hoenderkamps formula gives unconservative critical loads.

- **If the approximate methods are compared to the graphical method the approximate methods give better results then the graphical method and they are easier to use in the preliminary stages of the design (see table 8.1).**

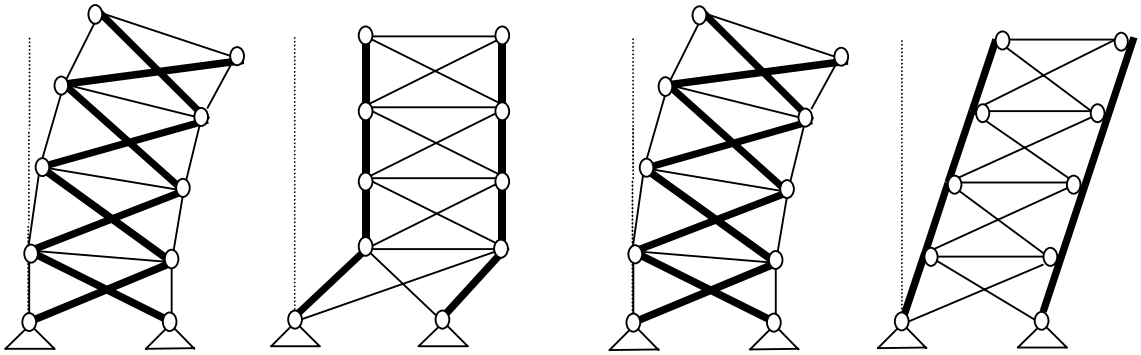

Figure 8.1 Buckling shapes of braced frames for loadcase F *and* $P + F$ *.*

8.1.2 Fixed rigid frames

8.1.2.1 Uniformly distributed loads

Zalka: continuum model

In 1998 Zalka [28] modelled a fixed rigid frame subjected to a vertical UDL by a continuum model and obtained a mathematical exact formula for the critical load by making use of a table or graph in which a critical load parameter $\hat{\alpha}$ is a function of a stiffness parameter $\hat{\beta}$

$$F_{cr} = \frac{r\left(\hat{\alpha} - \hat{\beta}\right)F_{cr;EI} + F_{cr;GA} + \dfrac{rF_{cr;EI}F_{cr;GA}}{F_{cr;EAc^2}}}{1 + \dfrac{F_{cr;GA}}{F_{cr;EAc^2}}} \tag{8.9}$$

Where:

- Individual bending critical load is:

$$F_{cr;EI} = \frac{7.837\alpha_s EI}{l^2} \tag{8.10}$$

- Global bending critical load is:

$$F_{cr;EAc^2} = \frac{7.837\alpha_s EAc^2}{l^2} \tag{8.11}$$

- Global racking shear critical load is:

$$F_{cr;GA} = \left[\frac{h^2}{2\pi^2 EI_c} + \frac{ah}{12EI_b}\right]^{-1} \tag{8.12}$$

- Reduction factor α_s is:

$$\alpha_s = \frac{s}{s + 1.588} \tag{8.13}$$

- Stiffness parameter $\hat{\beta}$ is:

$$\hat{\beta} = \frac{F_{cr;GA}}{F_{cr;EI}} \tag{8.14}$$

- Combination factor r is

$$r = \frac{\dfrac{2\pi^2 EI_c}{h^2}}{\dfrac{2\pi^2 EI_c}{h^2} + \dfrac{12EI_b}{ah}} \tag{8.15}$$

Zalka: sandwich column with thin faces

In 1998 Zalka [28] modelled a fixed rigid frame subjected to a vertical UDL by a sandwich column with thin faces and obtained a mathematically exact formula for the critical load by making use of a table or graph in which a critical load parameter $\overline{\lambda}$ is a function of a stiffness parameter $\overline{\beta}$

$$F_{cr} = \overline{\lambda} F_{cr;GA} \tag{8.16}$$

Where:

- The stiffness parameter $\overline{\beta}$ is:

$$\overline{\beta} = \frac{F_{cr;GA}}{F_{cr;EAc^2}} \tag{8.17}$$

- Global bending critical load is:

$$F_{cr;EAc^2} = \frac{7.837 \alpha_s EAc^2}{l^2} \tag{8.18}$$

- Reduction factor α_s is:

$$\alpha_s = \frac{s}{s + 1.588} \tag{8.19}$$

- Global racking shear critical load is:

$$F_{cr;GA} = \left[\frac{h^2}{2\pi^2 EI_c} + \frac{ah}{12 EI_b} \right]^{-1} \tag{8.20}$$

Zalka: design formula (combination of sandwich column with thin faces and continuum model)

As both the continuum and sandwich models approach the same problem from a different direction, it seems to be sensible to combine the two relevant formula. Zalka [28] combined both methods and obtained a design formula by making use of a table or graph in which a critical load parameter $\hat{\alpha}$ is a function of a stiffness parameter $\hat{\beta}$ and in which a critical load parameter $\overline{\lambda}$ is a function of a stiffness parameter $\overline{\beta}$

$$F_{cr} = \frac{r F_{cr;EI} \overline{\beta} \left(1 + \hat{\alpha} - \hat{\beta} + 2\overline{\beta}\right) + F_{cr;GA} \left(1 + \overline{\lambda} + \overline{\lambda}\,\overline{\beta}\right)}{2\left(1 + \overline{\beta}\right)} \tag{8.21}$$

Where:

- Individual bending critical load is:

$$F_{cr;EI} = \frac{7.837 \alpha_s EI}{l^2} \tag{8.22}$$

- Global bending critical load is:

$$F_{cr;EAc^2} = \frac{7.837 \alpha_s EAc^2}{l^2} \tag{8.23}$$

- Global racking shear critical load is:

$$F_{cr;GA} = \left[\frac{h^2}{2\pi^2 EI_c} + \frac{ah}{12EI_b} \right]^{-1} \tag{8.24}$$

- Reduction factor α_s is:

$$\alpha_s = \frac{s}{s + 1.588} \tag{8.25}$$

- Stiffness parameter $\hat{\beta}$ is:

$$\hat{\beta} = \frac{F_{cr;GA}}{F_{cr;EI}} \tag{8.26}$$

- Stiffness parameter $\overline{\beta}$ is:

$$\overline{\beta} = \frac{F_{cr;GA}}{F_{cr;EAc^2}} \tag{8.27}$$

- Combination factor r is:

$$r = \frac{\dfrac{2\pi^2 EI_c}{h^2}}{\dfrac{2\pi^2 EI_c}{h^2} + \dfrac{12EI_b}{ah}} \tag{8.28}$$

Hegedüs and Kollár: sandwich column with thick faces

In 1984 Hegedüs and Kollár [13] modelled a fixed rigid frame subjected to a vertical UDL by a sandwich column with thick faces and obtained a mathematical exact formula for the critical load by making use of a table or graph in which c_1 is a numerical parameter

$$F_{cr} = c_1 \frac{EAc^2 + EI}{l^2} \tag{8.29}$$

Hegedüs and Kollár

In 1984 Hegedüs and Kollár [13] suggested an approximate formula for the critical load of a fixed rigid frame subjected to a vertical UDL

$$F_{cr} = \left[\frac{l^2}{7.837EAc^2} + \frac{h^2}{2\pi^2 EI_c} + \frac{ah}{12EI_b} \right]^{-1} + \frac{7.837EI}{l^2} \tag{8.30}$$

Stick-spring model

The critical load for a fixed rigid frame subjected to a vertical UDL in this project has been derived from a stick-spring model and can be written as

$$F_{cr} = \frac{7.837EI}{l^2} + \left[\frac{l^2}{7.837EAc^2} + \frac{s-0.5}{s} \frac{h^2}{2\pi^2 EI_c} + \frac{ah}{24EI_b} \right]^{-1} \tag{8.31}$$

In tabel 8.2 and 8.3 Zalka`s continuum model (see eq. (8.9)), Zalka`s sandwich column with thin faces (see eq. (8.16)), Zalka`s design formula (see eq. (8.21)), Hegedüs/Kollár`s sandwich column with thick faces (see eq. (8.29)), Hegedüs/Kollár`s approximate formulae (see eq. (8.30)) and the stick-spring model (see eq. (8.31)) are compared. Formulae which are based on tables and graphs are given with capital letter T and approximate formula with capital letter A in table 8.2 and 8.3.

Table 8.2. Critical loads for fixed rigid frames.

Number of storeys s [-]	Vertical UDL F						
	Critical loads F_{cr} [MN]						
	Zalka (continuum model) T	Zalka (sandwich column with thin faces) T	Zalka (design formula) T	Hegedüs/ Kollár (sandwich column with thick faces) T	Hegedüs/ Kollár A	Stick-spring model A	ANSYS
8	34.70	26.05	31.10	39.55	25.20	39.19	40.34
16	22.19	23.57	23.06	25.43	18.07	24.84	26.15
24	14.74	15.52	15.21	16.11	12.67	15.71	16.60
32	10.12	10.26	10.23	10.56	8.97	10.39	10.84
40	7.23	7.13	7.21	7.35	6.52	7.24	7.48

Table 8.3. Errors for fixed rigid frames.

Number of storeys s [-]	Vertical UDL F					
	Error Δ [%]					
	Zalka (continuum model) T	Zalka (sandwich column with thin faces) T	Zalka (design formula) T	Hegedüs/ Kollár (sandwich column with thick faces) T	Hegedüs/ Kollár A	Stick-spring model A
8	-14	-35	-23	-2.0	-38	-2.9
16	-15	-9.9	-12	-2.8	-31	-5.0
24	-11	-6.5	-8.4	-2.9	-24	-5.4
32	-6.7	-5.4	-5.6	-2.6	-17	-4.2
40	-3.3	-4.7	-3.6	-1.8	-13	-3.1

Conclusions:

- **If the approximate methods are compared to the FE method the stick-spring model gives the most accurate results (see table 8.2/8.3).**

- **If the graphical methods are compared to the FE method the sandwich column with thick-faces gives the most accurate results (see table 8.2/8.3).**

- **If the most accurate approximate method (stick-spring model) is compared to the most accurate graphical method (sandwich column with thick-faces) the graphical method gives more accurate results, but the approximate method is easier to use in the preliminary stages of the design (see table 8.2/8.3).**

- **The differences between the approximate methods are the racking shear critical loads of the beams and the racking shear critical loads of the columns. The racking shear critical load of the columns of eq. (8.31) is a factor $\frac{s}{s-0.5}$ higher then the racking shear critical load of the columns of eq. (8.30). This reduction factor is of little importance for tall buildings, because it decreases to one if the number of stories increases to infinite. The racking shear critical load of the beams of eq. (8.31) is a factor two higher then racking shear critical load of the beams of eq. (8.30) and therefore is extremely important (see table 8.2/8.3).**

8.1.3 Flexible rigid frames

8.1.3.1 Uniformly distributed loads

The methods introduced by Zalka for fixed frames are the same as for flexible frames.
There are also some differences:

- The bending critical loads of a fixed rigid frame (see eq. (8.22) and eq. (8.23)) are different from the bending critical loads of a flexible rigid frame (see eq. (8.33) and eq. (8.34)).

- The critical load parameter $\hat{\alpha}$ of a fixed rigid frame is different from the critical load parameter $\hat{\alpha}_p$ of a flexible rigid frame, because $\hat{\alpha}$ is based on a fixed connection to the base and $\hat{\alpha}_p$ on a pinned connection to the base.

- The supporting effect of the groundfloor beam has been taken into account in the design formula, but not in the continuum model and sandwich column with thin faces.

Zalka: continuum model

In 1998 Zalka [28] modelled a flexible rigid frame subjected to a vertical UDL by a continuum model and obtained a mathematically exact formula for the critical load by making use of a table or graph in which a critical load parameter $\hat{\alpha}_p$ is a function of a stiffness parameter $\hat{\beta}$

$$F_{cr} = \frac{r\left(\hat{\alpha}_p - \hat{\beta}\right)F_{cr;EI} + F_{cr;GA} + \dfrac{rF_{cr;EI}F_{cr;GA}}{F_{cr;EAc^2}}}{1 + \dfrac{F_{cr;GA}}{F_{cr;EAc^2}}} \tag{8.32}$$

Where:

- Individual bending critical load is:

$$F_{cr;EI} = \frac{7.837EI}{l^2} \tag{8.33}$$

- Global bending critical load is:

$$F_{cr;EAc^2} = \frac{7.837EAc^2}{l^2} \tag{8.34}$$

- Global racking shear critical load is:

$$F_{cr;GA} = \left[\frac{h^2}{2\pi^2 EI_c} + \frac{ah}{12EI_b}\right]^{-1} \tag{8.35}$$

- Stiffness parameter $\hat{\beta}$ is:

$$\hat{\beta} = \frac{F_{cr;GA}}{F_{cr;EI}} \tag{8.36}$$

- Combination factor r is:

$$r = \frac{\frac{2\pi^2 EI_c}{h^2}}{\frac{2\pi^2 EI_c}{h^2} + \frac{12EI_b}{ah}} \tag{8.37}$$

Zalka: sandwich column with thin faces

In 1998 Zalka [28] modelled a flexible rigid frame subjected to a vertical UDL by a sandwich column with thin faces and obtained a mathematical exact formula for the critical load by making use of a table or graph in which critical load parameter $\overline{\lambda}$ is a function of stiffness parameter $\overline{\beta}$

$$F_{cr} = \overline{\lambda} F_{cr;GA} \tag{8.38}$$

Where:

- The stiffness parameter $\overline{\beta}$ is:

$$\overline{\beta} = \frac{F_{cr;GA}}{F_{cr;EAc^2}} \tag{8.39}$$

- Global bending critical load is:

$$F_{cr;EAc^2} = \frac{7.837EAc^2}{l^2} \tag{8.40}$$

- Global racking shear critical load is:

$$F_{cr;GA} = \left[\frac{h^2}{2\pi^2 EI_c} + \frac{ah}{12EI_b}\right]^{-1} \tag{8.41}$$

Zalka: design formula (combination of sandwich column with thin faces and continuum model)

As both the continuum and sandwich models approach the same problem from a different direction, it seems to be sensible to combine the two relevant formula. Zalka [28] combined both methods and obtained a design formula by making use of a table or graph in which a critical load parameter $\hat{\alpha}_p$ is a function of a stiffness parameter $\hat{\beta}$ and in which a critical load parameter $\overline{\lambda}$ is a function of a stiffness parameter $\overline{\beta}$

$$F_{cr} = \frac{rF_{cr;EI}\overline{\beta}\left(1 + \hat{\alpha}_p - \hat{\beta} + \overline{\beta} + r\overline{\beta} - r\right) + F_{cr;GA}\left(1 + \overline{\lambda} + \overline{\lambda}\overline{\beta}\right)}{2\left(1 + \overline{\beta}\right)} \tag{8.42}$$

Where:

- Individual bending critical load is:

$$F_{cr;EI} = \frac{7.837EI}{l^2} \tag{8.43}$$

- Global bending critical load is:

$$F_{cr;EAc^2} = \frac{7.837EAc^2}{l^2} \tag{8.44}$$

- Global racking shear critical load is:

$$F_{cr;GA} = \left[\frac{h^2}{2\pi^2 EI_c} + \frac{ah}{12EI_b} \right]^{-1} \tag{8.45}$$

- Stiffness parameter $\hat{\beta}$ is:

$$\hat{\beta} = \frac{F_{cr;GA}}{F_{cr;EI}} \tag{8.46}$$

- Stiffness parameter $\overline{\beta}$ is:

$$\overline{\beta} = \frac{F_{cr;GA}}{F_{cr;EAc^2}} \tag{8.47}$$

- Combination factor r is:

$$r = \frac{\dfrac{2\pi^2 EI_c}{h^2}}{\dfrac{2\pi^2 EI_c}{h^2} + \dfrac{12EI_b}{ah}} \tag{8.48}$$

Hegedüs and Kollár

In 1984 Hegedüs and Kollár [13] suggested an approximate formula for the critical load of a fixed rigid frame subjected to a vertical UDL

$$F_{cr} = \left[\frac{l^2}{7.837EAc^2} + \frac{h^2}{2\pi^2 EI_c} + \frac{ah}{12EI_b} \right]^{-1} + \frac{7.837EI}{l^2} \tag{8.49}$$

This approximate formula can also be used for a flexible rigid frame.

Stick-spring model

The critical load for a flexible rigid frame subjected to a vertical UDL in this project has been derived from a stick-spring model and can be written as

$$F_{cr} = \left[\frac{l^2}{7.837EI} + \frac{l}{2C} \right]^{-1} + \left[\frac{l^2}{7.837EAc^2} + \frac{s-0.5}{s} \frac{h^2}{2\pi^2 EI_c} + \frac{ah}{24EI_b} \right]^{-1} \tag{8.50}$$

In tabel 8.4 and 8.5 Zalka`s continuum model (see eq. (8.32)), Zalka`s sandwich column with thin faces (see eq. (8.38)), Zalka`s design formula (see eq. (8.42)), Hegedüs/Kollár`s approximate formulae (see eq. (8.49)) and the stick-spring model (see eq. (8.50)) are compared. Formulae which are based on tables and graphs are given with capital letter T and approximate formula with capital letter A in table 8.4 and 8.5.

Table 8.4. Critical loads for fixed rigid frames.

Number of storeys s [-]	Vertical UDL F					
	Critical loads F_{cr} [MN]					
	Zalka (continuum model) T	Zalka (sandwich column with thin faces) T	Zalka (design formula) T	Hegedüs/ Kollár A	Stick-spring model A	ANSYS
8	28.15	26.11	27.26	25.20	38.65	32.12
16	19.82	24.19	22.04	18.07	24.76	25.32
24	13.64	16.19	14.94	12.67	15.68	16.54
32	9.55	10.66	10.11	8.97	10.38	10.83
40	6.84	7.37	7.11	6.52	7.24	7.47

Table 8.5. Errors for fixed rigid frames.

Number of storeys s [-]	Vertical UDL F				
	Error Δ [%]				
	Zalka (continuum model) T	Zalka (sandwich column with thin faces) T	Zalka (design formula) T	Hegedüs/ Kollár A	Stick-spring model A
8	-12	-19	-15	-38	+20
16	-22	-4.5	-13	-31	-2.2
24	-18	-2.1	-9.7	-24	-5.2
32	-12	-1.6	-6.6	-17	-4.2
40	-8.4	-1.3	-4.8	-13	-3.2

Conclusions:

- **If the approximate methods are compared to the FE method the stick-spring model gives the most accurate results (see table 8.4/8.5).**

- **If the graphical methods are compared to the FE method the sandwich column with thin-faces gives the most accurate results (see table 8.4/8.5).**

- **If the most accurate approximate method (stick-spring model) is compared to the most accurate graphical method (sandwich column with thin-faces) the graphical method gives more accurate results, but the approximate method is easier to use in the preliminary stages of the design (see table 8.4/8.5).**

- **The differences between the approximate methods are the rotation spring critical load, the racking shear critical loads of the beams and the racking shear critical loads of the columns. Eq. (8.49) neglects the influence of the rotation spring critical load and eq. (8.50) not, but the influence of the rotation spring critical is of very little importance. The racking shear critical load of the columns of eq. (8.50) is a factor $\frac{s}{s-0.5}$ higher then the racking shear critical load of the columns of eq. (8.49). This reduction factor is of little importance for tall buildings, because it decreases to one if the number of stories increases to infinite. The racking shear critical load of the beams of eq. (8.50) is a factor two higher then racking shear critical load of the beams of eq. (8.49) and therefore is extremely important (see table 8.4/8.5).**

8.2 Comparison of all investigated structures

The following structures have been investigated:

- X-braced frames with non-continous columns pin-connected to the base (see fig. 8.2a).
- X-braced frame with continous columns pin-connected to the base (see fig. 8.2b).
- Fixed rigid frames (see fig. 8.2c).
- Flexible rigid frames (see fig. 8.2d).

In this section these structures will be compared. The best way to do so is to compare their critical loads. In this way it can be concluded, which of the structures is the most effective.
The characteristics of the frames can be found in table 6.1. The critical loads of these structures have been computed by a finite element method ANSYS and the results are given in table 8.6.

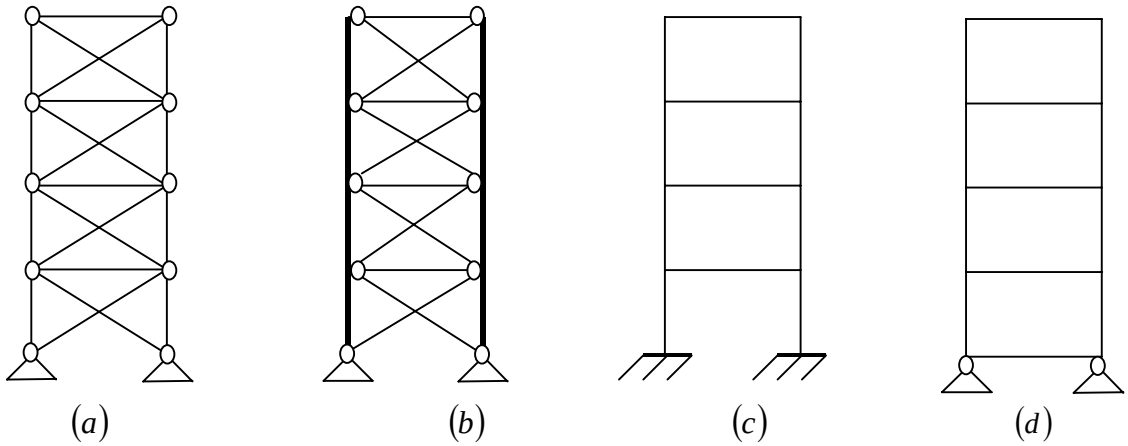

Figure 8.2 Investigated structures.

Table 8.6 Critical loads of one-bay structures subjected to UDL.

Vertical UDL F					
Critical loads F_{cr} [MN]					
Number of storeys s [-]	8	16	24	32	40
Braced frames with non-continous columns	180.0	51.37	23.43	13.30	8.55
Braced frames with continous columns	179.7	51.04	23.26	13.20	8.48
Fixed rigid frames	40.34	26.15	16.60	10.84	7.48
Flexible rigid frames	32.12	25.32	16.54	10.83	7.47

Conclusions:

- **Braced frame are more effective then rigid frames**, because the critical loads are higher (see table 8.6).

- **If the number of stories increases the difference in performance of the structures becomes smaller,** because the difference between the critical loads of the structures decreases. This is because all structures eventually develop global bending deformation only if the number of stories increases (see table 8.6).

- **The difference in performance of braced frames with non-continous and with continous columns is negligible for tall buildings which are dominated by global bending**, because the critical loads are nearly the same (see table 8.6).

- **The suggested formula give good results for the preliminary design of practical tall braced and rigid frames within a maximum error of 10%.**

9 Recommendations

Many recommendations can be made for further research involving the critical load of a structure. In this chapter these recommendations will be summed up.

In this project only frames have been investigated with a width of 3 m and a storey height of 3 m, but for tall buildings it would be better to investigate frames with a width of 7.2 m and a storey height of 3.6 m.

The parameter study for frames is restricted in this project. It could be useful to expand this parameter study.

The approximate formula for fixed and flexible rigid frames obtained by the stick-spring model gives high unconservative errors if these rigid frame are dominated by global racking shear (see table 7.4 and 7.10). It could be interesting to investigate the buckling behavior of fixed and flexible rigid frames which are dominated by global racking shear further.

In this project only one-bay X-braced frames pin-connected to the base have been investigated. It could be useful to investigate one-bay braced frames with other types of bracing (see fig. 9.1). For example N-bracing (see fig. 9.1a), K-bracing (see fig. 9.1b) and Knee-bracing (see fig. 9.1c).

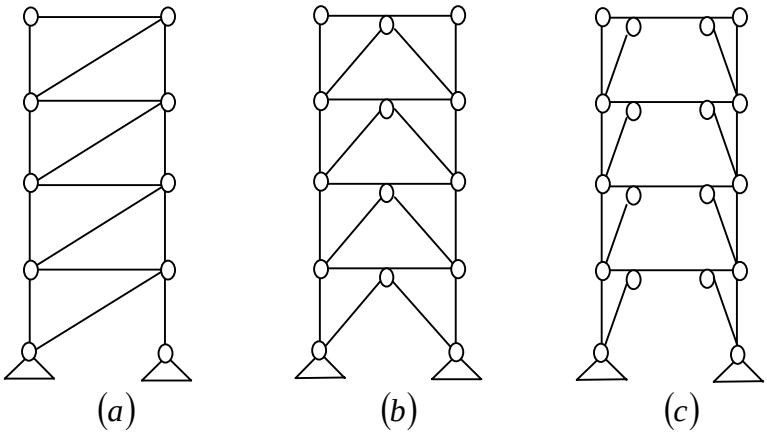

Figure 9.1 Different type of bracing.

Only one-bay X-braced frames and one-bay rigid frames have been investigated. It can be interesting to investigate frames with more then one-bay (see fig. 9.2).

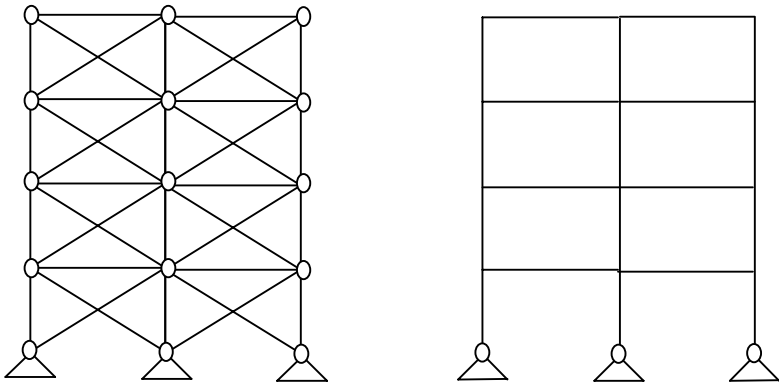

Figure 9.2 Two-bay frames.

Only one-bay rigid frames fix- and flexibly connected to the base have been investigated. It can be fascinating to investigate other types of rigid frames (see fig. 9.3). For example rigid frames pin-connected to the base.

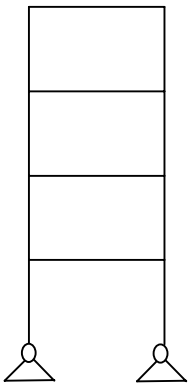

Figure 9.3 Rigid frame pin-connected to base.

For rigid frames shear deformations in the beams and columns will normally be neglected.
For coupled walls the influence of the shear deformations of the columns and beams could be taken into account, because the beams and columns are compact. It can be useful to investigate the influence of the shear deformations of the beams and columns on the overall critical load of a coupled wall (see fig. 9.4).

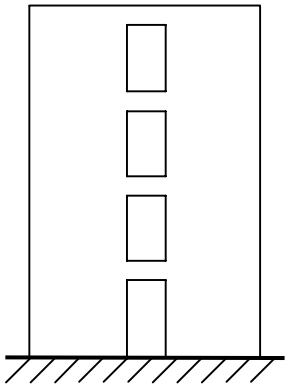

Figure 9.4 Coupled walls.

Only regular structures have been investigated, which means structures with uniform stiffness up the height or uniform width up the height and all storeys have the same storey height.
It can be interesting to investigate non-regular structures (see fig. 9.5). For example frames with varying width up the height (see fig. 9.5a), frames with varying stiffness parameters up the height (see fig. 9.5b) and frames with longer first storey columns (see fig. 9.5c).

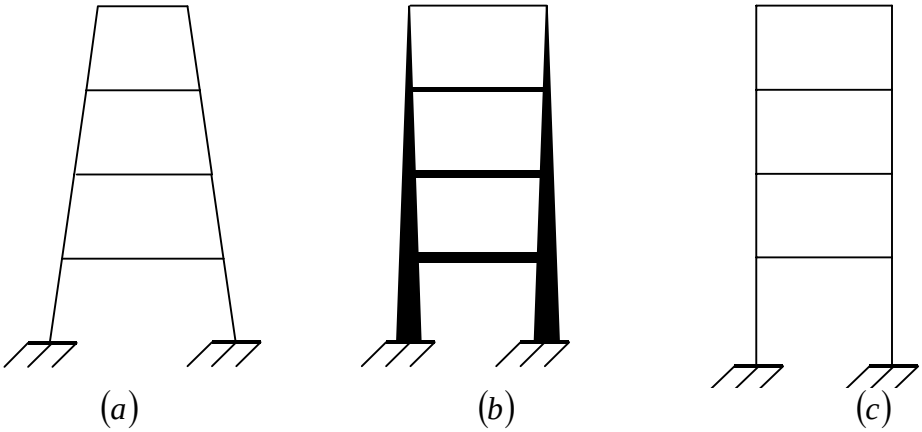

Figure 9.5 Non-regular structures.

In this project loads are applied symmetrically, but this is not always the case and sometimes columns are overloaded in comparison with others, which affects the critical load and the buckling shape.
It could be interesting to investigate the influence of assymetrical loading on the critical load of frames (see fig. 9.6).

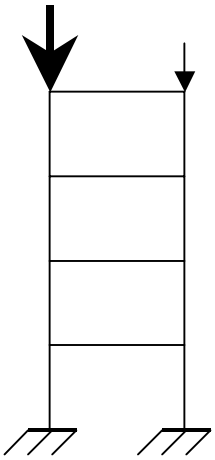

Figure 9.6 Assymetrically loaded frames

Only the buckling behavior of separate braced and rigid frames has been investigated.
It can be interesting to investigate the critical load of a combination of structures.
For example a combination of a core, braced frame, rigid frame and coupled wall (see fig. 9.7).

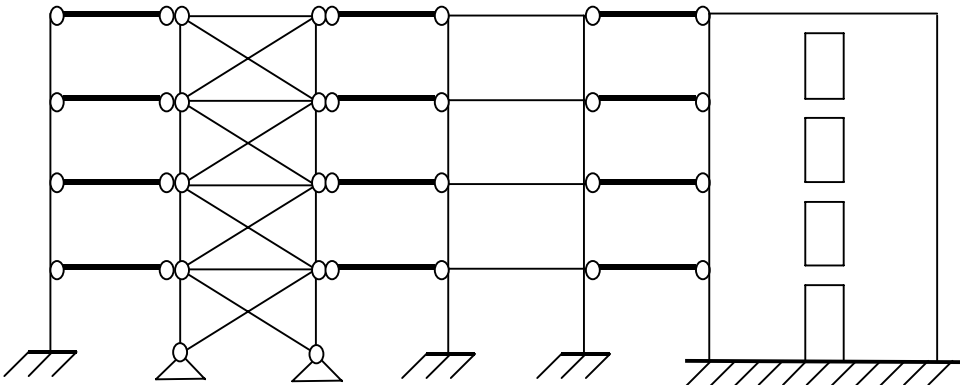

Figure 9.7 Combination of a core, braced frame, rigid frame and coupled wall.

Summary

Introduction
Tall buildings are usually subjected to horizontal wind loading and vertical gravity loading.
The horizontal wind loading causes first-order deflections. These deflections cause eccentricities of the vertical loads, which cause additional bending moments and additional deflections. These additional deformations and additional bending moments are called second-order effects. Building space is scarce and therefore buildings become taller and slender and are more vulnerable to horizontal windloading and second order effects. It is possible to estimate these second order effects in the preliminary stages of the design by defining the elastic critical load of and the vertical load on the structure.

Objective
Obtain simplified equations for estimating the elastic critical load of lateral load resisting braced and rigid frames in the preliminary stages of design of tall buildings, which combine the major modes of behavior.

Model
The stick-spring model will be used to obtain this simplified equation for the elastic critical load.

Structures to investigate
The following one-bay sway structures will be investigated:

- Braced frames (see fig. 0.1a).
- Rigid frames (see fig. 0.1b).

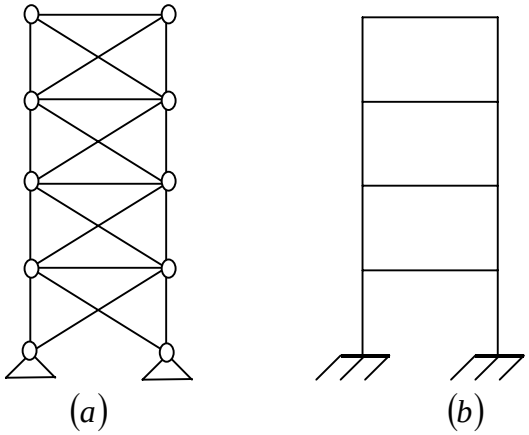

Figure 0.1 Structures to investigate.

Loadcases to investigate
The sway-structures are subjected to three different loadcases (see fig. 0.2):

- Vertical top loads (see fig. 0.2a).
- Uniformly distributed vertical loads (see fig. 0.2b).
- Load combinations (see fig. 0.2c).

For tall buildings only uniformly distributed vertical loads are interesting.

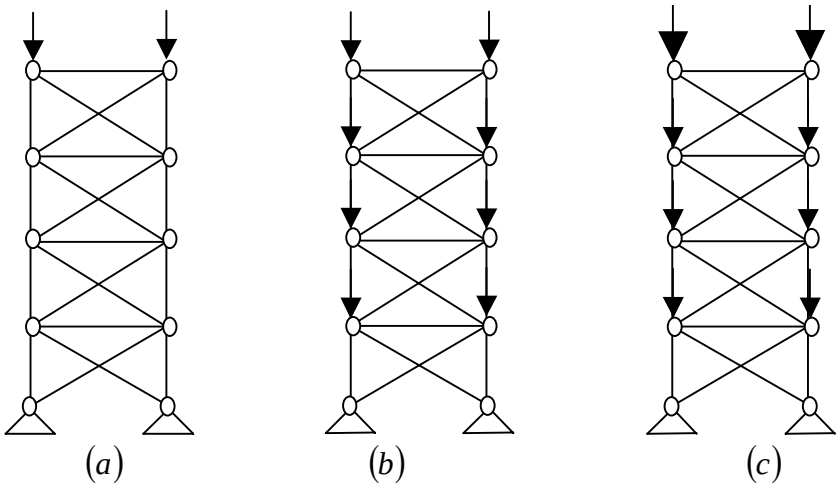

Figure 0.2 Loadcases sway structures.

Braced frames

The buckling behaviour of a braced frame can be divided into 2 modes of deformation:

- Global bending (EAc^2): axial deformation in the columns (see fig. 0.3a).
- Racking shear (GA): axial strains in the diagonals (see fig. 0.3b).

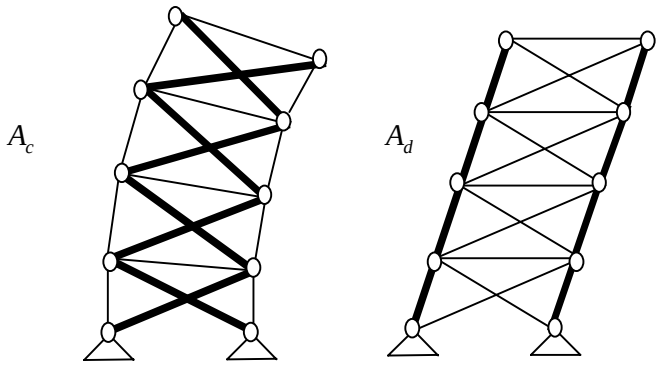

Fig 0.3 Modes of deformation of a braced frame.

Each mode of deformation is related to an individual critical load and a buckling shape.
The overall critical load of a braced can be obtained by combining all individual critical loads

$$F_{cr} = \left[\frac{1}{F_{cr;EAc^2}} + \frac{1}{F_{cr;GA}} \right]^{-1} \tag{0.1}$$

Where:

- Global bending critical load is:

$$F_{cr;EAc^2} = \frac{7.837 EAc^2}{l^2} \tag{0.2}$$

- Racking shear critical load is:

$$F_{cr;GA} = \eta GA \tag{0.3}$$

where reduction factor η is:

$$\eta = \frac{s}{s - 0.5} \tag{0.4}$$

Rigid frames

The buckling behaviour of a rigid frame can be divided into 4 modes of deformation:

- Individual bending (EI): single curvature bending of the vertical members (see fig. 0.4a).
  Global bending (EAc^2): axial deformation in the columns (see fig. 0.4b).
- Racking shear of the columns (GA_c): double curvature bending in the columns (see fig. 0.4c).
- Racking shear of the beams (GA_b): double curvature bending in the beams (see fig. 0.4d).

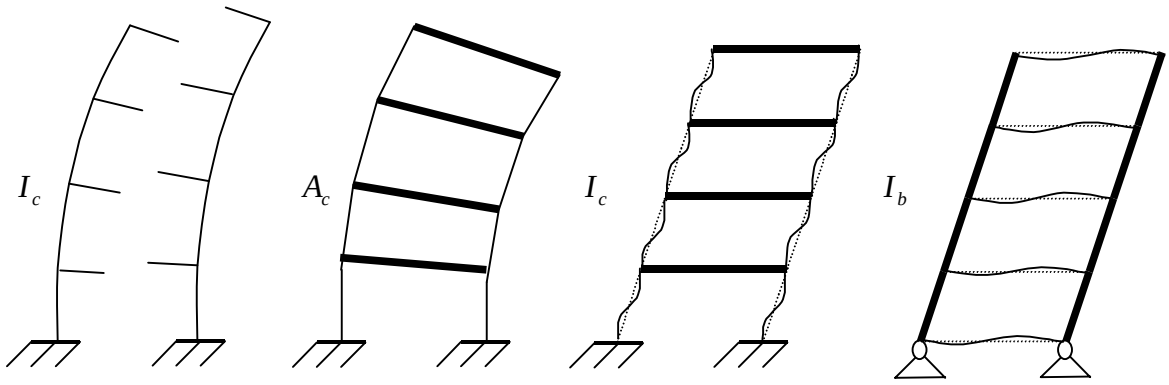

Fig 0.4 Modes of deformation of a rigid frame.

The overall critical load of a rigid frame can be obtained by combining all individual critical loads

$$F_{cr} = F_{cr;EI} + \left[\frac{1}{F_{cr;EAc^2}} + \frac{1}{F_{cr;GA_c}} + \frac{1}{F_{cr;GA_b}} \right]^{-1} \tag{0.5}$$

Where:

- Individual bending critical load is:

$$F_{cr;EI} = \frac{7.837EI}{l^2} \tag{0.6}$$

- Global bending critical load is:

$$F_{cr;EAc^2} = \frac{7.837EAc^2}{l^2} \tag{0.7}$$

- Racking shear critical load of the columns:

$$F_{cr;GA_c} = \eta \frac{2\pi^2 EI_c}{h^2} \tag{0.8}$$

- Racking shear critical load of the beams:

$$F_{cr;GA_b} = \frac{24EI_b}{ah} \tag{0.9}$$

The accuracy of the stick-spring model will be checked by a finite element analysis.

Conclusion

- **All suggested formula give good results for the preliminary design of practical highrise braced and rigid frames within a maximum error of 10%.**

References

[1] Dicke, D. (1991). Stability for Designers, Delftse Publishing Company: Delft, The Netherlands (in Dutch).
[2] Dicke, D. (1991). Knik en Stabiliteit, Stichting Professor Bakkerfonds: Delft, The Netherlands (in Dutch).
[3] Rosman, R. (1973). Dynamics and stability of shear wall building structures, Proc. Instn. Civ.
[4] Euler, L. (1744). Methodes inveniendi lineas curvas maximi minimive proprietate gaudentes, Appendix I, De curvis elaticis, Lausanne/Geneva 1744.
[5] Timoshenko S, Gere J. (1961). Theory of elastic stability (2nd edn). McGraw-HiIl: New York.
[6] Föppl, L. (1933). Über das Ausknicken von Gittermasten, insbesondere von hohen Funktürmen. ZAMM 13, pp. 1-10.
[7] Papkovich, P.F. (1963). On structural mechanics in chipbuilding. 4, Stability of beams, trusses and plates (in Russian). Sudpromgiz, Leningrad.
[8] Zalka KA. (1979). Buckling of a cantilever subjected to distributed normal loads, taking shearing deformation into account. Acta technica Academiae Scientiarum Hungaricae, Tomus 89 (3-4), pp. 497-508.
[9] Csonka (1961). Buckling of bars elastically built in along their entire length. Acta Technica. Tomus XXXII Fasciculi (3-4), pp. 423-427.
[10] Southwell, R.V. (1922). On the free transverse vibrations of an uniform circular disc clamped at its centre; and on the effects of rotation. Proceedings of the Royal Society of London. A, pp. 101, 133-153.
[11] Zalka KA. (1980). Torsional buckling of a cantilever subjected to distributed normal loads with the aid of the method of continuum. Acta technica Hung., 90, pp. 91-108.
[12] Hegedüs, I and Kollár, L. (1984). Buckling of sandwich columns with thin faces under distributed normal loads. Acta Technica Hung. 97, 111-122.
[13] Hegedüs, I and Kollár, L. (1984). Buckling of sandwich columns with thick faces subjected to distributed normal loads of arbitrary distribution. Acta Technica Hung. 97, 123-132.
Engrs., 55, 411-423.
[14] Tarnai, T. (1980). Generalization of Southwell`s and Dunkerley`s theorems for quadratic eigenvalue problems, Acta Technica Hung. 91, pp. 201-221.
[15] Tarnai, T. (1981). Generalization of the Dunkerley theorem and its application in the theory of elastic stability. 9th International Congress on the application of Mathematics in Engineering Science,Weimar.
[16] Dunkerley S. (1894). On the whirling and vibration of shafts. Philosophical Transactions of the Royal Asociety of London, Ser. A, 185, pp. 279-360.
[17] Zalka KA. (2000). Global Structural Analysis of Buildings, E & FN Spon, London.
[18] Hoenderkamp, J.C.D. (2002). Critical Loads of Lateral Load Resisting Structures for Tall Buildings, The Structural Design of Tall Buildings, USA, Vol.11, No.3, pp. 221-232.
[19] Hoenderkamp, J.C.D. (2002). Simplified Second Order Analysis of Braced Frames, Proceedings of the 7th International Conference on Steel & Space Structures, Edited by S.P. Chieuw, ISBN:981-04-5826-6, Singapore Structural Steel Society, Singapore, Oct. 2-4, pp. 19-26.
[20] Hoenderkamp, J.C.D. (2002). Kritische belastingen van stabiliteitselementen, Bouwen met staal:Mechanica, Nr. 167, Aug., pp.46-52.
[21] Hoenderkamp, J.C.D. (2002). Kritische belastingen van stabiliteitselementen voor verdiepingbouw, Syllabus van de bouwen met Staal Techniekdag, ISBN 90-6814-134-1, eindhoven, maart, pp. 25-42.
[22] Kollár L. (1999). Structural Stability in Engineering Practice, E&FN Spon, London.
[23] Stafford Smith B, Coull A. (1991). Tall Building Structures: Analysis and design. John Wiley & Sons: New York.
[24] Zalka KA. (1999). Full-height buckling of frame with cross-bracing. Proc. Inst. Civ. Engrs. Structures & Buildings, Vol. 134, May, pp. 181-191.
[25] Astalos, Z. (1972) Buckling of single-bay, multi-storey frameworks by the continuum method, taking column shortening into consideration (in Hungarion). Magyar Épitöipar. pp. 471-474.

[26] Hegedüs and Kollár. (1999) Buckling analysis of laced columns using difference equations and the continuum method. Acta Tech. Hung. Civil Eng. (In press).
[27] Hegedüs and Kollár. (1987) Stabilitätsuntersuchung von Rahmen und Wandscheiben mit der Sandwichtheorie. Die Bautechnik, 64, 420-425.
[28] Zalka KA. (1998b). Equivalent wall for frameworks for the global stability analysis. Building Research Establishment, N33/98, Watford.